A study of Salmon Pituitary Tissue using Magic Angle Spinning ^{1}H-NMR

Merethe Birkeland

Master Thesis in NMR Spectroscopy

University of Bergen

2019

Acknowledgements

First of all I would like to thank my supervisor John Georg Seland for all his guidance, feedback and encouragement throughout this thesis. Thanks for being available and eager to help whenever needed. I would also like to express my gratitude towards Signe Steinkopf for the amazing follow-up and support in the writing process. A great motivator with constructive feedback. I am also grateful to Willy Nerdal for guidance during the experimental work and for getting us in touch with the Institute of Marine Research (HI). Matre Research Department of HI provided samples for this study, and for that I am grateful, a special thanks to Ragnar Nordtvedt for the cooperation. I would like to thank Henrik Sørgård for being available and helping me with the NMR instrument.

Lastly, I am grateful for my family and friends for supporting me throughout my Master´s degree.

Abstract

The aim of this pilot study was to evaluate the use of HR-MAS NMR spectroscopy in qualitative and quantitative analysis of the pituitary content from healthy farmed fish. Global aquaculture has grown continuously and rapidly the last decades, and accounts for nearly 50 percent of food fish worldwide. The pituitary gland in teleosts produces hormones which regulate sexual maturation. Growth and age at sexual maturity are traits influencing the quality of the salmon and are important breeding goals for continued economic growth in the industry. Achieving an overview of the hormone activity throughout the life cycle of salmon is a requirement to delay maturation by hormone regulation, and thus the quality.

The study composes of 6 female and 6 male pituitary gland samples obtained from matured farmed salmon with different backgrounds. The samples was given by the Institute of Marine Research (HI) from the Matre Research Department. The thesis features ^{1}H 1D HR-MAS NMR experiments with applied T_2 filter, in addition to H,H-COSY NMR experiments, both acquired with presaturation of water. All the experiments were performed at 277 K with spinning rates of 4000 Hz. All the samples weighed less than 0,08 g and more than 90 % of the proton signals came from water.

The study lead to some main findings. A triplet at 0,9 ppm is assumed to originate from a methyl group, presumably from the amino acids Ile, Leu and Val. Two doublets at 1,13 and 1,27 ppm are also considered due to the presence of methyl groups, but in Val, Ala and Thr. Further are Lys and Cys assumed present in the samples proven by signals and couplings in the ^{1}H NMR spectra. However, the triplet is only observed in three of the samples, and the lack of the methyl signal in all other spectra could be due to low concentrations of the hormones making it difficult to detect. A high intensity singlet at 2,0 ppm was also found in six of the spectra, and is assumed to be a contamination of the brain metabolite NAA.

The attempt to distinguish hormones from each other in healthy salmon pituitaries using HR-MAS NMR was challenging. However, the results from this pilot can be used to design a study where all the salmons are comparable considering maturity, breeding conditions and genetic background. In addition, the samples should be collected from the fish at another time in their life cycle with higher hormone activity.

Abbreviations

ACTH	adrenocorticotropic hormone
Ala	Alanine
Asn	Asparagine
Asp	Aspartic acid
BMRB	Biological Magnetic Resonance Bank
BPG-axis	brain-pituitary-gonad-axis
COSY	Correlated Spectroscopy
Cys	Cysteine
DQF	Double Quantum Filtered
DSS	4,4-dimethyl-silapentane-1-sulfonic acid
FSH	Follicle stimulating hormone
GH	Growth hormone
GTH	Gonadotropic hormone
HMDB	Human Metabolome Database
HR-MAS	High Resolution Magic Angle Spinning
Ile	Isoleucine
Leu	Leucine
LH	Luteinizing hormone
Lys	Lysine
Met	Methionine
MRI	Magnetic Resonance Imaging
NAA	N-acetyl aspartate
NMR	Nuclear Magnetic Resonance
ns	number of scans
ppm	parts per million
PRL	Prolactin
Thr	Threonine
TSH	Thyroid stimulating hormone
Tyr	Tyrosine
TPPM	Two-pulse phase-modulated decoupling
Val	Valine

Symbol

P	Angular moment
I	Spin quantum number
$\hbar$	Planck´s constant divided on 2π
h	Planck´s constant (6,6256*10^{-34} Js)
μ	magnetic moment
γ	Gyromagnetic ratio
m	Magnetic quantum number
B_0	Static magnetic field
α	Low energy state (m= +1/2)
β	High energy state (m= -1/2)
E	Energy
ΔE	Energy difference between two energy states
N_α	Spin population in the lower energy level
N_β	Spin population in the upper energy level
k	Boltzmann´s constant (1,38*10^{-23} JK^{-1})
T	Temperature (Kelvin)
ω	Larmor frequency
θ	Flip angle
M_0	Magnetization vector
B_1	Applied electromagnetic pulse
τ_p	pulse duration
T_1	Longitudinal relaxation
T_2	Transverse relaxation
p1	Pulse length
p2	Pulse length
d1	Delay time
rg	Receiver gain
p19	Power level of presaturation
d20	Fixed echo time
L4	Loop times four
t_1	Evolution time
d0	Incremented delay

Table of Contents

1. Introduction

1.1 Background

Global aquaculture has grown continuously and rapidly the last decades, and today it accounts for nearly 50 percent of food fish worldwide.[1] It is fast becoming one of the most important sources of food production in the world. The early 70´s was the beginning of the industrial fairy tale that is Norwegian aquaculture which according to Statistics Norway (SSB) produced more than 1,2 tonnes of salmon in 2017. With rapid growth and production, the aquaculture sector faces challenges which is necessary to comprehend when it is the key to feeding humans in the future. One important challenge is fulfilling the consumer´s requests as the production is of economic importance. The demand of higher quality of farmed fish is increasing, and quality traits are now included in large-scale breeding productions.[2]

Growth, age at sexual maturity, improved resistance to disease and other traits influencing the quality of the salmon are important breeding goals for continued economic growth in the industry.[3] Early sexual maturity is a problem in many farmed fish species, including salmon.[4] The maturation affects the growth performance, flesh composition, behaviour, health, welfare and external appearance. Controlling the age and growth of fish is not possible to do without knowing the exact mechanisms triggering puberty of a given species in addition to the external and internal factors.[5] Puberty onset in teleosts (bony fish) is activated by the brain-pituitary-gonad-axis (BPG-axis), and is linked to genetic factors, as well as nutritional status and body growth rate.[6]

The pituitary gland in teleosts produces gonadotropic hormones (GTH) which regulate sexual maturation. The GTH´s are the follicle stimulating hormone (FSH) and the luteinizing hormone (LH) which targets the ovaries. In addition there are other important hormones present in the pituitary which are important in controlling the maturation, for example the growth hormone (GH) and the adrenocorticotropic hormone (ACTH). Optimally there would be a method to detect and determine the amount of hormones in a

pituitary. Quantitative information about the hormones in the fish pituitary at different stages of the fish´s life cycle is essential to observe trends in the hormone activity, especially during maturation, thus making it possible to delay maturation of farmed fish by manipulating the pituitary hormone activity. NMR technology is useful in this aspect as it is a completely non-invasive, not very time consuming method, which can yield both qualitative and quantitative information of the observed material.

1.2 Previous work

1.2.1 Pituitary

The interest in the pituitary gland of teleosts was significantly increased when Pickford and Atz published their work *The Physiology of the Pituitary Gland of fishes* in 1957.[7] Since then a number of reviews about the morphology, function and control of pituitary cells have appeared. A great deal of the earlier works published are regarding the structure of the pituitary and the physiology of these cells. An overview of the cells and their structure present in the teleost pituitary in addition to their location are accomplished by many histochemical [8-10] and in situ hybridization studies.[6, 11] Later investigations involve how the teleost pituitary cells behave by electrophysiological techniques.[12-14] To my knowledge these investigations does not yield detailed quantitative information about the chemical composition of the different parts of the teleost pituitary apart from morphometric studies.[15, 16] Morphometric studies are quantitative analysis based on form with high standard deviations. The challenge with endocrine screenings are the need to identify thousands of chemicals.

1.2.2 Biological NMR applications

Application of NMR in the field of biological materials began in 1957 with studies on simple amino acids which helped initiate studies of proteins.[17] Some years later research which gave rise to the area of metabolic investigations was published.[18, 19] The high-resolution magic-angle spinning (HR-MAS) NMR method was developed in the late 1990´s and made it possible for non-invasive analysis of biological material [20]. NMR spectroscopy has since developed to become a powerful tool for analyzing structure, dynamics, and interactions of biological molecules.

NMR spectroscopy has been used in many different studies of fish since the method was developed. Analysis of fat and oil in addition to metabolites using HR-MAS [21, 22], and tumor and tissue analysis using Magnetic Resonance Imaging (MRI)[23] are some of the NMR studies performed on fish. Generating good 1D spectra from fish tissue using HR-MAS NMR has been achieved in many studies, and are often used for quantitative in addition to qualitative analysis. The compounds under investigation in these studies are usually oils, fat and metabolites, and the interpretation is generally manageable.[21, 22, 24-26] In addition to regular 1D spectra, good resolved 2D COSY spectrum can be achieved of biological material in the solid state, with water supression.[22, 27, 28]

There is a lot of research on pituitaries using NMR spectroscopy, both from extracts of the organ and directly on the organ in solid state. Most of the research in solid state is based on MRI and are metabolite studies of cancer tumors in the pituitary organ.[29-33]

1.3 Objective

The aim of this work is to evaluate the use of HR-MAS NMR spectroscopy in qualitative and quantitative analysis of the pituitary content from healthy farmed fish. This was given as a pilot project. To identify the amino acids and thus hormones present in a healthy pituitary gland a reliable HR-MAS NMR technique needs to be developed. With this aim both ^{13}C and ^{1}H NMR analysis are performed on the pituitary samples, although the fundament of the work are the ^{1}H 1D HR-MAS NMR experiments. H,H-COSY NMR experiments are acquired for additional information to support the discoveries in the 1D experiments. To my knowledge this is the first attempt in obtaining qualitative and quantitative information of healthy fish pituitaries.

2. Theory

2.1 NMR spectroscopy

Nuclear Magnetic Resonance (NMR) spectroscopy is a method used to study biological, physical and chemical properties of complex molecules. In chemistry it is mostly used to determine the static and dynamic properties of a molecule. The first experiment by use of NMR spectroscopy were made by F. Block and E. M. Purcell who in 1946 successfully demonstrated NMR of condensed matter.[34, 35] It is thus a relative new technique under constant development.

2.1.1 The NMR phenomenon

NMR is a phenomenon which occurs when a nucleus is exposed to a static magnetic field ($\mathbf{B_0}$). The nucleus is subsequently subjected to a second oscillating magnetic field to be excited. The phenomenon is present in atoms where the nucleus possesses spin property. Spin is a fundamental property of protons, electrons and neutrons. The spin of a nucleus yields an angular moment, and is defined in quantum mechanics by the following equation.

$$P = \sqrt{I(I+1)}\hbar \qquad \text{Eq. 2.1}$$

Where I is the spin quantum number with possible values of I=0, ½, 1, 3/2, 2.. up to six and $\hbar = h/2\pi$ where h is Planck´s constant ($6{,}6256*10^{-34}$Js) [36]. The angular moment **P** is associated with the magnetic moment $\boldsymbol{\mu}$. The vector quantities are proportional to each other and are shown as:

$$\mu = \gamma P \qquad \text{Eq. 2.2}$$

Where γ is the gyromagnetic ratio which is a constant for each nuclide. Nuclei with low gyromagnetic ratio are said to be NMR insensitive and nuclei with large gyromagnetic

values are sensitive. By combining **equation 2.1** and **2.2** the following expression of the magnetic moment μ is obtained:

$$\mu = \gamma\sqrt{I(I+1)}\hbar \qquad \text{Eq. 2.3}$$

Nuclides with spin I= 0 do not possess a magnetic moment and are therefore not observed in NMR spectroscopy. If a nucleus with angular moment **P** and magnetic moment μ is exposed to a static magnetic field $\mathbf{B_0}$ the angular moment is oriented along the field in the same or opposite direction (z-direction). The z-component of the angular moment is oriented as follows:

$$P_z = m\hbar \qquad \text{Eq. 2.4}$$

Where m is the magnetic quantum number with values m= I, I-1,…-I. By combining **equation 2.2** and **2.4** the components of the magnetic moment along the field direction z, are obtained.

$$\mu_z = m\gamma\hbar \qquad \text{Eq. 2.5}$$

Totally there are (2I+1) different values of m, which yields possible orientations for the angular and the magnetic moment.

2.1.2 Zeeman energy levels and population

Protons and ^{13}C nuclei possess spin I=1/2, giving m=$\pm$1/2 when exposed to a magnetic field. The energy of the magnetic dipole in a magnetic field $\mathbf{B_0}$ is:

$$E = -\mu_z B_0 \qquad \text{Eq. 2.6}$$

By combining **equation 2.5** and **2.6** the following expression of the energy state for a nucleus with 2I-1 possible orientations are obtained (**equation 2.7**).

$$E = -m\gamma\hbar B_0 \qquad \text{Eq. 2.7}$$

The energy states are called the Zeeman energy levels. The alpha (α) spin is parallel, and the beta (β) spin is antiparallel to the static magnetic field **B_0** as illustrated in **figure 2.1.**

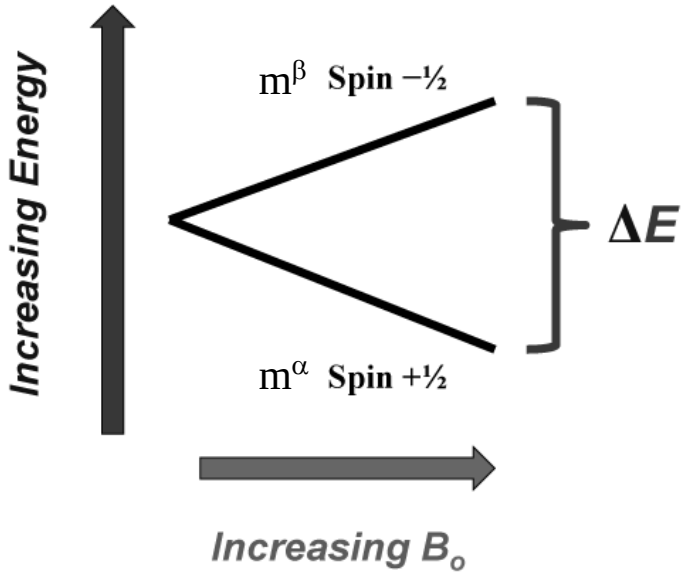

Figure 2.1: Illustration of the interaction between a nucleus with spin I=1/2 and the external magnetic field B_0 leading to splitting of the energy. The splitting is proportional with the magnetic field. The figure is made with small adjustments from mriquestions.com 27.02.2019.

The energy difference between the energy levels of a proton (m=±1/2) is expressed in **equation 2.8. Equation 2.8 and figure 2.1** clearly shows that the energy difference increases as the external magnetic field increases.

$$\Delta E = \gamma\hbar B_0 \qquad \text{Eq. 2.8}$$

The energy difference ΔE is proportional to the population difference between the two Zeeman levels [37]. The nuclei are distributed between the available energy levels according to the Boltzmann distribution (**eq.2.9**)

$$\frac{N_\beta}{N_\alpha} = e^{-\frac{\Delta E}{kT}} \qquad \text{Eq. 2.9}$$

Where k is the Boltzmann´s constant ($1{,}38*10^{-23}JK^{-1}$) , T is the absolute temperature in Kelvin and kT expresses the thermal energy acquired to reorient the spins. N_β represents the spin population in the upper energy level and N_α is the spin population in the lower level. For all nuclei the energy difference ΔE will be much smaller compared to the thermic conditions kT which yields a small population difference in the energy levels. The absorption of energy, and hence the intensity of the spectroscopic transition is dependent of the population difference. NMR is therefore a relatively insensitive technique, and thus it is crucial to optimize signal strengths by for example using high magnetic field strengths B_0.

2.1.3 Pulse NMR

The dipole of the nuclei precesses about the z-axis with frequency proportional to the static magnetic field $\mathbf{B_0}$ where ω is the Larmor frequency (**eq.2.10**). Nuclei can only absorb and emit energy that matches the Larmor frequency of the nucleus in the magnetic field [36].

$$\omega = \frac{\gamma}{2\pi} B_0 \qquad \text{Eq.2.10}$$

One type of nuclei are excited in the sample by an electromagnetic radiofrequency (RF) pulse. The pulse is applied to the sample during a certain amount of time, τ_p, to induce NMR transitions between the energy levels and thus bring the magnetization along the z-direction ($\mathbf{M_0}$) out of equilibrium [34]. The weaker electromagnetic RF pulse $\mathbf{B_1}$ oscillating with the Larmor frequency ω is applied perpendicular to the strong constant static magnetic field B_0 in the x´-direction. The x´ and y´ denotation indicates that the scheme is in a rotating coordinate system where the x- and y-axis rotate with the Larmor frequency. The angle between the z-direction and the induced magnetization after application of the RF pulse is called the flip angle and is expressed as follows [36]:

$$\theta = \gamma B_1 \tau_p \qquad \text{Eq. 2.11}$$

θ is the flip angle which is typically set to 90° or 180°. **Figure 2.2** illustrates how the RF pulse influences the magnetization depending on the different flip angles. When the flip

angle is set to 90°x´ the longitudinal magnetization (**M_z**) is flipped down and converted to transverse magnetization (**M_{xy}**). When the flip angle is 180°x´ the net magnetization ends up in the negative z-direction (**$-M_0$**). The receiver coil which detects the signals is fixed in the xy-plane, thus the magnetization has to exist in the xy-plane to yield signal.

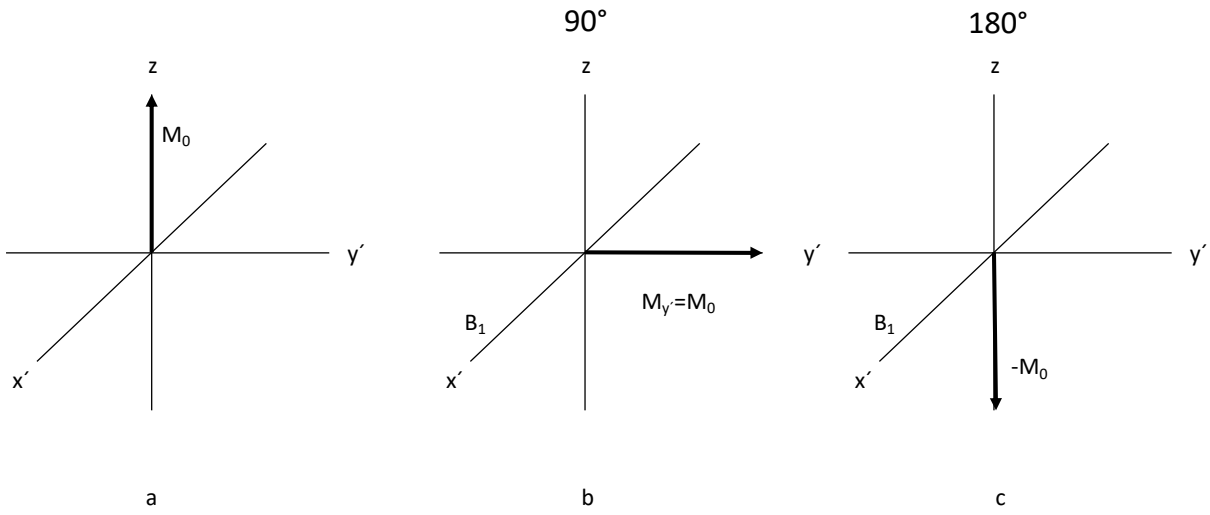

Figure 2.2: Illustration of how a 90° and a 180° pulse affect the net magnetization in a rotating coordinate system. a) Before the pulse is added to the system and the net magnetization is due to the static magnetic field in the z-direction b) After application of a 90°x´ pulse and the magnetization is flipped into the y´-direction c) After application of a 180°x´ pulse and the magnetization is flipped into the negative z-direction. The figure is drawn based on an illustration from Friebolin page 11. [36].

2.1.4 Relaxation

As shown in **figure 2.2**, the magnetization along the z-axis is flipped out of equilibrium when exposed to the RF pulse. When the pulse is turned off the magnetization reverts to its equilibrium state. How the nuclei release energy and the spin system rotates back to its original state is called relaxation. There are two relaxation processes; the longitudinal or spin-lattice relaxation (T_1) and the transverse or spin-spin relaxation (T_2) [36].

2.1.4.1 Longitudinal relaxation (T_1)

In its equilibrium state the magnetization in the z-direction is noted $\mathbf{M_0}$. The longitudinal relaxation describes how the $\mathbf{M_z}$ magnetization changes from zero to $\mathbf{M_0}$ after the RF pulse is turned off. T_1 relaxation occurs due to how the nuclei release the absorbed pulsed energy to the surroundings and it can be described as the rate of change of $\mathbf{M_z}$ by the following equation [36]:

$$\frac{dM_z}{dt} = -\frac{M_z - M_0}{T_1} \qquad \text{Eq. 2.12}$$

Where T_1 corresponds to the rate constant of the relaxation process in the longitudinal direction. There are many different interactions that contribute to the longitudinal relaxation, but the most important one is the dipolar interactions. The dipolar interaction occurs when a nucleus with magnetic moment interacts with other magnetic nuclei through space.

2.1.4.2 Transverse relaxation (T_2)

The transverse relaxation describes how the induced signal in the xy-plane changes when the RF pulse is turned off. The transverse magnetization $\mathbf{M_{xy}}$, approaches zero as the systems reverts to equilibrium. This relaxation effect is noted T_2 relaxation. The rate constant T_2 for the exponential decay in the xy-plane is defined by the following equations [34]:

$$\frac{dM_{x'}}{dt} = -\frac{M_{x'}}{T_2}, \quad \frac{dM_{y'}}{dt} = -\frac{M_{y'}}{T_2} \qquad \text{Eq. 2.13}$$

This yields:

$$\frac{M_{xy}(t)}{M_0} = e^{-\frac{t}{T_2}} \qquad \text{Eq. 2.14}$$

The $\mathbf{M_{xy}}$ magnetization consists of spin in phase coherence and when the RF pulse is turned off the spins will gradually loose phase coherence and fan out in the xy-plane. This relaxation effect is due to the nuclei experiencing slightly different magnetic fields caused by inhomogeneities in the magnetic field $\mathbf{B_0}$ and is noted T_2'. The sum of the two transverse relaxation effects T_2 and T_2' is the apparent relaxation T_2^*. T_2 can never be longer than T_1 because it is a necessity that the transverse magnetization fully decays for the longitudinal magnetization to reach its equilibrium state. Thus T_2 is often shorter than T_1 [36].

$$T_2 \leq T_1 \qquad \text{Eq. 2.15}$$

2.1.5 Chemical shift and spin-spin coupling

The NMR spectra yield the chemical shift and peak intensity of a nuclei in a magnetic field. The chemical shift is expressed in parts per million (ppm) by frequency [36]. The factor influencing the chemical shift of a nuclei is the total magnetic field. The experienced magnetic field of a nuclei varies with chemical environments. The nuclei are always surrounded by electrons and other atoms which produce an induced field opposed to the applied field. The nuclei experience a shielding. Chemically non-equivalent nuclei are shielded to different extents and give separate resonance signals in the spectrum [36].

In addition to the chemical shifts, the nuclei yield different shapes in the NMR spectrum depending on the environment. In a molecule the neighboring magnetic dipoles interact with each other, called spin-spin coupling. This coupling affects the magnetic field at the position of the nuclei, and alters the resonance frequencies [36]. The indirect spin-spin coupling (J-coupling) is the effect through chemical bonds and applies to nuclei up to three bond lengths apart.

2.1.6 Solid State NMR

NMR spectroscopy is one of the most versatile analytical methods used to study biological, physical and chemical properties of matter, solution or gas. By detecting the different magnetic interactions between the nuclei it is possible to obtain valuable structural and dynamic information about the sample. The isotropic or anisotropic interactions between the nuclei contributes to the NMR spectra, and some interactions are more dominating.

In solution there is random and rapid movement of molecules which leads to isotropic properties and yields a NMR spectrum with sharp absorptions and high resolution. In solid state NMR the spectra are dominated by anisotropic (e.g. orientation dependent) interactions, especially dipolar and/or quadrupolar interactions, which leads to broad featureless absorptions [38].

2.1.6.1 Magic Angle Spinning (MAS)

To yield high resolution spectrum in solid state NMR the anisotropic interactions need to be partly or fully eliminated. This is solved by a technique called Magic Angle Spinning (MAS). The technique involve adding artificial molecular motion to the system, Thus, averaging the dipolar or quadrupolar interactions to zero and the chemical shift and spin-spin interactions to their isotropic values. The artificial motion is added by adjusting the sample in 54.74° to the static magnetic field B_0 and spinning the sample as illustrated in **figure 2.3**.

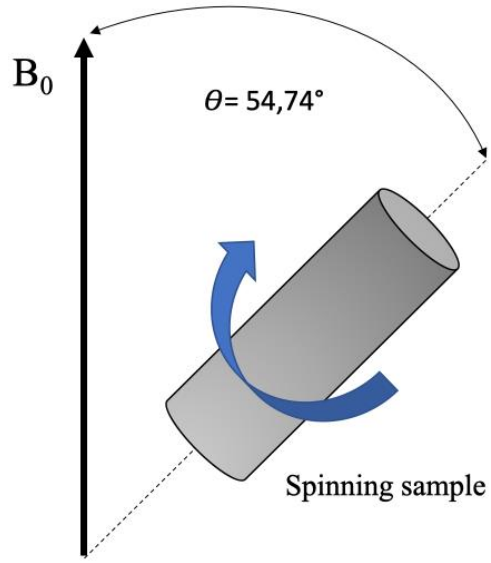

Figure 2.3: Schematic representation of a spinning sample related to the magnetic field B_0 with the angle set at θ= 54.74°: The Magic Angle. The figure is drawn with adjustments from figure in Penzel. [39].

The angle where the mathematical expression (**eq.2.16**) of dipolar and quadrupolar interaction equals to zero is 54,74°, the Magic Angle [37]. For the interactions to be fully averaged to zero or their isotropic values, the sample has to spin with a rate equal or higher than the line width of the anisotropic interactions (can be several kHz). When these requirements are met the spectrum yields sharp signals with high resolution, and are possible to interpret. Thus, the expression Magic Angle Spinning originates from the angle between the sample and the static magnetic field, and the spinning of the sample.

$$(3cos^2\theta - 1) \qquad \text{Eq. 2.16}$$

2.2 Salmon and endocrinology

2.2.1 Atlantic Salmon

There is only one species of salmon in the Atlantic Ocean called the Atlantic salmon (*Salmo salar, L*). The Atlantic Salmon is an anadromous species which means it spawns in freshwater streams, and thereafter returns to the sea. It takes up to five years for a salmon to mature, one to three years in freshwater and one to two years in seawater. By using the earth´s magnetic field the species is able to locate the river of origin to spawn throughout their lifetime. Currently, the farmed Atlantic Salmon is one of the most important farmed fish along the coasts in the North Atlantic Ocean and plays an important role in providing food.

2.2.2 Fish and aquaculture

Fish consists mainly of protein and are valuable as a food resource because of the high food conversion value (FCV). FCV is the amount of food it takes to produce a unit weight of the product [40]. In addition there is a high value of marine omega-3 in Atlantic salmon which benefits health. Because of the high FCV, high omega-3 content and the capabilities to produce farmed fish , the aquaculture is developing to feed an increased population that is exposed to overfishing and climate change.

Early sexual maturity is a problem in many farmed fish species, including the different salmon species [4]. The maturation affects the growth performance, flesh composition, behaviour, health, welfare and external appearance [41]. Different measurements have to be taken to achieve the customers quality demands and control the fish puberty. Sexual maturation in fish can be delayed in various ways, but the most common way is to expose the fish to continuous light affecting the perception of season [5]. Another way to control the maturation is to control the hormone production.

2.2.3 Pituitary

The pituitary in teleost fish (bony fish) is an endocrine gland that produces hormones in addition to control activity of three other endocrine glands. The pituitary is an advanced organ and in addition to hormones it contains tissue, fat and receptors (**table 2.1)** [42]. The amount of the individual hormones present in the pituitary varies with different conditions: Life cycle, salt concentrations, stress and light accessibility. The hormones are not evenly portioned throughout the pituitary, they exist as aggregates in the different parts of the endocrine gland.

Gonadotropic hormones (GTH) are produced in the pituitary, and teleost fish have to types of GTH: the follicle stimulating hormone (FSH) produced during the entire germ cell development, and the luteinizing hormone (LH) produced later in the germ cell development [43]. Testis and ovaries are the main target for the gonadotropic hormones and leads to release of sex hormones (testosterone and oestrogen) and thus maturation. In addition other hormones control factors that triggers the BPG-axis in teleost fish, thus there are several hormones of importance to the sexual maturation present in the pituitary.

Table 2.1 The table shows the different elements present in the pituitary gland of teleost fish and their target system.

Hormone	**Target**
Luteinizing hormone (LH)	Gonad (testes and ovaries) (GTH)
Follicle stimulating hormone (FSH)	Gonad (testes and ovaries) (GTH)
Growth hormone (GH)	Growth
Thyroid stimulating hormone (TSH)	Stimulates metabolism
Adrenocorticotropic hormone (ACTH)	Stress (adrenalin)
Prolactin (PRL)	Osmoregulation
Gonadotropin-releasing hormone (GnRH)	GTH´s
Melanin Concentration Hormone (MCH)	Skin pigmentation
Melanocyte-stimulating hormone (MSH)	MCH
Somatolactin hormone (SL)	Growth
Receptors (protein)	Hormones
Fat	-

Tissue	-
Lipids	Membranes

2.2.4 Hormones

The hormones investigated in this study are control factors that triggers the BPG-axis and the gonadotropic hormones that triggers maturation in teleost fish. Hormones have diverse chemical structures, they can consist of amino acid residues in long chains, or steroids with a four ring core with attached side groups or as glycoproteins. The hormones of interest consist mainly of the common 20 amino acid residues **(appendix 1),** but TSH, LH and FSH are glycoproteins. Glycoprotein hormones are proteins which contain oligosaccharide chains attached to the amino acid chain, they are complex and have high molecular mass. **Figure 2.4.** shows the general structure of an amino acid with varying side chain (R).

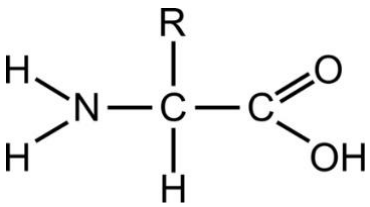

Figure 2.4: The general structure of all amino acids. The R-group represents the side chain which separates the amino acids from each other. The illustration is based on wikibooks.com 12.03.2019.

The amino acids are attached by peptide bonds, creating a long chain with varying side groups (**figure 2.5**). The chain folds in a specific conformation dependent on the peptide back-bone restriction and the interaction between the side groups of the amino acids. The hormones of interest in salmon are TSH, LH, FSH, GH and ACTH among others and they consist of a variety of amino acids (**appendix 2**). In comparison GH consists of 210 amino acids, and ACTH consist of 39 amino acids. All the 20 common amino acids are represented in almost all of the hormones investigated. The amino acid with the highest abundancy in the pituitary is Leucine (Leu) [44-52] (**figure 2.6**).

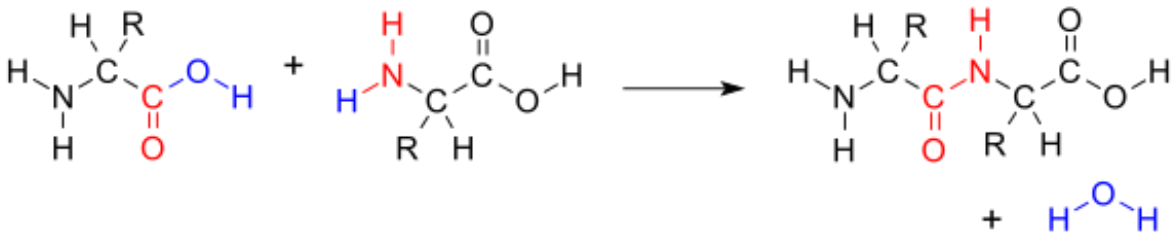

Figure 2.5: The formation of a peptide bond (red) between two amino acid residues. The illustration is based on Wikipedia.org 12.03.2019

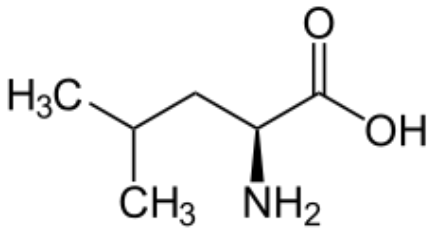

Figure 2.6: The molecular structure of the amino acid Leucine (Leu). The illustration is taken from wikibooks.com 12.03.2019.

The chemical shifts of the different amino acids are taken from the Biological Magnetic Resonance Data Bank (BMRB) and the Human Metabolome Database (HMDB) which are obtained under the same conditions (298 K and 7,4 pH).

3. Methods

3.1 Experimental materials and samples

The samples used for the ^{1}H MAS NMR analysis are all from the pituitary gland collected from farmed salmon (*Salmo salar, L.).* The Institute of Marine Research (HI) contributed with farmed salmon from the Matre Research Department in western Norway. Both male and female mature salmon are investigated in this study (12 samples). The extractions of the samples were completed by the researchers at Matre. Samples 1-6 were extracted the 17th of December 2017, and samples 7-12 were extracted the 5th of December 2018. The two different batches were bred at different conditions, but the maturation status is comparable. The first sample has been investigated frequently in initial experiments and is thus treated differently than the other samples. During three months, the first sample was thawed and prepared for initial experiments and then frozen to -80°C. This procedure was done repeatedly. Thus, sample number 1 is not regarded in the final study. The pituitary in teleost fish and its location in the brain is illustrated in **figure 3.1.**

The samples were stored at -80°C after the extraction and transported to the laboratory at the Chemical department at The University of Bergen. The samples did not thaw during transportation and was kept at -80°C in the laboratory until preparation for running NMR experiments. Samples 1-6 were stored at -50°C for six months and at -80°C before sample preparation. Different storing conditions of the samples were due to a broken freezer at the Chemical Department. The samples were kept at low temperatures to avoid the pituitaries to oxidise and decompose. Extraction and preparation was identical for all the samples.

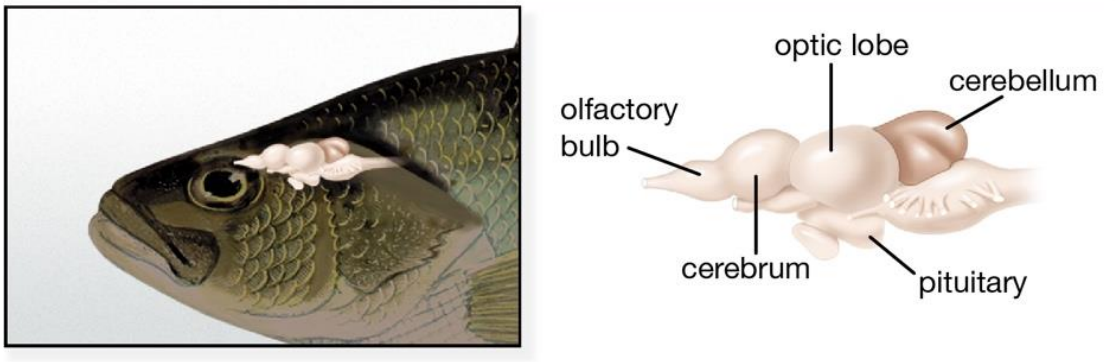

Figure 3.1: Location and description of the brain compartments of teleost fish including the pituitary gland. [53].

Information about gender, maturity and length of the fish are presented in **table 3.1** The weight of the pituitary samples are listed in **table 3.2,** and are used for quantitative analysis of hormones in salmon pituitaries by NMR.

Table 3.1: The table shows an overview of the gender, length and maturity of the fish used in the study. The length of the individuals are measured in centimetres. The males are noted with M, while F is the notation of the female fish.

Sample	Length [cm]	Gender	Maturity
1	105	M	x
2	106	M	x
3	109	M	x
4	97	F	x
5	88	F	x
6	91	F	x
7	88	F	x
8	79	F	x
9	72	F	x
10	74	M	x
11	63	M	x
12	91	M	x

Table 3.2: The weight of the pituitary samples used for quantitative analysis. The weight is measured in grams.

Sample	Weight [g]
1	0,03822
2	0,07830
3	0,07381
4	0,07415
5	0,06132
6	0,05926
7	0,06536
8	0,06064
9	0,04564
10	0,04296
11	0,02487
12	0,06112

3.2 Sample preparation

The method used in this project is solid state nuclear magnetic resonance spectroscopy (NMR). The experiments were performed with a Bruker AVIII 500 MHz WB NMR/MRI instrument at the Department of Chemistry, University of Bergen.

It is desirable to keep as much of the pituitary intact during sample preparation to get proper results. The samples were therefore kept frozen during the sample preparation to prevent degradation. In addition the samples were inserted in the test tubes under argon atmosphere to avoid oxidation. **Figure 3.2** shows a picture of pituitary sample preparation for NMR experiments.

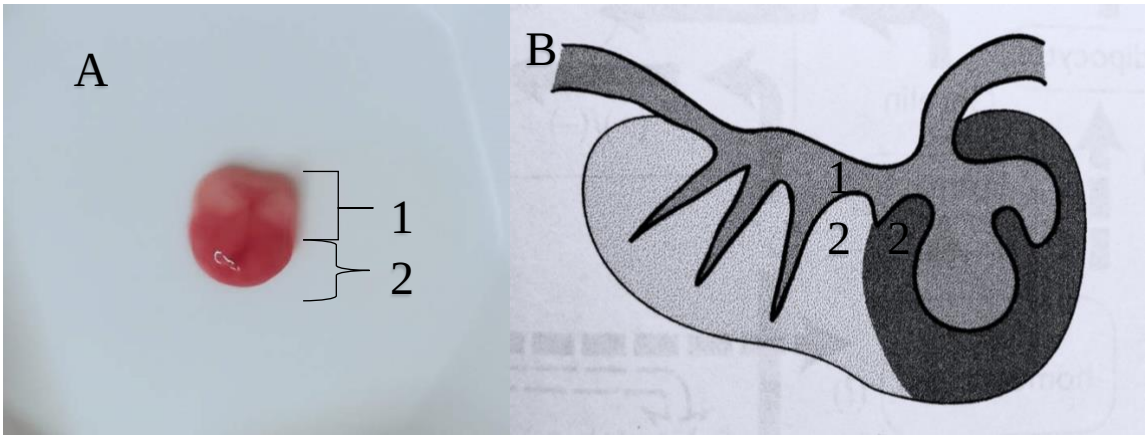

Figure 3.2: A) A small pituitary from a mature male salmon (sample number 10). The two main sections of the pituitary are visible. Area 1 shows the neurohypophysis in light red and area 2 the adenohypophysis in dark red. B) A simple illustration of a teleost pituitary where area 1 is the neurohypophysis and area 2 is the adenohypophysis. The illustration is taken from Bone page 265 [54].

The pituitary weight vary with the size of the investigated fish. The pituitary was sliced carefully with a scalpel to fit into the insert (test tube) depicted in **figure 3.3.A**. To fit the entire pituitary into the insert it has to be more compact which is solved by centrifugation of the sample. The insert was then packed into a rotor. The samples were packed into an insert and into the 50µl ZrO_2 (zirconia) MAS rotors depicted in **figure 3.3.B.** The samples with volumes higher than the insert volume were inserted directly into the rotor. When the rotor was not sufficiently packed a removable top plug was used with the rotor depicted in **figure 3.3.B.** The top plug has a ventilation hole for easy bubble removal. The sample was injected into the NMR probe head. The instrument temperature was set to 277 K to prevent decomposition of the pituitary during the experimental time.

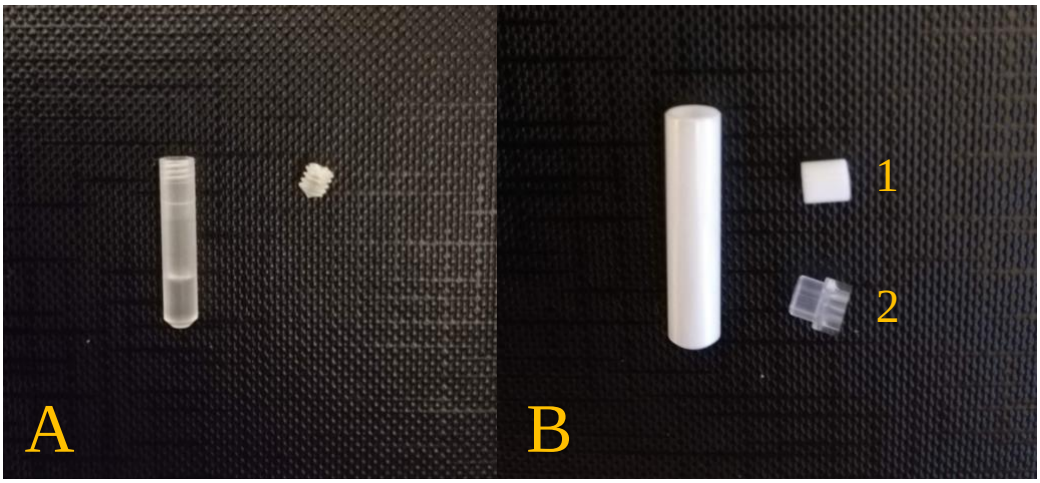

Figure 3.3: ***Sample tubes:*** *A) The insert and insert cap for small samples~ 12µl. This test tube is inserted in the rotor for NMR analysis. B) The* 50µl *ZrO_2 rotor with associated top plug (1) with ventilation hole for easy bubble removal are used with viscous samples and rotor cap (2) to keep the sample in place.*

The equipment used during sample preparation was washed with distilled water and rinsed thoroughly with chloroform in-between every sample. The rotor material is zirconia which is a homogeneous ceramic material structure that contains no ^{1}H or ^{19}F and is mechanically durable. Kel-F (polychlorotrifluoroethylene) is chemical resistant, near-zero moisture absorptive and a strong mechanical polymer which makes up the rotor cap.

3.3 Experimental methods

3.3.1 Field drift and calibration

This thesis features ^{1}H and ^{13}C NMR studies performed on a Bruker AVIII magnet at 500 MHz WB. There is a naturally occurring magnet drift in the instrumental field which can lead to artefacts and inaccurate chemical shifts in the resulting data. A field calibration before every experiment was therefore necessary to adjust the field and avoid these artefacts. Adamantane is a typically used compound as an external ^{13}C standard to calibrate the field for solid state NMR experiments when using a probe that does not use a field frequency block [55]. By running a few scans of adamantane with a 4000Hz spinning rate at room temperature (298K) the two carbon signals were easily detected, the carbon signal at 28,6 ppm is commonly used for calibration and are illustrated in **figure 3.4** [56]. After

calibration a double distilled water sample was recorded at the same conditions to control the chemical shift at 4,7 ppm [57].

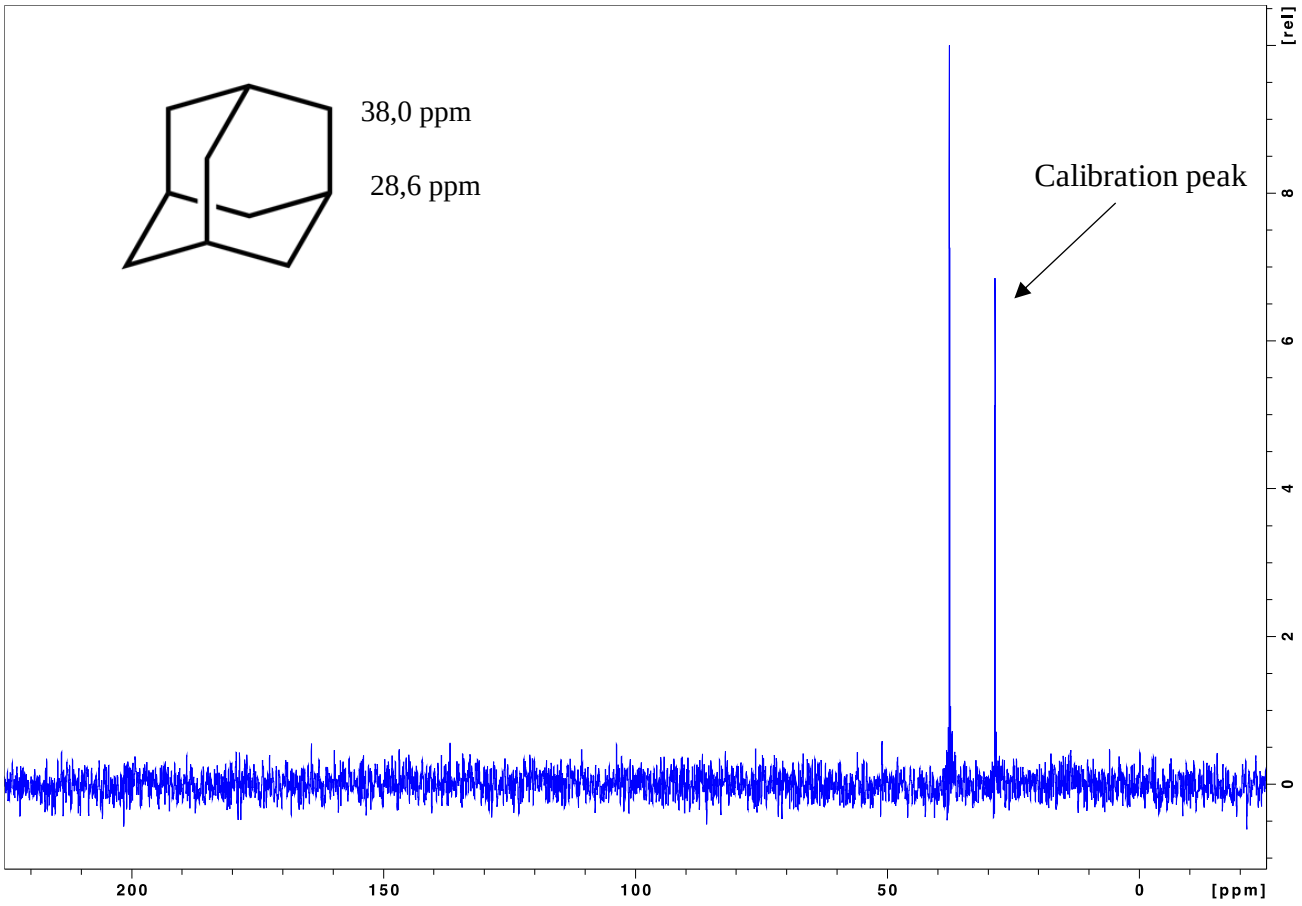

Figure 3.4: A spectrum of the two ^{13}C chemical shifts of adamantane. The shift at 28,6 ppm is used for field calibration.

3.3.2 ^{13}C MAS NMR experiment

A ^{13}C magic angle spinning experiment was performed using the pulse program "hpdec" with parameters presented in **appendix 4.A.3**. Based on previous quantitative and qualitative ^{13}C studies of metabolites in muscle and brain tissue this method is expected to provide useful information regarding hormones in salmon pituitaries [25, 58, 59]. **Figure 3.5** illustrates the standard Bruker "hpdec" (high-power proton decoupling) pulse sequence used. Poor signal to noise ratio of the experiment states that this procedure is insufficient for analysing hormones in salmon pituitary, despite the 44000 number of transients in the experiment. The spectrum shows that the molecules in the sample are more rigid than expected which provides a poor signal to noise ratio. In addition, it is necessary with an

intrusive preparation and higher sample volume for the ^{13}C nucleus to provide useful spectra [59]. No ^{13}C experiments are further performed in this work.

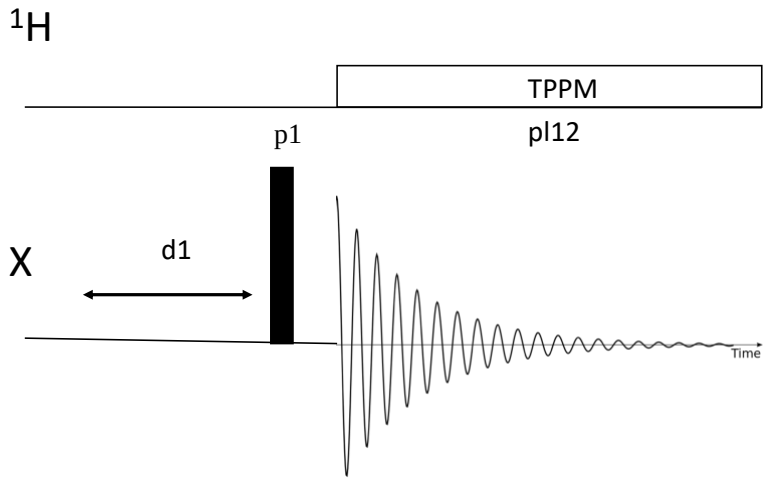

Figure 3.5 The schematic illustration of the "hpdec" pulse sequence. d1 is the delay time, pl12 is the power level for standard proton decoupling, tppm is the two-pulse phase-modulated decoupling scheme and X is the nuclei detected, in this case carbon. Illustration taken from the Bruker Topspin 3.0 User Manual 15.04.2019.

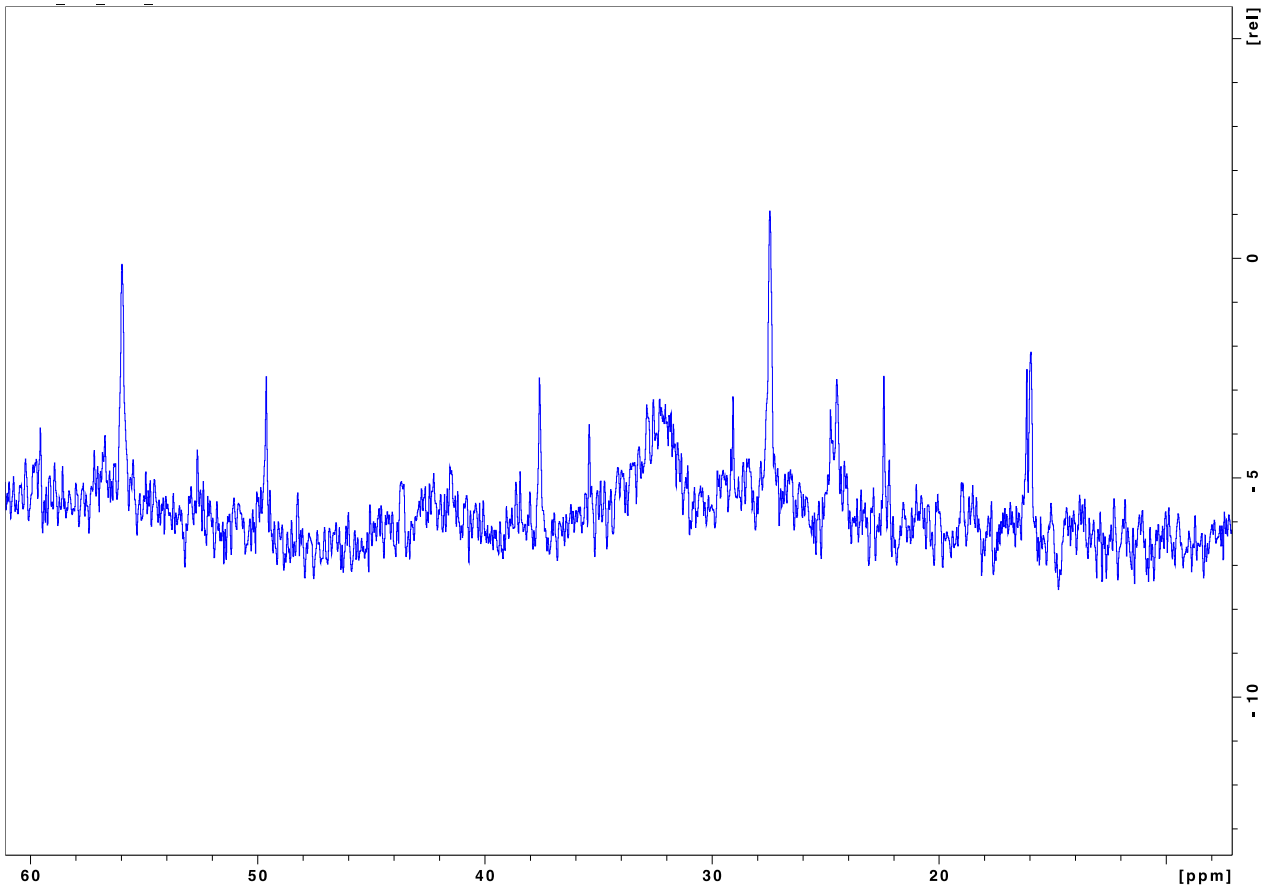

Figure 3.6: ^{13}C spectrum of salmon pituitary. The signal to noise ratio is poor and the spectrum provides insufficient data even after 44000 transients.

3.3.3 Water suppression

Pituitary glands contain several different molecules, and the non-invasive NMR experiment detects all of them. The pituitary tissue contains large volumes of water molecules and in a regular ^{1}H NMR analysis the water signal would mask signals from molecules of lower concentrations in the pituitary. To obtain good resolved signals from the samples, the resonance from water has to be suppressed.

A ^{1}H NMR spectrum was recorded of the sample using the "onepulse" pulse program (**figure 3.7**) to determine the chemical shift of water at the same temperature conditions for all experiments. The parameters used in the experiment are listed in **appendix 4.A.4**. The determined chemical shift of water is used for presaturation of the water resonance. A low power pulse applied at the water frequency during the preparation delay excites the water signal. Thus, there is no water signal detected during acquisition. It is recognized that

presaturation of the water resonance is undesirable in different protein NMR experiments, as it can lead to exchange of protons due to the Nuclear Overhauser effect (NOE) and attenuation of signal with similar chemical shift as water [60]. This work does not include structure elucidation making the NOE effects irrelevant. Attenuation of signal with chemical shift near the water signal does on the other hand occur and can affect the qualitative and quantitative determination.

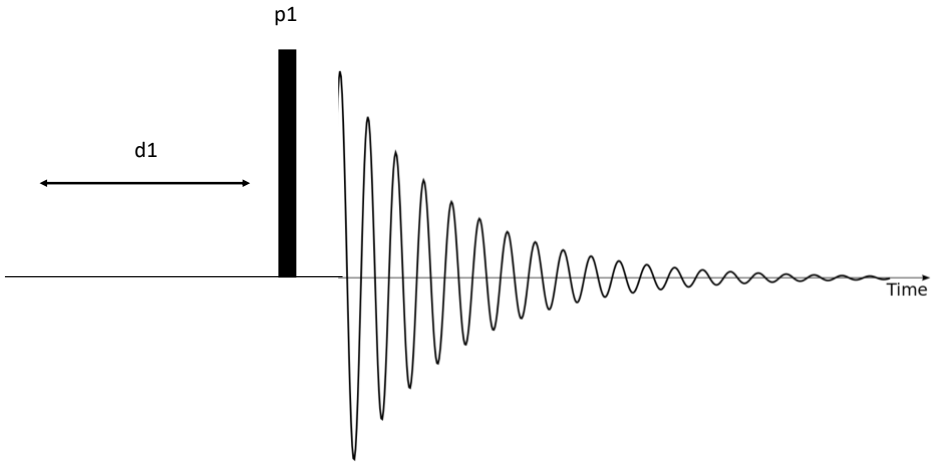

Figure 3.7: The illustration shows the "onepulse" pulse sequence, where d1 Is the delay time, the p1 is the excitation pulse length. The sequence is used to detect the water signal of the water samples, of the water in the pituitary samples and the water in the buffer sample. The illustration is taken from the Bruker Topspin 3.0 User Manual 15.04.2019.

3.3.4 Quantification

In addition to collecting the water signal from the samples, three double distilled water samples of different, but known weights are collected (**table 3.3**). By using the integrals of the peaks of the predetermined water weights, it is possible to make a calibration curve to estimate the area and intensity of peaks from other signals acquired with the same parameters. Ideally this method yields precise quantifications of the water signal in the experiments and the signals originating from the hormones. The water spectra are conducted under the conditions listed in **appendix 4.A.5**. with temperatures at 277K and with the receiver gain (rg) set to 8.

Table 3.3: An overview of the double distilled water samples and their weight in gram.

Water sample	**Weight [g]**
W1	0,016726
W2	0,01800
W3	0,01609

3.3.5 pH dependency of chemical shift

It is well established that the pH-values are dependent on temperature changes in ectotherm (cold blooded) vertebrates such as teleost fish [61]. The pituitary samples featured in this thesis are extracted at room temperature and stored at -80°C in freezer. The experiments were performed at 277 K.

To adjust the chemical shifts of the analysed protons in the pituitary samples a Phosphate buffer solution was prepared as an internal standard. The phosphate buffer have pH 7,4, and the samples are assumed to have pH 7,4. By comparing the chemical shifts of the water signal in the buffer and the samples it is possible to determine if the pH in the samples have changed or remains at pH 7,4. If the samples start to decompose it is expected that the pH value decreases. The experiments on the Phosphate buffer were conducted under identical conditions as the pituitary samples (**appendix 4.A.5**).

It is known that the pH dependence of the chemical shift of water is around 0,02 ppm per pH unit (nmrwiki.org 15.02.2019). A pH change even at one unit is not likely to occur for the investigated samples. Systems like a pituitary that contains fat, tissue and hormones have high chemical stability and are thus expected to maintain stable pH values. pH stability is an important property for function of biological systems.

3.3.6 Temperature dependency of chemical shift

The chemical shift of the water protons depends on temperature more than pH. It has been proposed that **equation 3.1** can be used as an internal standard of aqueous samples to calculate the chemical shift dependence of temperature, and is valid at pH 5,5.[62]

$$\delta(H_2O) = 7{,}83 - \frac{T}{96{,}9} \qquad \text{Eq. 3.1}$$

Where δ is the chemical shift in ppm and T is the temperature in Kelvin. The samples investigated are operated under different temperature conditions during sample storing and preparation. However, during the NMR experiment, the temperature was 277K. Using **equation 3.1** it is possible to predict the change in ppm of the water signal in the samples. The samples in the study are expected to have pH 7,4, which is almost 2 pH values from the valid pH given by the equation. It is expected that the chemical shift changes with 0,04 ppm with pH. **Table 3.4** shows the expected chemical shifts of the water protons with temperatures at 298 and 277 K with pH 5,5 and 7,5.

*Table 3.4: The table presents the expected chemical shifts of water protons dependent on temperature and pH using **equation 3.1**. The temperatures represented are 298K and 277K with pH values 5,5 and 7,5.*

Temperature [K]	Chemical shift pH 5,5 [ppm]	Chemical shift pH 7,5 [ppm]
298	4,75	4,71
277	4,97	4,93
Change	0,22	0,22

3.3.7 1D ^{1}H NMR

The ^{1}H HR-MAS 1D data was acquired using the standard Bruker pulse program "zgcppr" at 277K. Based on previous qualitative ^{1}H HR-MAS studies of metabolites in different tissues the method is expected to provide reasonable results [63, 64]. The 1D experiments

contribute with the most detailed data featured in this thesis thus the method is fully optimized for the tissue samples extracted from farmed salmon. The parameters of the optimized sequence are presented in **appendix 4.A.6**, and MAS spinning rates at 4000 Hz are applied. The spinning rate reduces spectral broadening caused by bulk magnetic susceptibility and thus resolves the water spinning side band (SSB). In addition, the low spinning rates protect the tissue structures from MAS NMR centrifugal damage [65]. The 1D sequence applied is a standard Bruker "zg cppr" pulse sequence with pre-saturation and composite pulses for selection [66]. It provides a more complete saturation by compensating for inhomogeneities in the applied field using a series of 90° pulses as illustrated in **figure 3.8.** The sequence yields a narrow residual water signal thus beneficial for all other molecules in the sample and molecules with chemical shift near the water resonance.

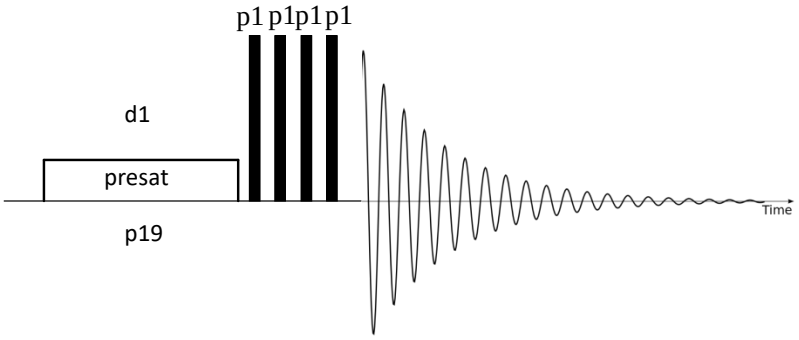

Figure 3.8: A schematic drawing of the composite "zg cppr" presaturation pulse sequence developed to suppress water signal in NMR. d1 is the delay time, p19 is the power level for presaturation and p1 is the composite pulse length. The illustration is taken from the Bruker Topspin 3.0 User Manual 15.04.2019.

3.3.8 Spin-Echo

The Spin-Echo sequence is a method to determine transversal magnetization (T_2) where inhomogeneity contribution is eliminated [67]. This thesis features the 1D ^{1}H experiment with T_2 filter using the Carr-Purcell-Meiboom-Gill version of the sequence with presaturation [68]. In the Carr-Purcell version the 90° excitation pulse is followed by a 180° pulse, as in the Hahn version the excitation pulse is followed by another 90° pulse. **Figure 3.9** shows the complete pulse sequence and how each step in the sequence affects the spin system.

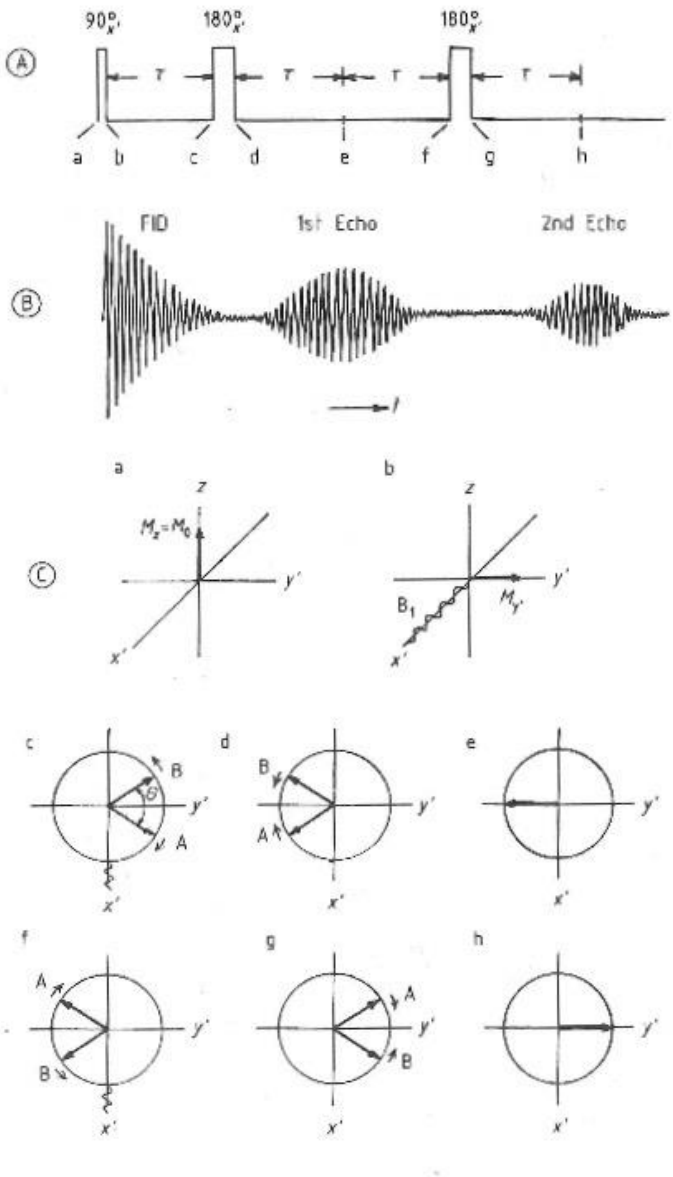

Figure 3.9. Schematic drawing of the Carr-Purcell spin-echo experiment based on that of Hahn. A) The complete spin-echo pulse sequence B) The FID and echo over time C) Vector diagram showing the stages of evolution of the spin system labeled a-h. The illustration is obtained from Horst Friebolin page 180 [36].

The spin system is initially in its equilibrium condition with the macroscopic magnetization at the z-axis as illustrated in **figure3.9.C** in diagram "a". A 90° excitation pulse turns the magnetization along the y-axis, as illustrated in "b". When the 90° pulse is turned off, the nuclei shown as A and B in diagram "c" are precessing after time τ with different frequencies due to inhomogeneities in the magnetic field which leads to the nuclei dephasing. This is the T_2' effect. In the illustration nucleus A precesses with a higher

frequency than nucleus B. The rotation directions of the nuclei compared to the coordinate system rotating with the Larmor frequency are noted in diagram "c". A 180° pulse follows which alternates the magnetization 180° into the y-plane as diagram "d" shows. After time τ the nuclei are refocused along the y-axis and an echo with full intensity occurs as illustrated in diagram "e". The echo with full intensity occurs due to reversal of the inhomogeneities the nuclei experience from $\mathbf{B_0}$. After another time τ the new dephasing is inverted by a 180° pulse, and again after an additional time τ a second echo occurs. The intensity of the second echo will be less than the first echo due to spin-spin relaxation. By repeating this sequence several times the reduction of the echo signals will provide a value of T_2, as the T_2' is reversed with each refocus.

The standard Bruker sequence for the spin-echo experiment with presaturation used is "cpmgpr1d" (**figure 3.10**). The sequence consists of a 90° excitation pulse followed by a loop of 180° pulses. Molecules with high molecular mass like hormones are rigid and therefore hold short T_2 values, but the side groups of the hormone chains are more mobile and thus have a longer T_2 value. By applying a T_2 filter, the echo time is adjusted to be longer. This adjustment makes it possible for better detection of the mobile parts in the sample which is under examination. The broad signals from the rigid parts disappears because of the short T_2 time leaving sharp signals from the mobile parts in the spectra. In addition to disregarding signals from the rigid parts of hormone molecules, the method excludes signals from other rigid molecules.

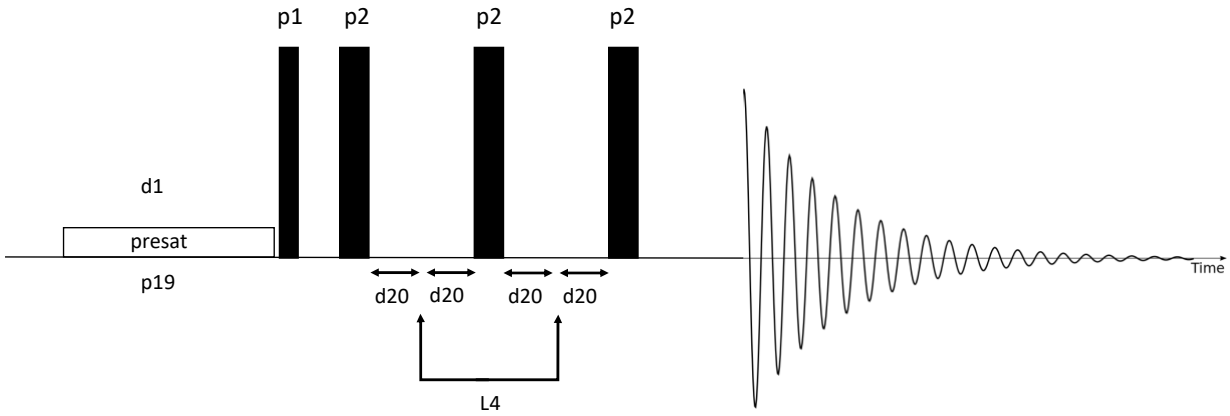

Figure 3.10: A schematic drawing of the "cpmgpr1d" pulse sequence. d1 is the delay time, p19 is the power level for presaturation, p1 is the 90° excited pulse length, p2 the 180° pulse length, d20 is the fixed echo time and L4 is a loop. The illustration is taken from the Bruker Topspin 3.0 User Manual 15.04.2019.

For application of the "cmpgpr1d" sequence different values of ns (number of transients), d20 and l4 are studied. d20 is the fixed echo time, and l4 is the denotation of a loop performed l4 times. ns is set to 512 scans during one experiment and to 261 scans in another experiment, while all other parameters are identical. The difference in number of transients does not reveal any evident changes in the resolution or quality of the spectrum information, but leads to a huge difference in experimental time. From 512 ns to 261 ns the number of scans are halved and the experimental time is reduced from 3,0 to 1,5 hours. Regulation of d20 and l4 values decide the echo time thus filter out molecules with short T_2 values, an overview of the experimental parameters applied are presented in **appendix 4.A.7**.

3.3.9 DQF- COSY

1D experiments performed on large complex molecules like hormones are challenging to interpret due to the amount of information and overlapping resonances in the obtained spectra. The data can be simplified by introducing a third dimension to the experiment, and a 2D experiment provides more supplementary information to solve assignment problems. The 2D experiment featured in this work is homonuclear H,H correlated.

2D homonuclear H,H correlated NMR experiments yield spectrum in which both frequency dimensions are ^{1}H chemical shifts, and the two axes are correlated with each other [36]. The method, known as Correlated spectroscopy (COSY) is based on the pulse sequence illustrated in **figure 3.11** where the first pulse angle is 90° and the second pulse angle after the time t_1 usually is 90°, 45° or 60°. The first pulse excites the magnetization in to transverse magnetization. During the evolution time t_1, which is varied in the COSY experiment, the magnetization components evolve chemical shift as a result of their different frequencies, and J-coupling. The following pulse mixes the magnetization components that belong to the same coupled system. The experiment provides information of ^{1}H resonances that are connected via scalar coupling (through bond) i.e. the cross peaks show which pairs of protons are J- coupled.

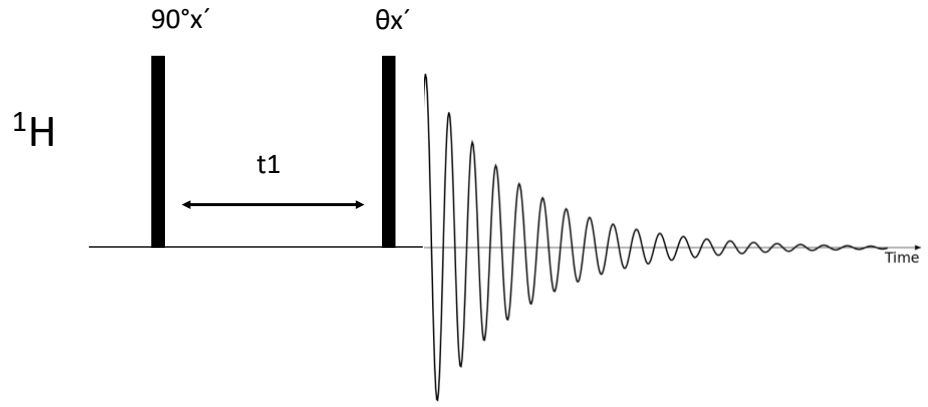

Figure 3.11: A schematic illustration of the pulse sequence of the 2D homonuclear H,H correlated NMR experiment COSY. The illustration is drawn from Horst Friebolin page 263 [36].

However, COSY has the disadvantage of intense diagonal peaks because they are in-phase with the cross peaks and cover a large area of the two dimensional NMR spectrum [69]. Consequently, cross peaks close to the diagonal can be difficult to detect. Double quantum filtered COSY (DQF-COSY) has the advantage of higher resolution and thus multiplet structure can be seen which allows proton-proton couplings to be measured. This is achieved by causing the diagonal peaks to be antiphase with the cross peaks. In addition there is a partial cancellation of the diagonal peaks in the DQF- COSY experiments[70] and strong signals from e.g. solvents and singlets are eliminated. Double quantum filters are

used to filter out single quantum magnetization and allow double magnetization. The pulse sequence consists of three pulses as illustrated in **figure 3.12**, and the parameters applied are presented in **appendix 4.A.8**.

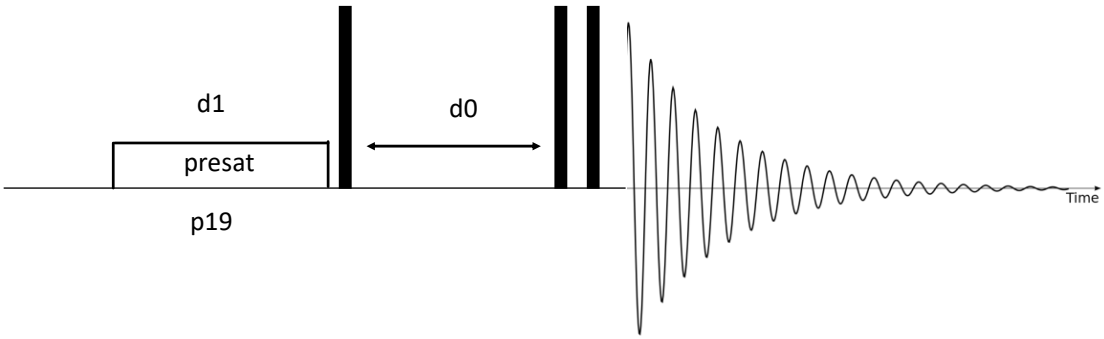

Figure 3.12: A schematic illustration of the "cosydfphpr" pulse sequence. The 2D homonuclear H,H correlated NMR experiment is phase sensitive with DQF and presaturation. D1 is delay time, p19 is the power level for presaturation and d0 is incremented delay. The illustration is taken from the Bruker Topspin 3.0 User Manual 15.04.2019.

The COSY spectrum of the twenty common amino acids are well established. By analysing the data of the 1D spectrum and compare it to the information retrieved from the 2D COSY experiment there is a chance for qualitative analysis of hormones in salmon pituitary.

4. Results

All the ^{1}H NMR spectra of the pituitary samples have the same general features (**appendix 3**). An example of a spectrum of salmon pituitary is shown in **figure 4.1.** At 4,7 ppm the suppressed water signal is observed.[57] There are several different components contributing to the NMR-signals, and some of the signals in the experimental spectra are overlapping.

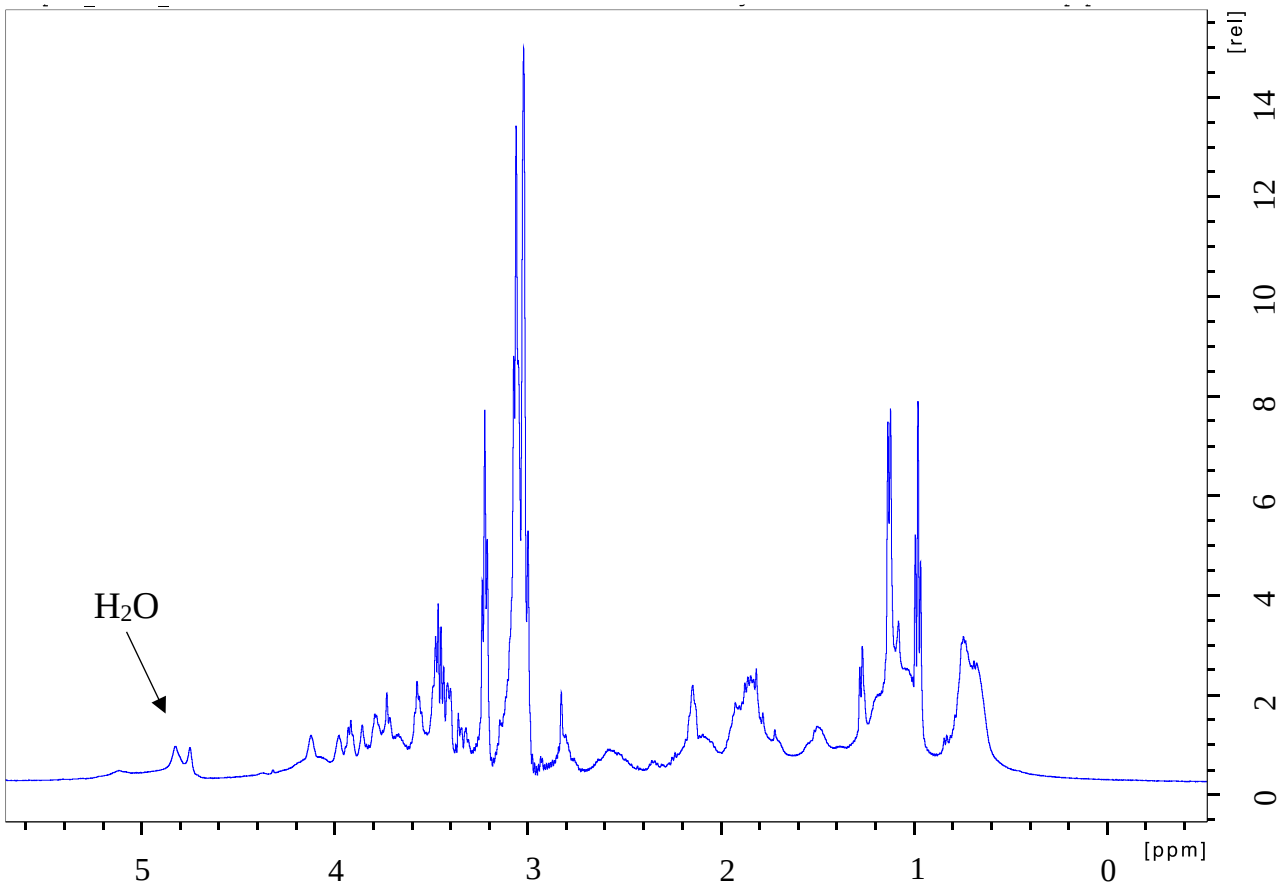

Figure 4.1: ^{1}H NMR spectrum of a bred salmon pituitary (sample 7) at 277 K. The horizontal axis is set to parts per million (ppm) and the vertical axis represents the relative intensity (rel).

4.1 pH and temperature dependency of chemical shift

4.1.1 pH

It is necessary to monitor the temperature and pH as the chemical shifts of the signals depend on these factors. The spectra shown in **figure 4.2.A** display the water signal in the buffer and the pituitary sample (sample 12) acquired at identical conditions (277 K). It shows that the chemical shift of water is identical in both the buffer solution and the sample. **Figure 4.2.B** shows the same signals at 298 K. The buffer and sample signals do not occur at the same chemical shifts, but at at 4,60 and 4,61 ppm respectively. The buffer solution have pH 7,4. **Table 4.1** shows the chemical shifts of water in the buffer of all the samples at 277 K. The difference between the chemical shifts of water within an experimental set is ≤0,01 ppm, however, sample 3 shows a difference of 0,06 ppm.

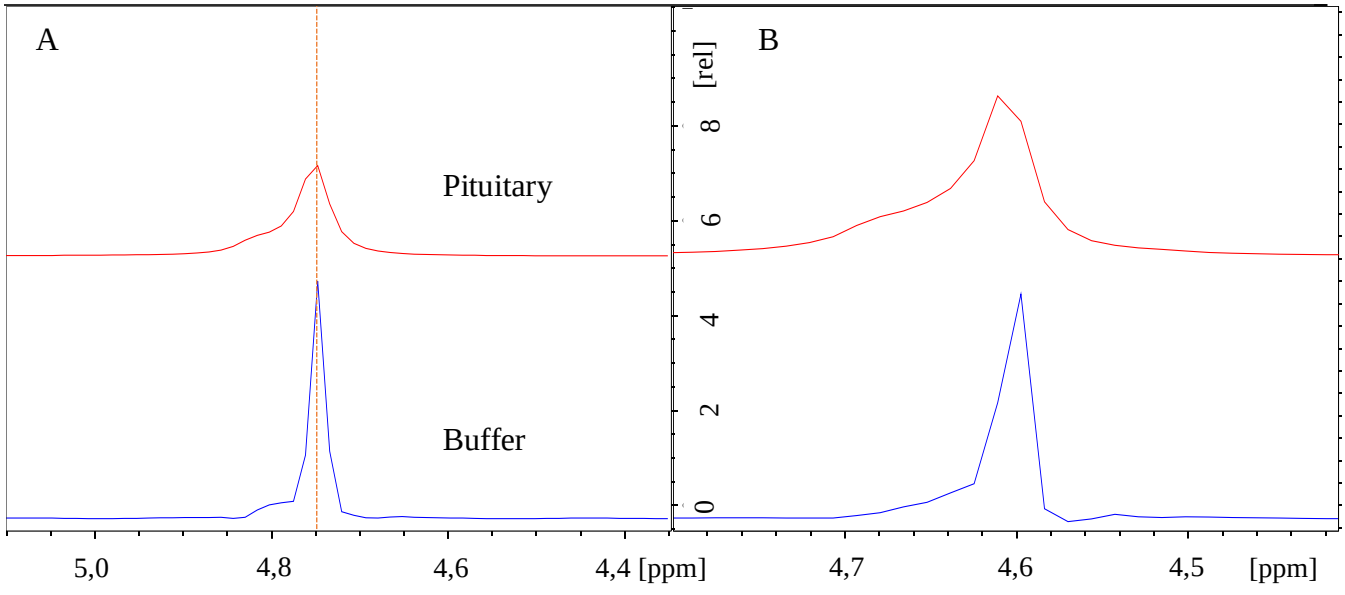

Figure 4.2: A) The ^{1}H NMR spectrum of the water signal in buffer solution (blue) and a pituitary sample (sample 12)(red) at 277 K. The water signal is at 4,75 ppm in both spectra. B) The ^{1}H NMR spectrum of the water signal in buffer solution (blue) and a pituitary sample (sample 12)(red) at 298 K. The water signal in the buffer and the sample occurs almost at the same chemical shift; at 4,60 and 4,61 ppm respectively.

Table 4.1: The overview of the chemical shifts of water in the buffer solution and the samples at 277 K.

Sample	Water, Sample [ppm]	Water, Buffer [ppm]
2	4,72	4,73
3	4,77	4,71
4	4,72	4,72
5	4,78	4,77
6	4,75	4,75
7	4,75	4,75
8	4,72	4,72
10	4,72	4,72
11	4,69	4,68
12	4,75	4,75
Difference	0,09	0,09

4.1.2 Temperature

The main experiments in this thesis are all performed at 277 K. However, to monitor the temperature dependence of the chemical shift, proton experiments are performed at both 277 and 298 K. This was only completed for one sample. The expected chemical shifts of the water signals are calculated from **equation 3.1**. Considering the experimental pH, the water signal at 298 and 277 K should appear at 4,71 and 4,93 ppm respectively. **Figure 4.2** shows the NMR spectra of the water signal in a pituitary sample (sample 12) at different temperatures. The chemical shifts are 4,61 and 4,75 ppm, at 298 and 277 K respectively. There is a temperature dependent change in the chemical shift of 0,14 ppm. **Figure 4.3** shows the ^{1}H NMR spectrum of a pituitary sample (sample 12) at 277 and 298 K with presaturation. The ^{1}H NMR spectra reveal that the chemical shift of the water protons change with temperature, but the other signals do not change.

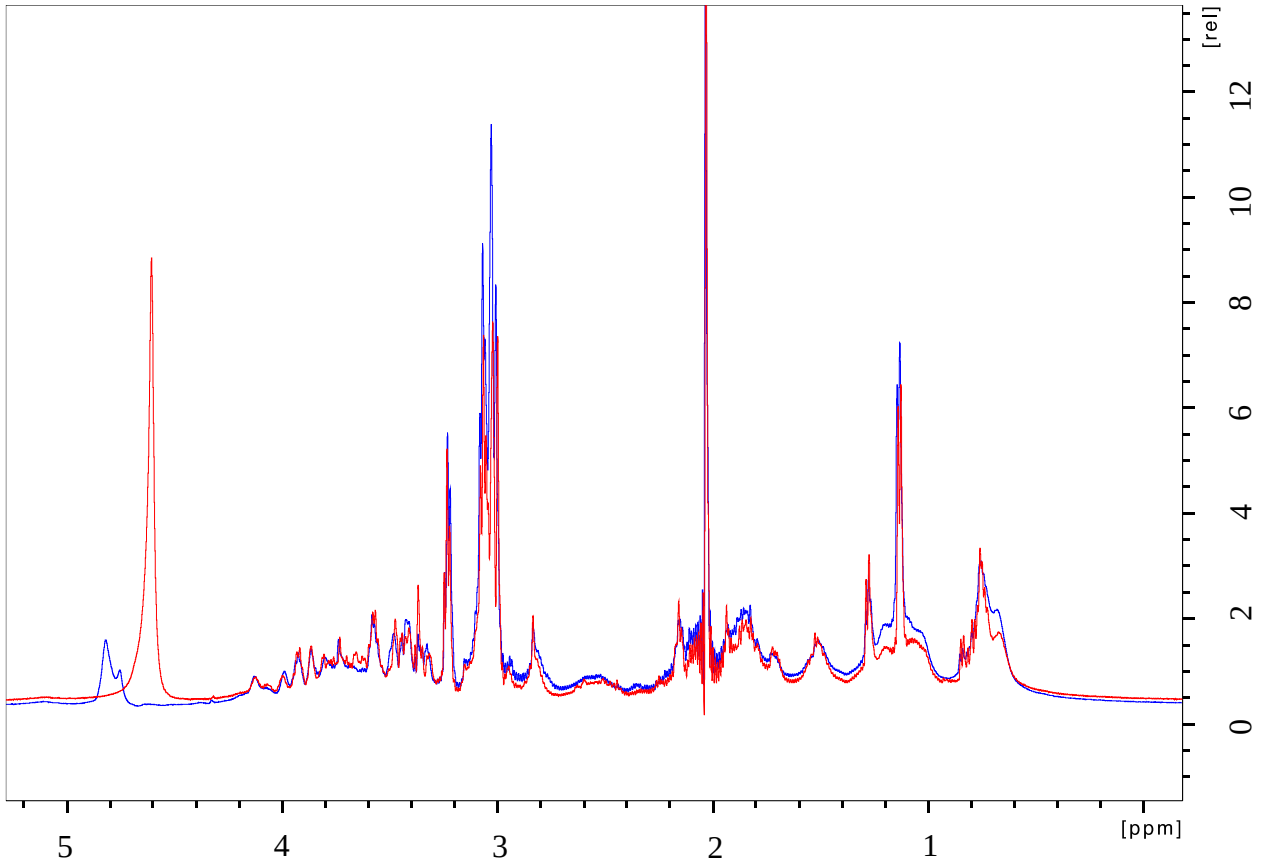

Figure 4.3: The *^{1}H NMR spectrum of a pituitary sample (sample 12) with water suppression at 277K (blue) and 298K (red). The proton signals from water have different chemical shifts depending on the temperature, but the other signals do not change.*

4.2 T_2 filter

The salmon pituitary contains other compounds than the studied hormones [42]. To remove signals from large immobile molecules and to improve the spectral resolution, a T_2 filter is applied. The 1D proton spectrum of a pituitary (sample 7) with and without applied T_2 filter is shown in **figure 4.4**. The chemical shift area from 3,0 to 4,2 ppm is shown in **figure 4.5**. The signals are noticeably decreased in intensity and some signals have disappeared. The signal around 1,2 ppm in **figure 4.4** shows significant reduction of the broad signal when the T_2 filter is applied, and the broad signal around 2,5 ppm seem to have totally disappeared. Signals from rigid molecules like membrane lipids, membrane proteins and receptors are filtered out of the spectra, leaving the sharper peaks that originate from the mobile intracellular material.

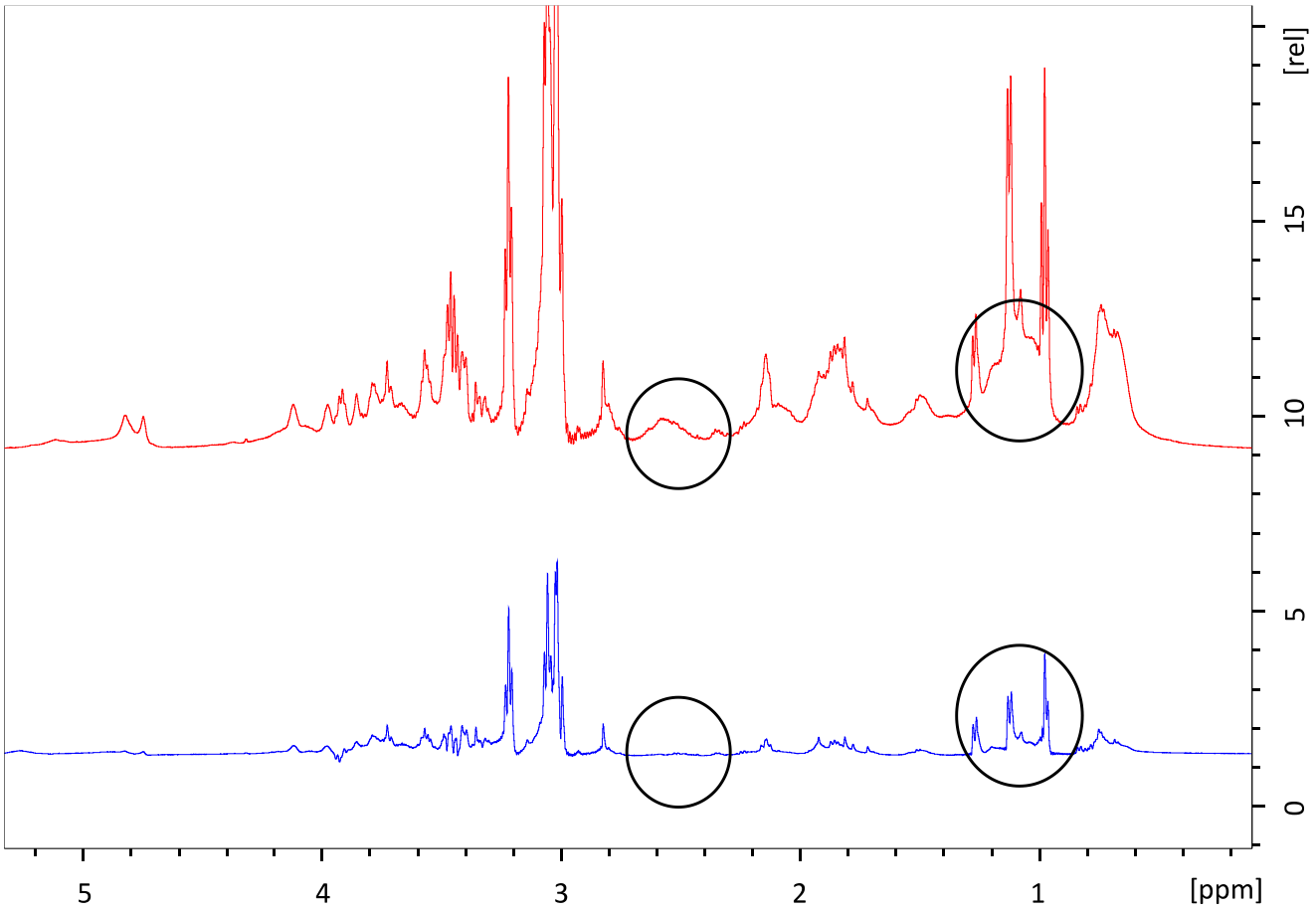

Figure 4.4: A ^{1}H *NMR spectrum of a pituitary sample (sample 7) with (blue) and without (red) applied* T_2 *filter. The disappeared signal between 2-3 ppm and the reduced signals around 1 ppm are marked with circles.*

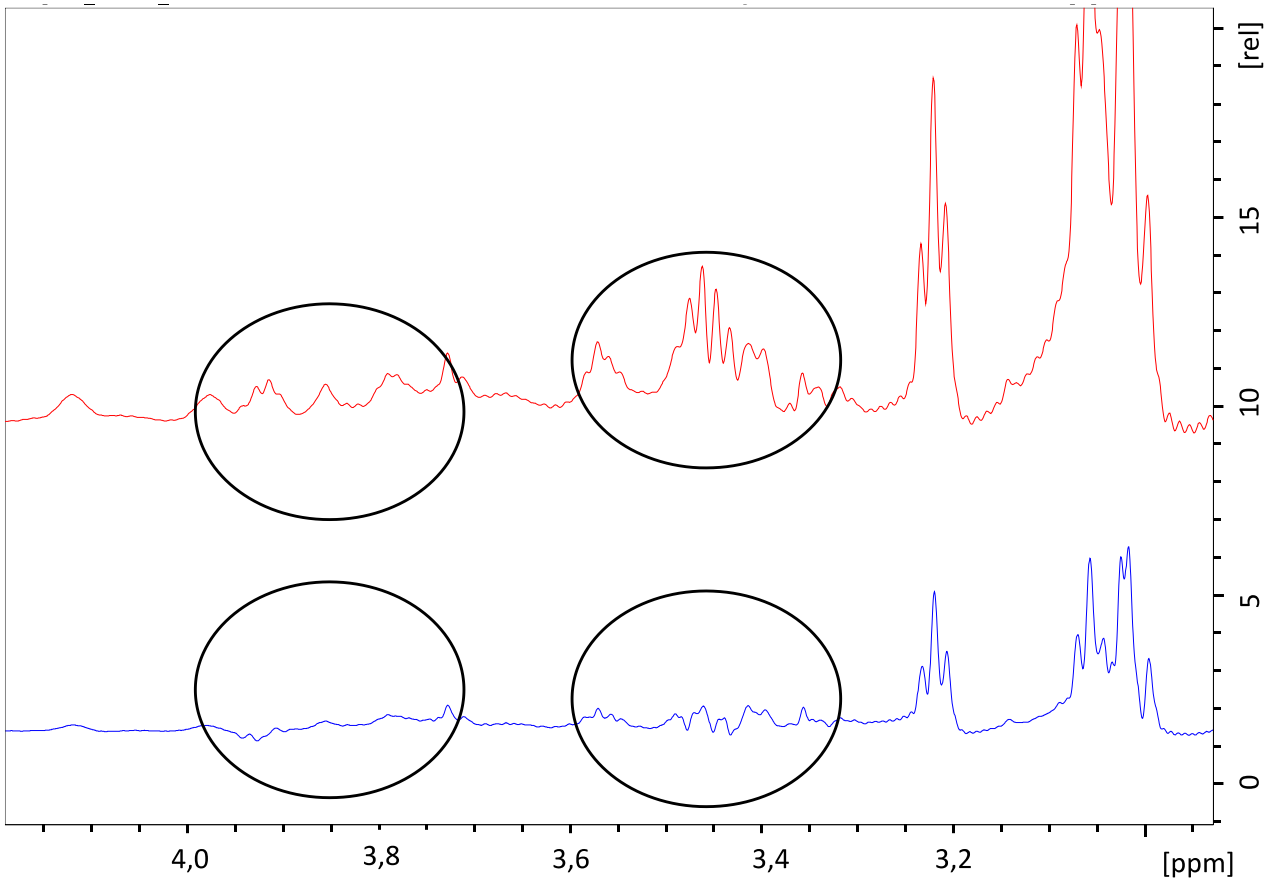

Figure 4.5: The ^{1}H NMR spectrum showing the chemical shift area of 3,0 to 4,2 ppm (sample 7). The lower spectrum is with, and the upper spectrum is without applied T_2 filter. In the lower spectra, the reduced signals are marked with circles.

4.3 Quantification of the water signal

The spectra of double distilled water samples acquired for quantification purposes show water peaks with undesirable shapes (**figure 4.6**) This might indicate that the samples are contaminated, and that the sample preparation was unsuccessful. Thus, these spectra can not be used for volume quantification. However, the volume percentage of water in each sample can still be found within a spectra. By integrating the water peak of the spectrum with no presaturation, and then integrating over all the peaks in the spectrum, the proton fraction is known. When the sample weight is known, this can further be used to calculate the amount of water in the sample. **Table 4.2** shows the sample weight and the percentage of the water signal.

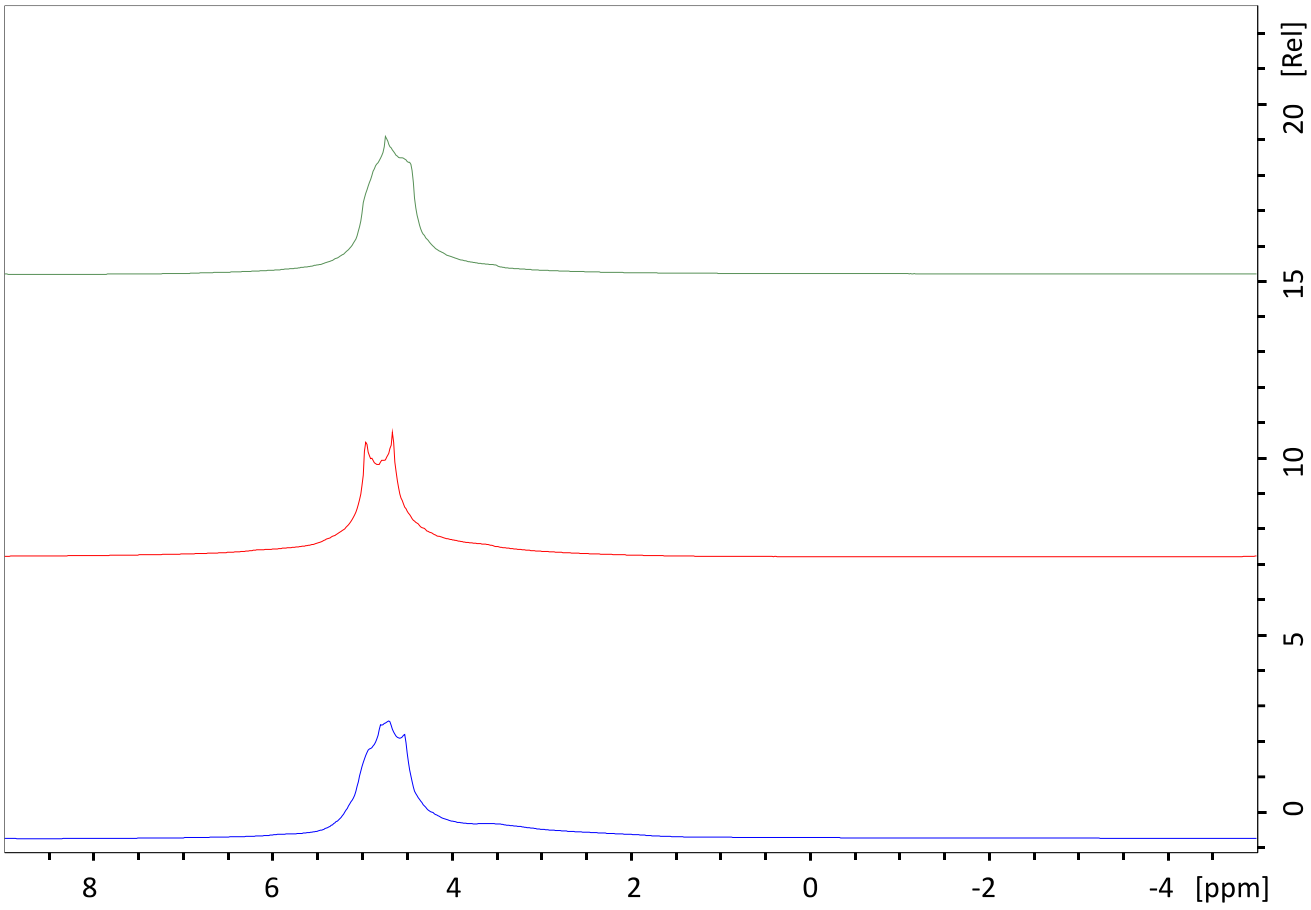

Figure 4.6: 1D ^{1}H-NMR spectra of the three double distilled water samples. The signals are broad with an undesirable form.

Table 4.2: The weight of the pituitary samples and the amount of water in the samples in percent and gram.

Sample	Weight [g]	Water [%]	Water [g]
2	0,07830	94,4	0,07391
3	0,07381	90,9	0,06710
4	0,07415	90,8	0,06733
5	0,06132	93,2	0,05715
6	0,05926	93,4	0,05535
7	0,06536	92,8	0,06065
8	0,06064	93,7	0,05682
10	0,04296	92,8	0,03986
11	0,02487	93,5	0,02325
12	0,06112	92,6	0,05660

4.4 Signal interpretation

The spectra show a multitude of signals (**figure 4.1)**, and have the same general features. However, there are signals that varies from sample to sample. **Table 4.3** shows an overview of the signals with additional sample information. Samples 1-6 were extracted the 17th of December 2017, and samples 7-12 were extracted the 5th of December 2018, noted batch 1 and 2.

Table 4.3: An overview of the pituitary samples with information about the sexes of the fish, the weight of the samples and ^{1}H NMR signal differences.

Sample	Batch	Sex	Weight [g]	Singlet at 2,0 ppm	Triplet at 0,9 ppm
2	1	M	0,07830		X
3	1	M	0,07381	X	
4	1	F	0,07415	X	
5	1	F	0,06132	X	
6	1	F	0,05926	X	
7	2	F	0,06536		X
8	2	F	0,06064		
10	2	M	0,04296		X
11	2	M	0,02487	X	
12	2	M	0,06112	X	

Depending on the sample there are two major differences observed in the spectra, a triplet at 0,9 ppm and a singlet at 2,0 ppm. The samples 1, 2, 7 and 10 show the presence of a triplet around 0,9 ppm, and samples 3, 4, 5, 6, 11 and 12 show a signal at 2,0 ppm. Sample 8 does not yield either signals, and sample 9 yields improper signals and is not further discussed. **Figure 4.7** shows the singlet observed in the spectrum of sample 4, the triplet of sample 7 and the spectrum of sample 8 with no uncommon signals relative to the other samples.

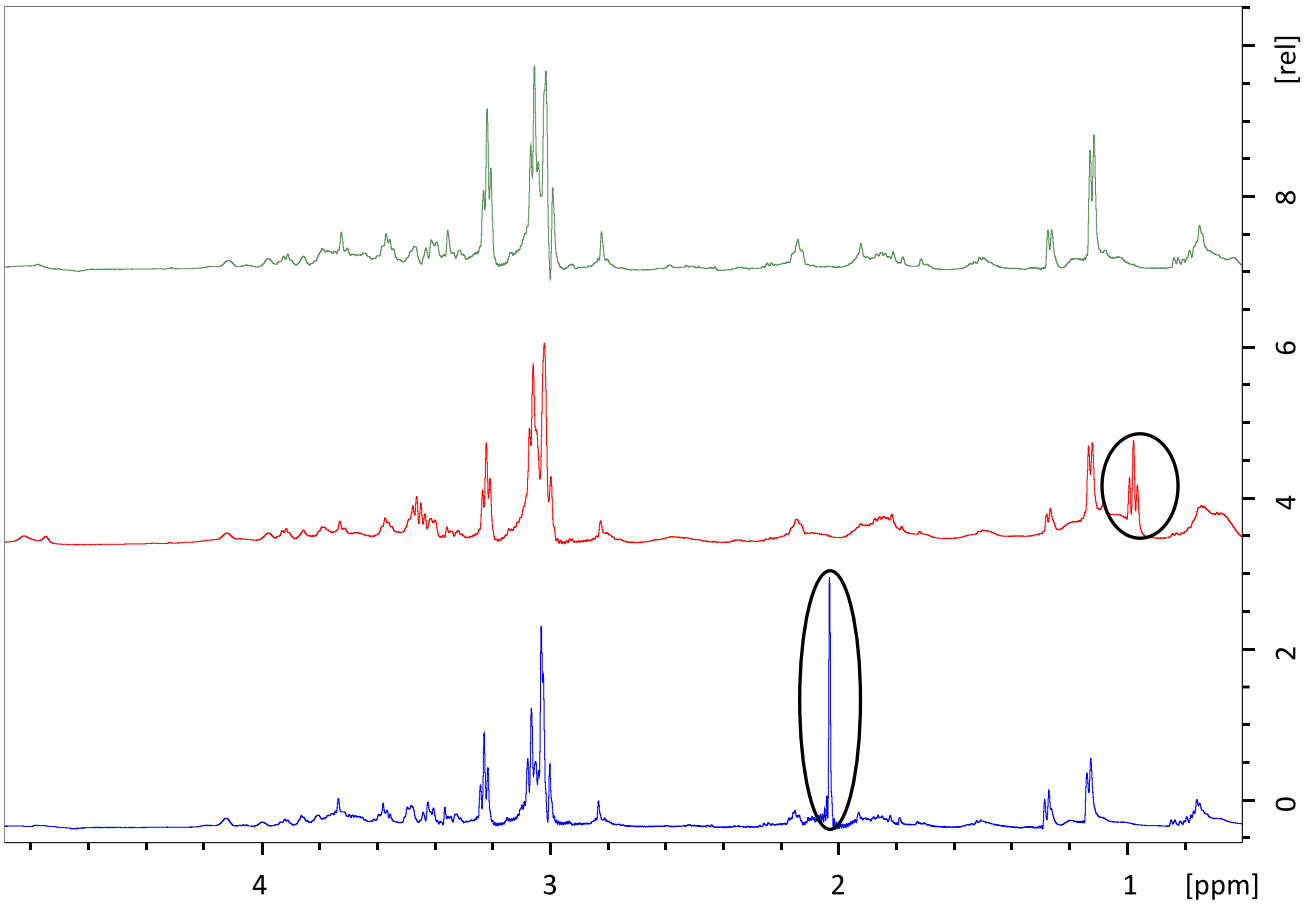

Figure 4.7: The ^{1}H NMR spectrum of the pituitary samples 4 (blue), 7 (red) and 8 (green). Sample 4 shows a singlet at 2,0 ppm and sample 7 shows a triplet at 0,9 ppm (marked with circles).

4.4.1 The Methyl signal at 0,9 ppm

The triplet signal at 0,9 ppm has the chemical shift characteristic of a methyl signal. **Figure 4.8** depicts the COSY spectrum of sample 7 and this spectrum is used to identify protons that are coupled to the methyl signal. **Figure 4.9** shows an overview of the four proton environments coupled to the triplet in sample 7. **Table 4.4** shows an overview of the samples containing the triplet signal, and their chemical shifts.

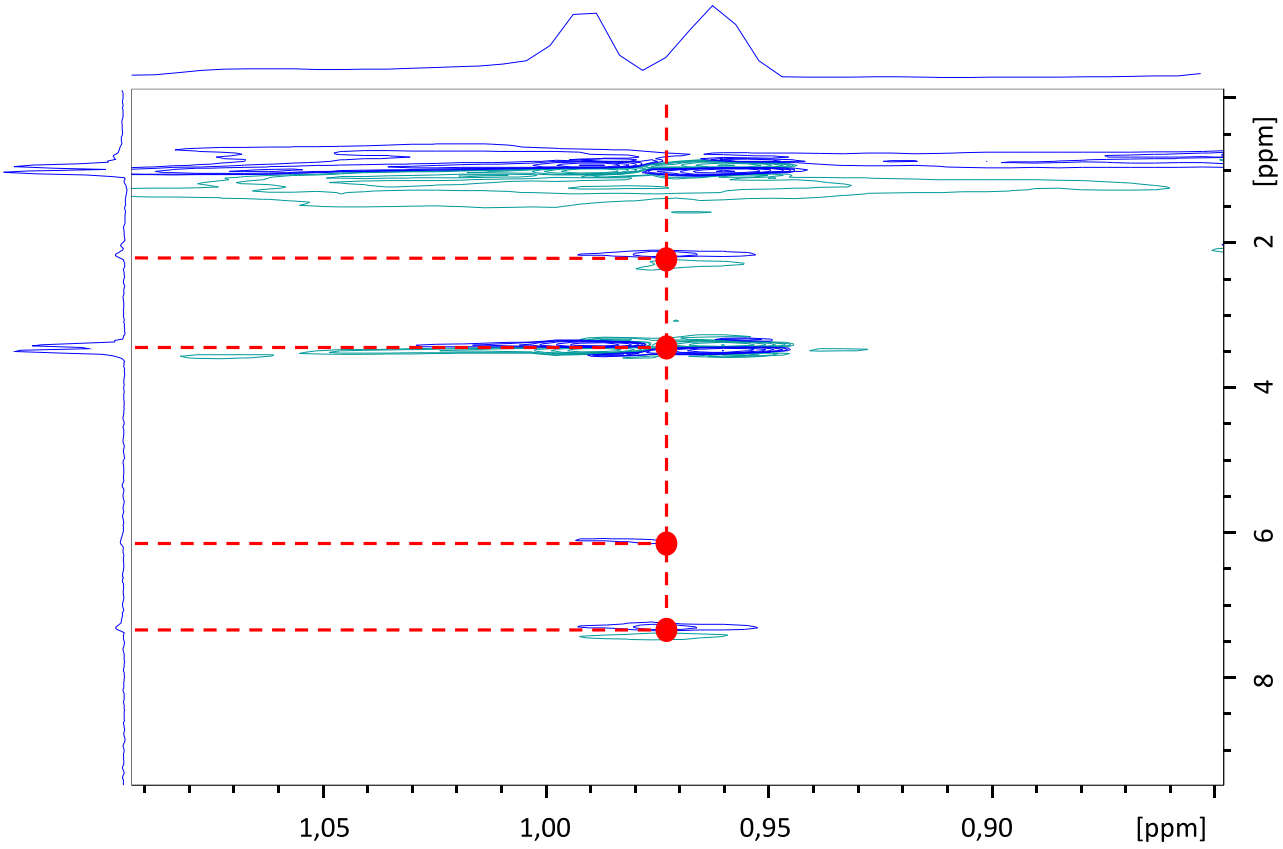

Figure 4.8: The H,H-COSY spectrum of sample 7, showing the couplings from the methyl triplet to other proton signals in the spectra.

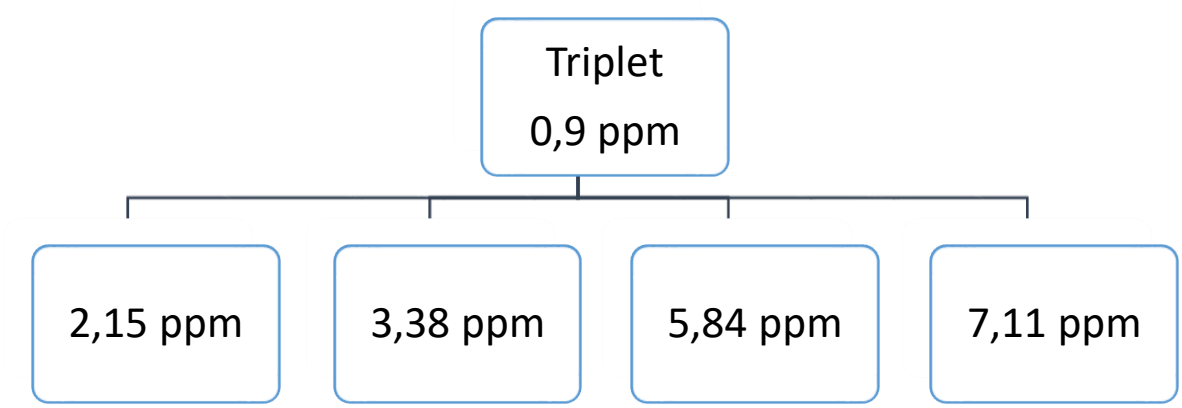

Figure 4.9: The chemical shifts of the cross peaks to the triplet at 0,9 ppm in sample 7.

Table 4.4: An overview of the samples containing a triplet signal, and the chemical shifts of the triplet and the signals that are making cross peaks with it.

Sample	Triplet at 0,9 [ppm]	Coupling 1 [ppm]	Coupling 2 [ppm]	Coupling 3 [ppm]	Coupling 4 [ppm]
2	0,98	2,15	3,49	6,12	7,29
7	0,99	2,15	3,38	5,84	7,11
10	0,99	2,24	3,49	5,91	7,17

The triplet is making cross peaks to four signals, that make further cross peaks with other resonances. **Figure 4.10** depicts a COSY spectrum of the correlating signals of the triplet at 0,9 ppm (sample 7). An overview of further couplings are shown in **figure 4.11**. The COSY spectrum shows that the signal intensities are stronger above the diagonal than under. This occurs in all the COSY spectra. This might explain why the cross peak between 3,43 and 2,17 ppm under the diagonal is missing (**figure 4.10**). The cross peaks at 5,84 and 7,11 ppm show no further cross peaks.

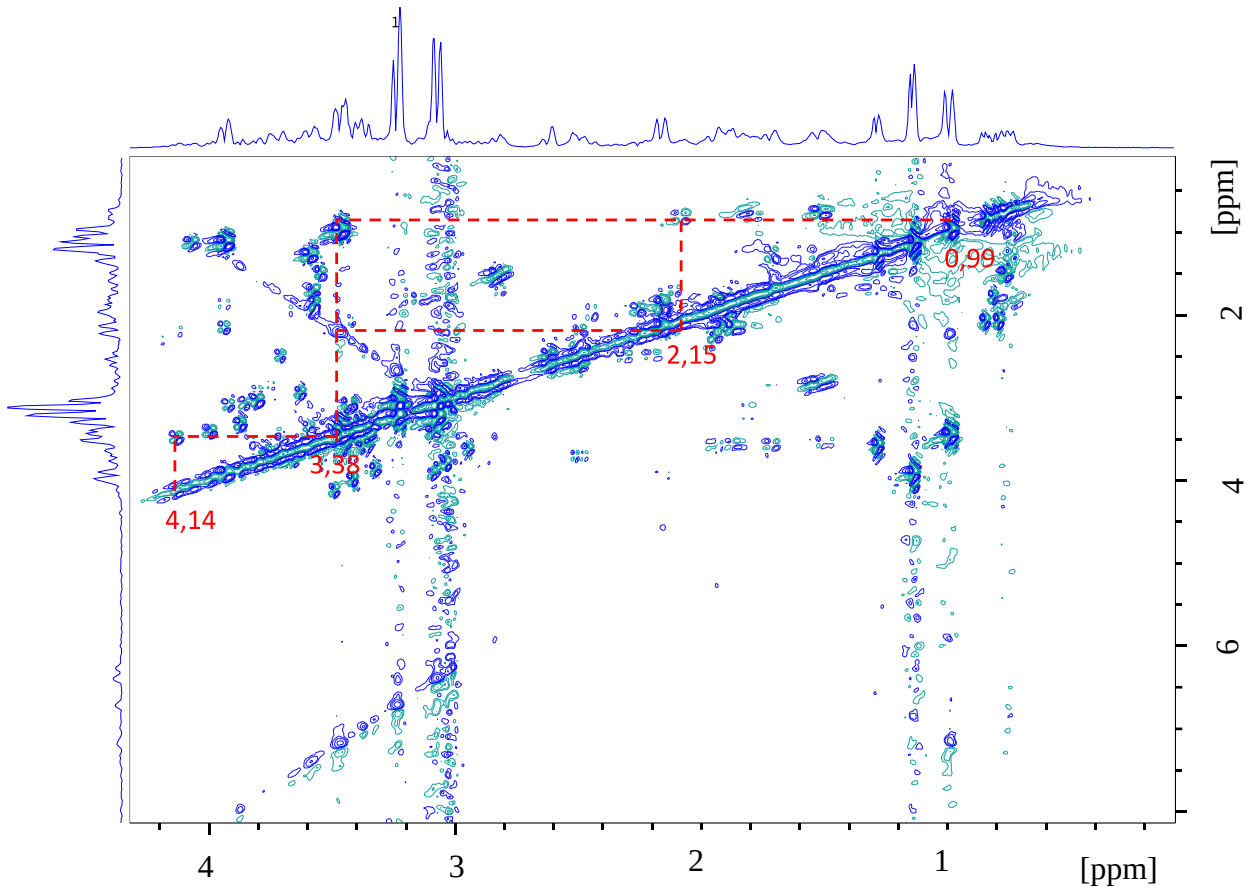

Figure 4.10: The H,H-COSY spectrum of sample 7. The coupled signals are marked with dotted lines, and the chemical shifts are noted at the diagonal.

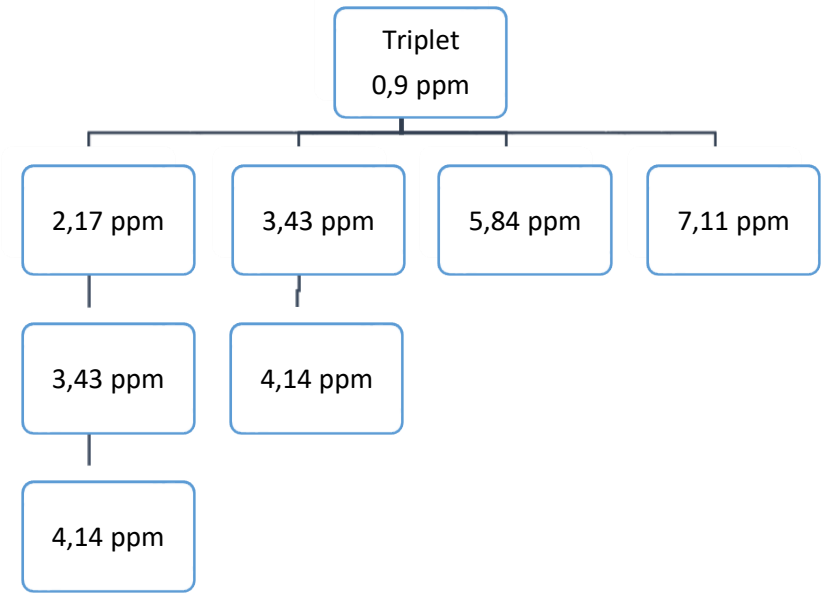

Figure 4.11: An overview of signals that makes cross peaks with the triplet at 0,9 ppm. The resonances at 5,84 and 7,11 ppm have no further couplings.

4.4.2 The Singlet at 2,0 ppm

The spectra of samples 3, 4, 5, 6, 11 and 12 show a singlet with high intensity at 2,0 ppm (**figure 4.12**). The chemical shifts of the signal in the samples are listed in **table 4.5**. To determine the signal´s origin, COSY spectra are acquired. **Figure 4.13** depicts the COSY spectrum of sample 4. The singlet at 2,0 ppm in the COSY spectrum shows reduced intensity compared to the 1D spectra. This is not unexpected since COSY yields J-couplings and since the signal is a singlet, the protons are equivalent and not coupled to other signals. There is no cross peaks at 2,0 ppm as expected due to the DQF-COSY which eliminates signals with no couplings.

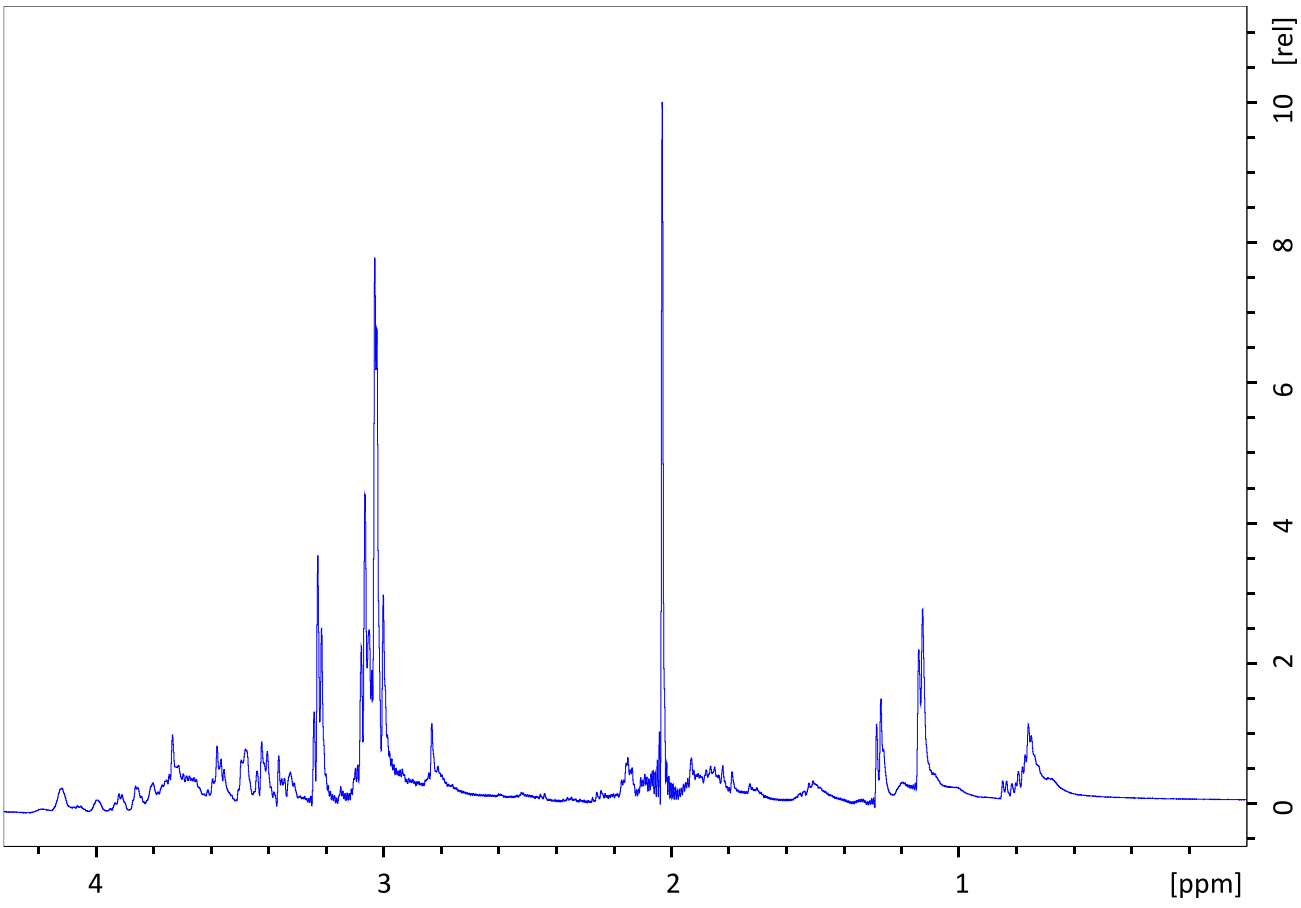

Figure 4.12:The ^{1}H NMR spectrum of sample 4. The spectrum shows a singlet at 2,0 ppm. The horizontal axis is in ppm and the vertical axis is the relative intensity (rel).

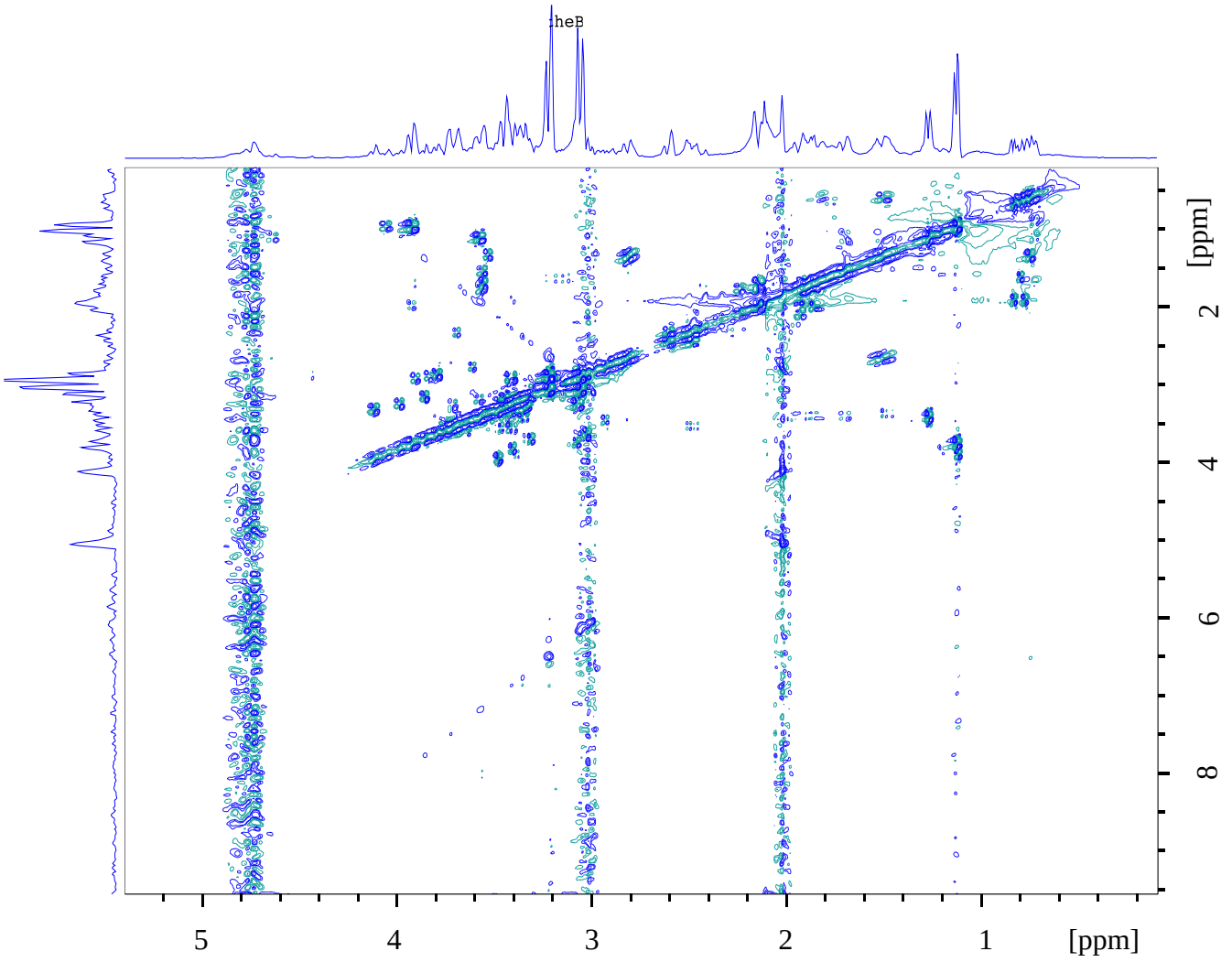

Figure 4.13: The H,H-COSY spectrum of sample 4. No cross peaks are shown at 2,0 ppm.

Table 4.5: The chemical shifts of the singlet in the different samples.

Sample	Singlet [ppm]
3	2,09
4	2,03
5	2,07
6	2,02
11	2,01
12	2,03

4.4.3 The doublets at 1,13 and 1,27 ppm

There are two doublets, at 1,13 and 1,27 ppm. **Figure 4.14** depicts the T_2 filtered 1D spectrum of sample 7 with the two doublets. All spectra show these two doublets, however the chemical shifts are not identical. The chemical shifts are listed in **table 4.6** where the doublets are denoted I and II depending on increasing chemical shift value. The change in the chemical shifts of all samples are 0,07 and 0,06 ppm of doublet I and II respectively. The COSY spectrum of sample 7 is depicted in **figure 4.15**. The doublet at 1,13 ppm is coupled to the two signals at 3,93 and 4,10 ppm. Further, the signal at 3,93 ppm is coupled to a resonance at 2,15 ppm. The second doublet at 1,27 ppm is coupled to a signal at 1,70 ppm and at 3,58. Further, these signals are coupled with each other as marked in red dotted lines in **figure 4.15**. **Figure 4.16** shows an overview of the coupled signals. The chemical shifts of the coupling signals of all the samples are shown in **table 4.6**.

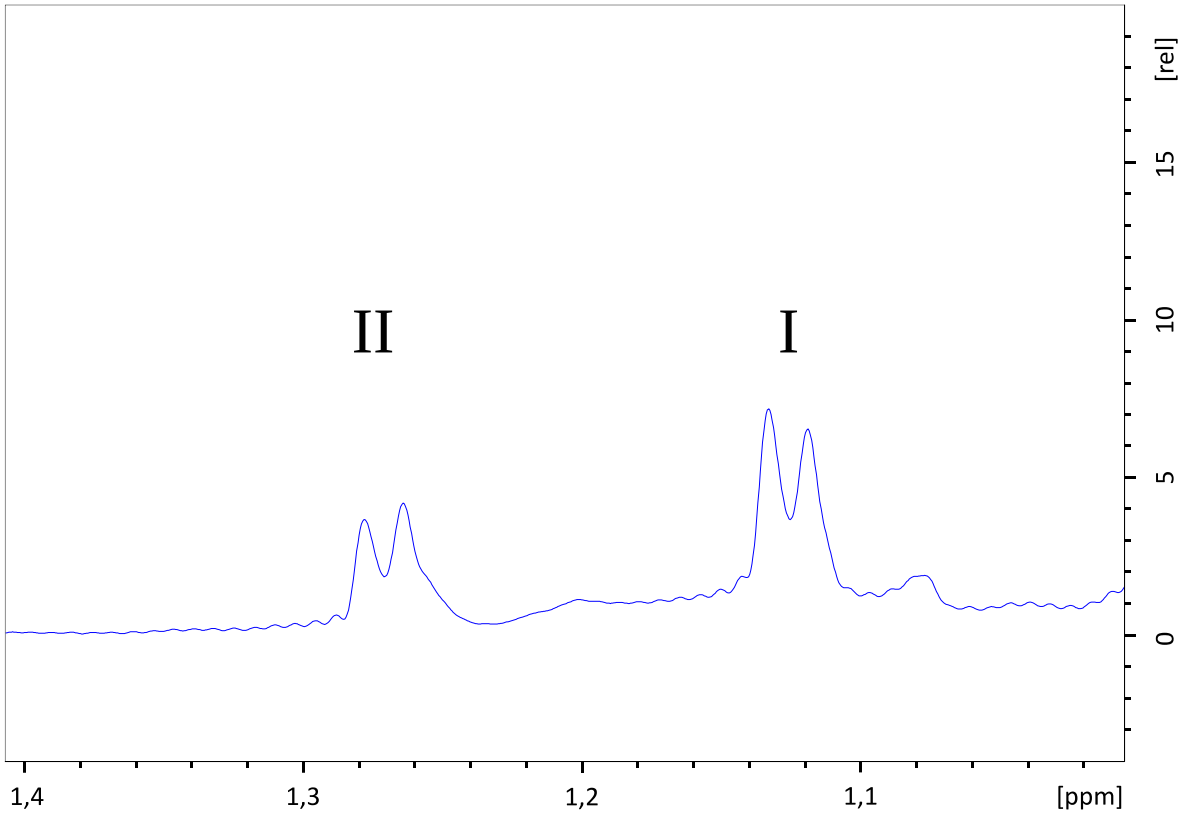

Figure 4.14: The T_2 filtered 1D spectrum of sample 7 showing the two doublets at 1,13 and 1,27 ppm.

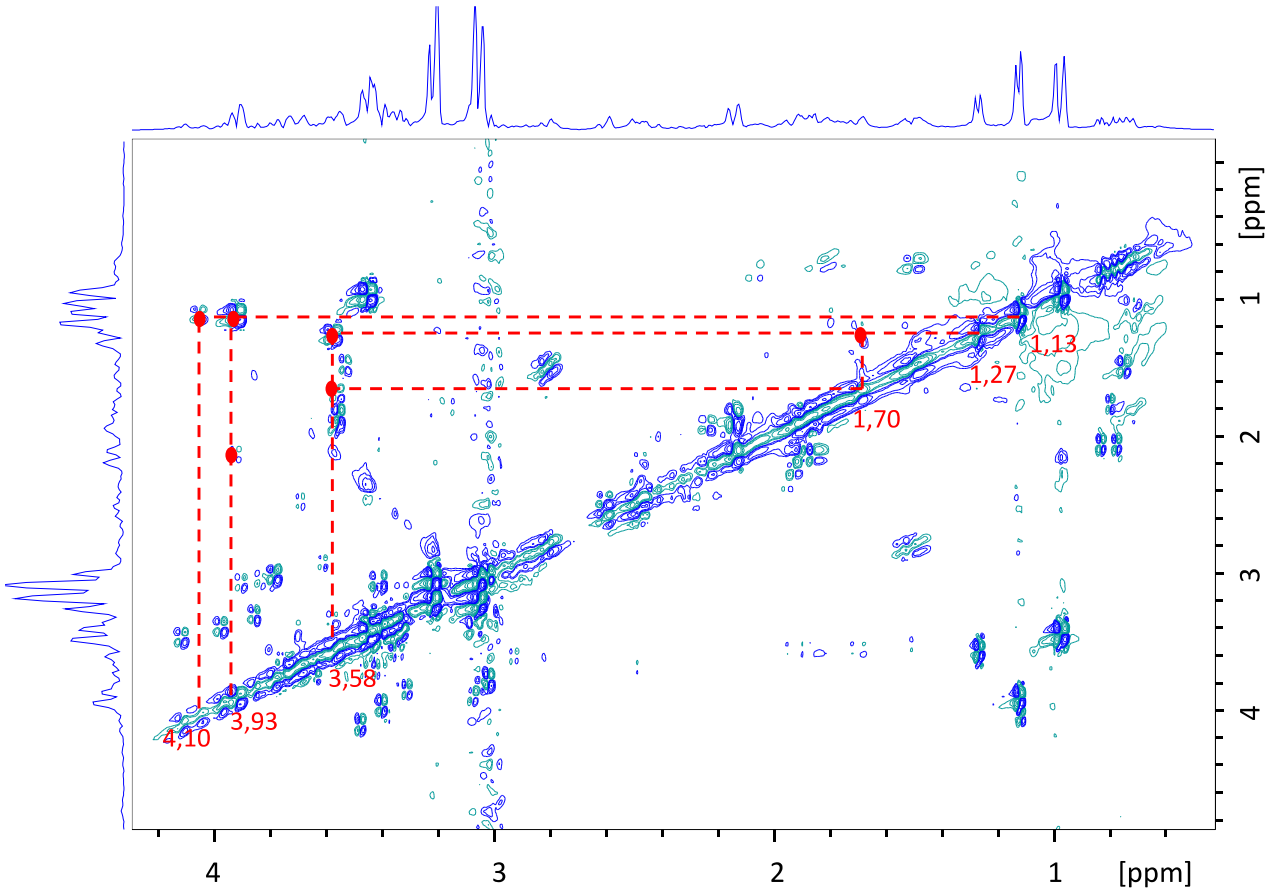

Figure 4.15: The H,H-COSY NMR spectrum of sample 7 showing the cross peaks coupled to the two doublets.

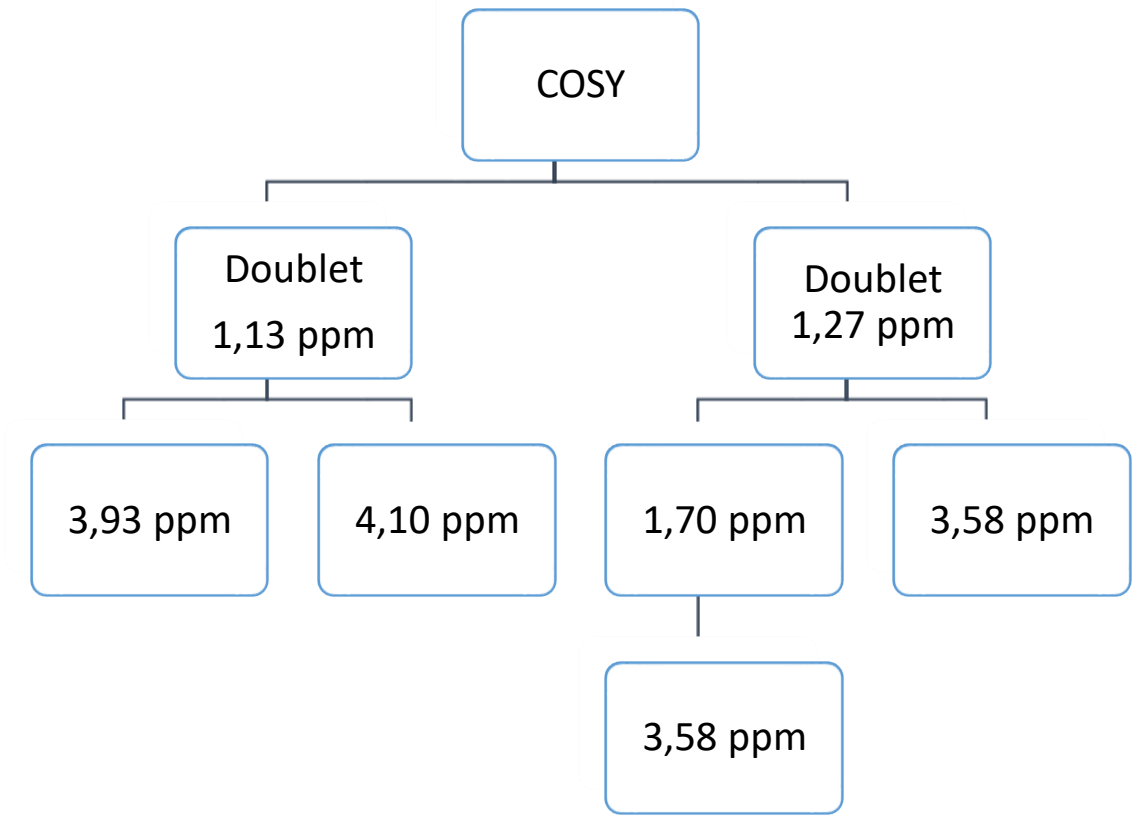

Figure 4.16: An overview of the cross peaks to the two doublets and further cross peaks in the COSY spectrum of sample 7.

Table 4.6: The table shows the chemical shifts of the two doublets and their cross peaks in all samples. The resonances in yellow corresponds to the highest and lowest occurring chemical shift value of each signal.

Sample	Doublet I [ppm]	Cross peak 1	Additional cross peak	Cross peak 2	Doublet II [ppm]	Cross peak 1	Cross peak 2
2	**1,14**	3,95	2,05	4,10	**1,29**	1,71	3,60
3	**1,18**	3,98	2,20	4,11	**1,32**	1,75	3,63
4	**1,13**	3,93	2,14	4,07	**1,28**	1,70	3,58
5	**1,17**	3,97	2,20	4,11	**1,32**	1,73	3,63
6	**1,13**	3,93	2,00	4,06	**1,27**	1,70	3,58
7	**1,13**	3,93	2,15	4,06	**1,27**	1,70	3,58
8	**1,14**	3,94	2,17	4,08	**1,29**	1,71	3,59
10	**1,14**	3,94	2,17	4,07	**1,28**	1,71	3,59
11	**1,11**	3,91	2,13	4,05	**1,26**	1,69	3,56
12	**1,14**	3,95	2,15	4,07	**1,28**	1,71	3,58
Change [ppm]	**0,07**	0,07	0,20	0,06	**0,06**	0,06	0,07

4.4.4 Additional Resonances

There are signals with chemical shifts lower than 3,0 ppm in all the spectra. **Figure 4.17** depicts all these signals from samples 4, 7 and 8, and they clearly feature resembling signals. Three of these signals at 0,79, 1,52 and 2,82 ppm are coupled in the COSY spectrum as shown in **figure 4.18**. The signal at 1,52 ppm is also coupled to the resonance at 3,54 ppm. The figure also depicts two other signals with chemical shifts at 1,88 and 2,16 ppm. These are correlated to each other in addition to three other signals at 3,46, 3,55 and 4,13 ppm. The resonance at 2,16 ppm is also coupled to a signal at 3,94 ppm. Finally the two signals at 2,61 and 3,71 ppm are coupled, but the signal at 2.61 ppm is indistinct in the 1D NMR spectra. **Figure 4.19** shows an overview of the coupled signals.

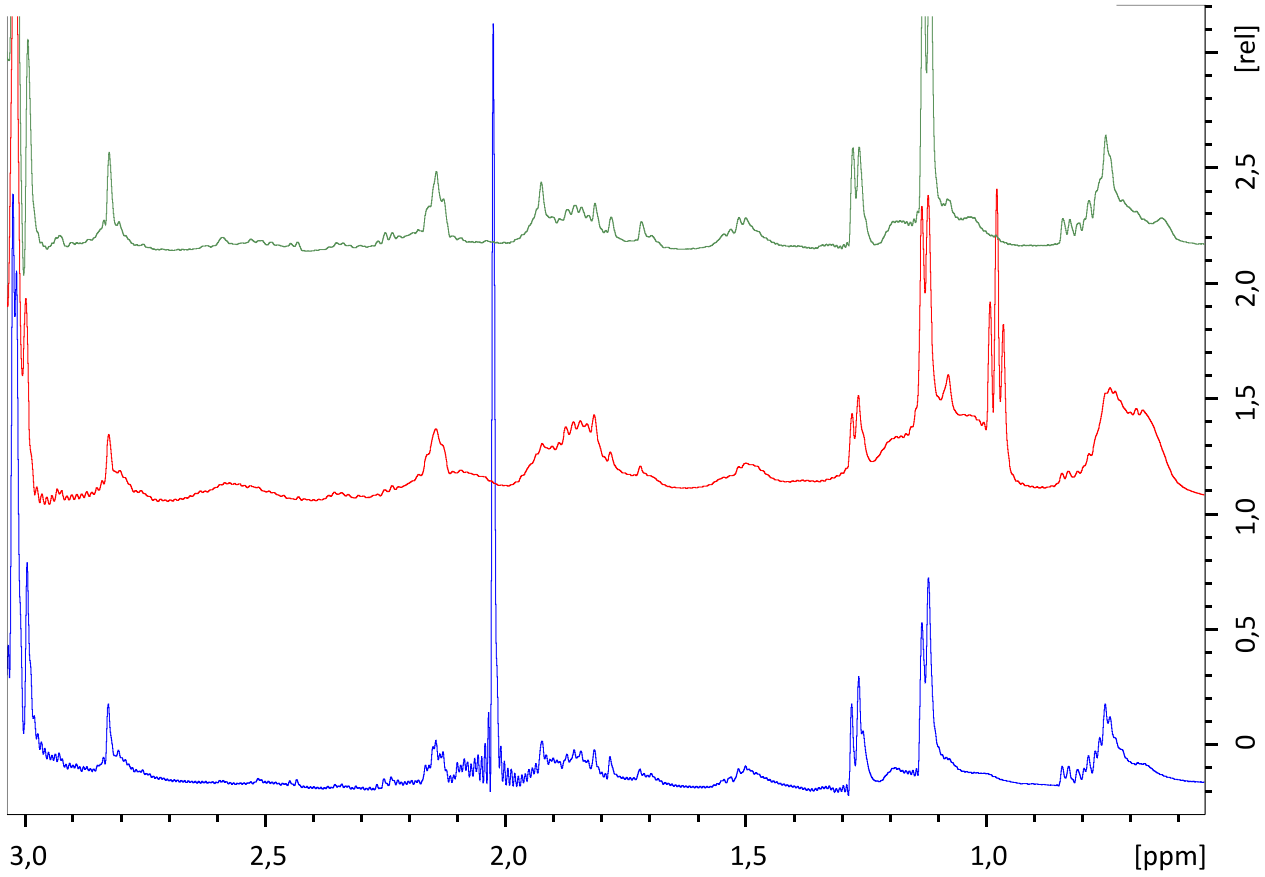

Figure 4.17: The T_2 filtered 1D spectrum of sample 4 (blue), 7 (red) and 8 (green) between 0 and 3,0 ppm.

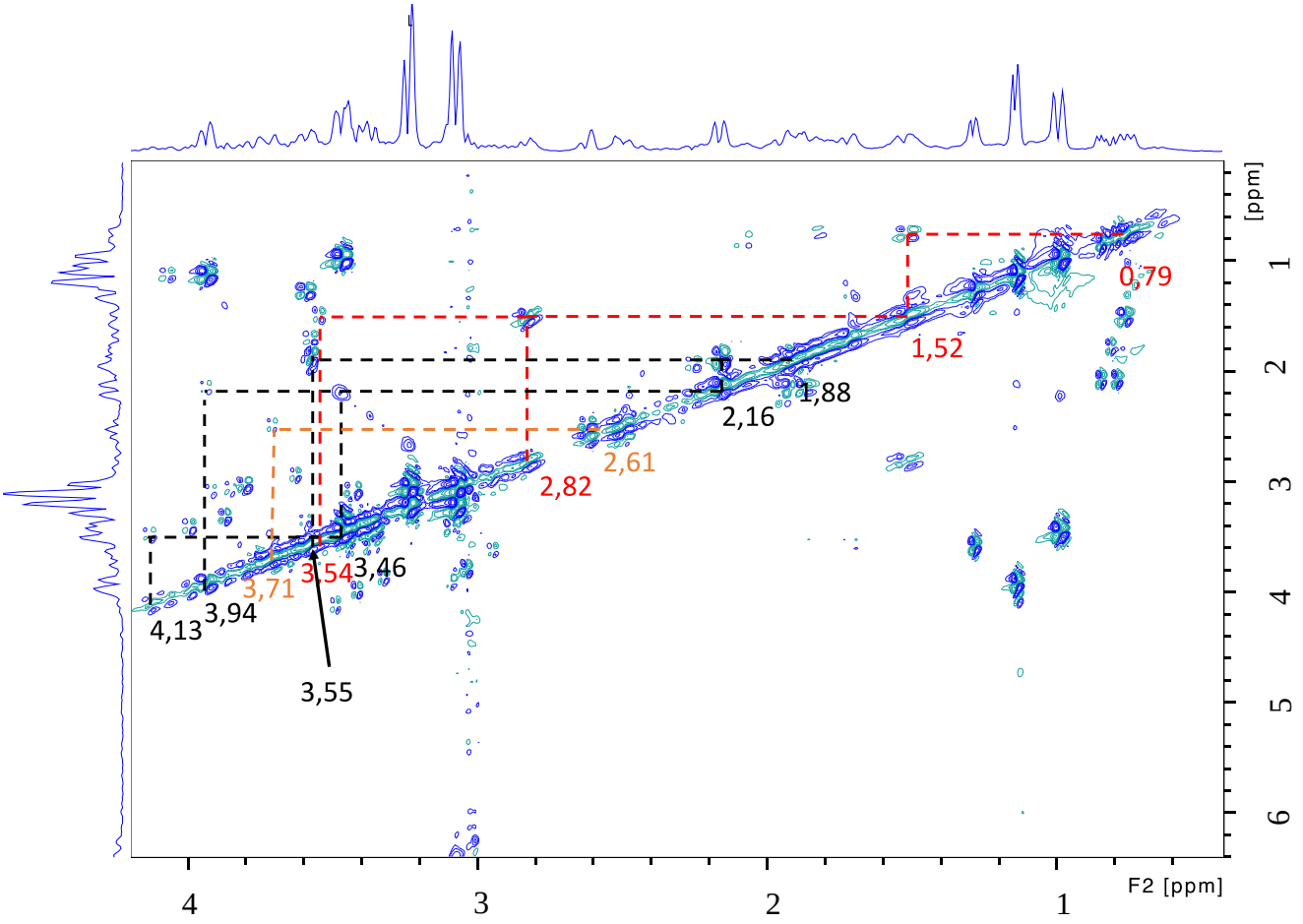

Figure 4.18: The COSY spectrum of sample 7 showing the cross peaks between the signals at 0,79, 1,52, 2,82 and 3,54 ppm (red). The correlations between signals at 1,88, 2,18, 3,46, 3,55, 3,94 and 4,13 ppm (black) are also included in the spectra. Lastly there is a correlation between the two signals at 2,61 and 3,71 ppm (orange). All the couplings are marked with dotted lines.

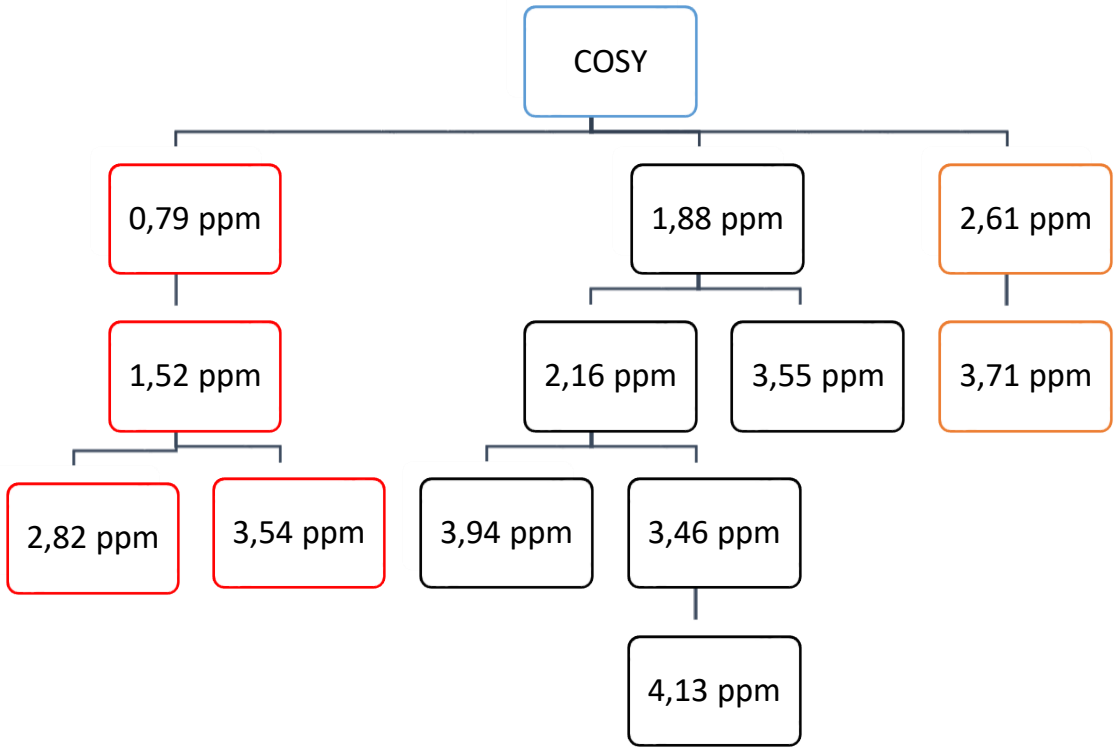

Figure 4.19: An overview of the remaining coupled signals below 5,0 ppm in the COSY spectrum (sample 7).

Figure 4.20 shows the spectrum of sample 7 with the resonances between 3,0 and 8,0 ppm. There are many overlapping resonances between 3,0 and 4,0 ppm and are thus hard to interpret. There are a few resonances between 6,0 and 8,0 ppm with low intensities. This area is typical for double carbon-carbon bonds and aromatic compounds. **Figure 4.21** depicts the COSY spectrum of the resonances between 3,0 and 8,0 ppm (sample 7). The couplings are marked with red dotted lines.

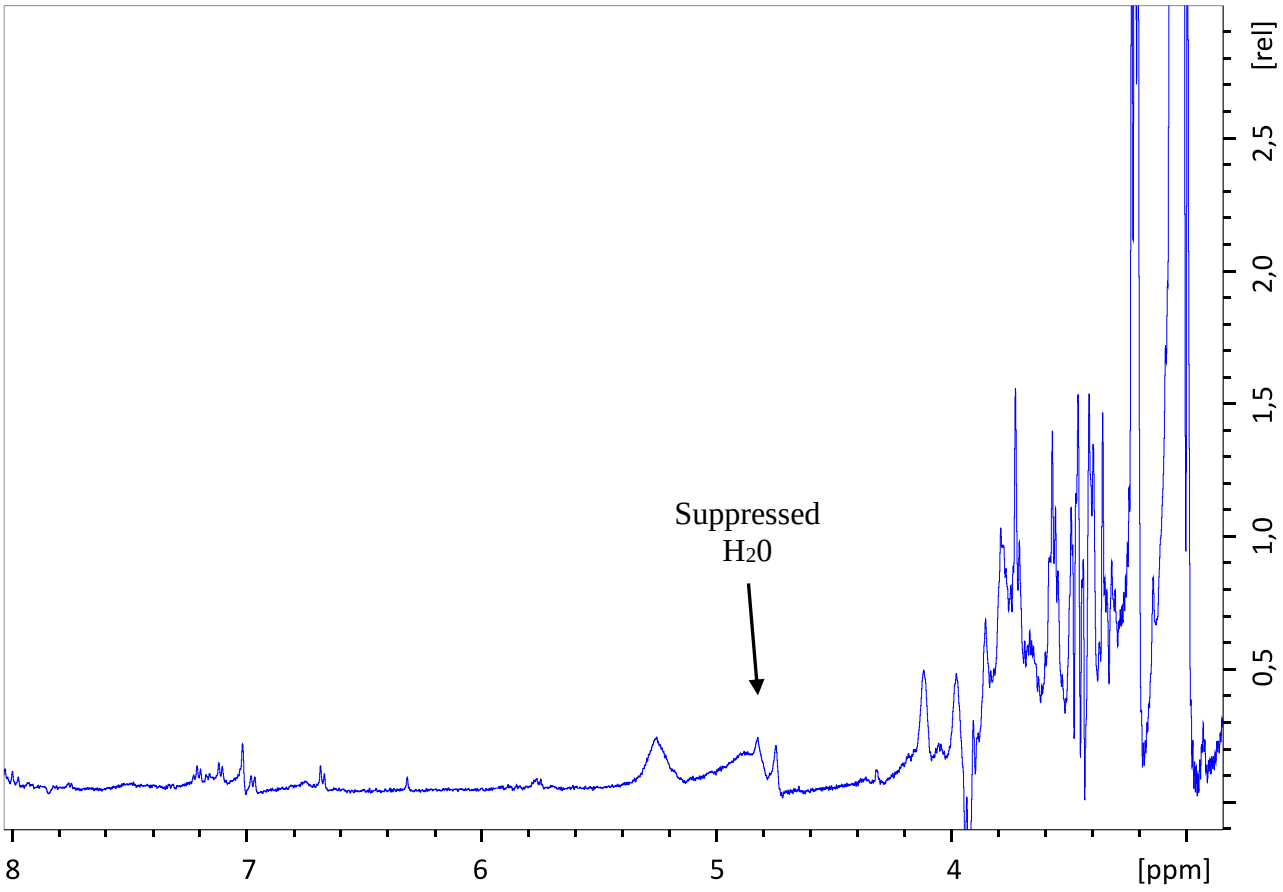

Figure:4.20: The 1D proton NMR spectrum of sample 7. The spectrum shows the resonances between 3,0 and 8,0 ppm. The signals from this chemical shift area are typical for double carbon-carbon bonds and aromatic compounds.

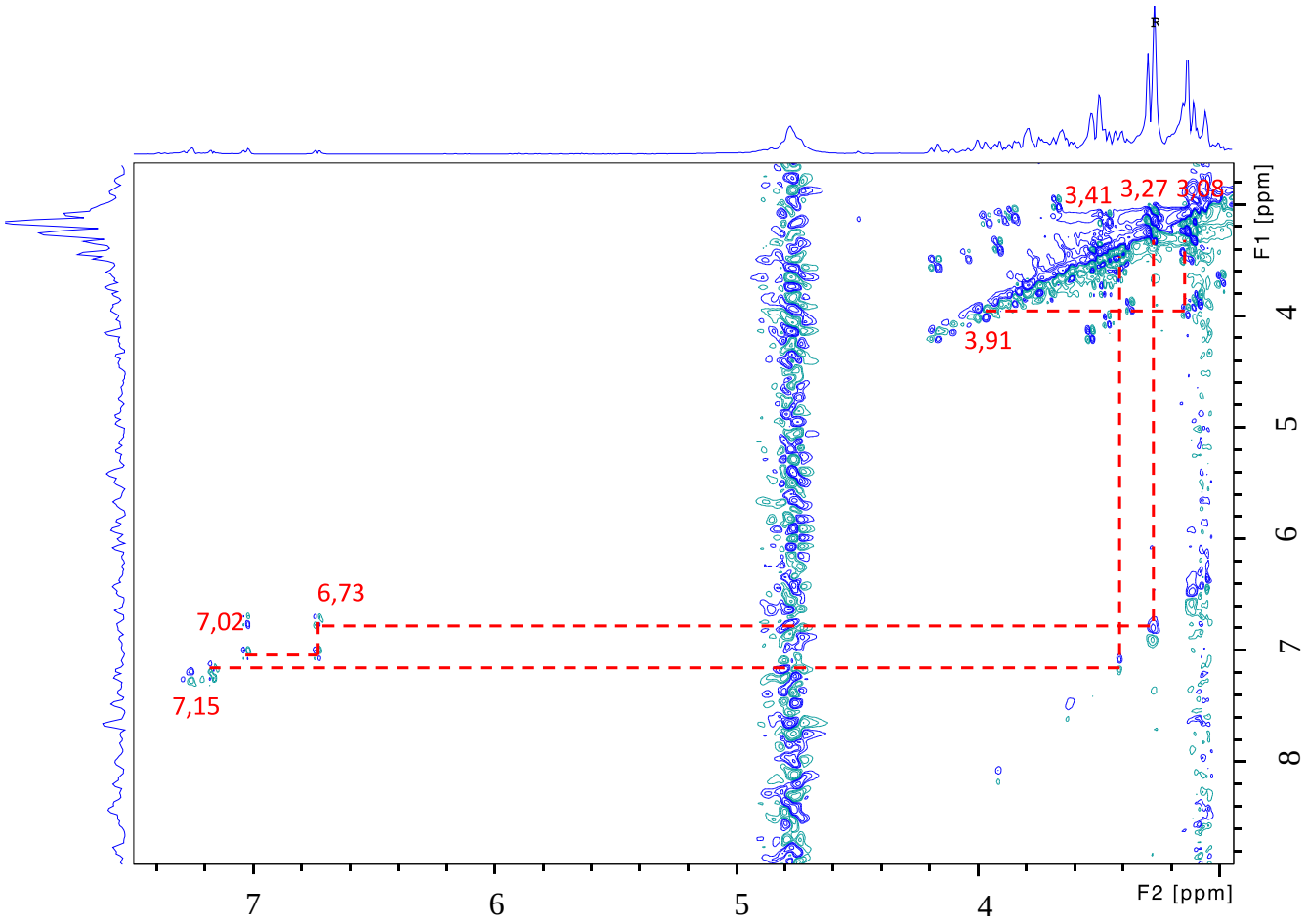

Figure 4.21: The H,H-COSY spectrum of sample 7 between 3,0 and 8,0 ppm. The couplings are marked with red dotted lines.

5. Discussion

The samples investigated were handled with care throughout the project, and they were stored at -80°C. The exceptions are samples 1-6 that were stored at -50°C in six months due to a broken freezer. Nothing in the spectra indicates that the different storing have influenced the samples (**appendix 3**) Thus it is assumed that all samples are stored under conditions which leads to no or equal loss of pituitary components.

5.1 pH and temperature dependency of chemical shift

5.1.1 pH

The spectra shown in **figure 4.2.** display the water signal from the buffer and the pituitary sample (sample 12) acquired at 277 (**A**) and 298 K (**B**). The chemical shifts listed in **table 4.1** show that there is little to no difference in the chemical shift of the water signal in the buffer and samples per set of experiments. The exception is sample 3, the chemical shift of water change with $\leq$0,01 ppm. This indicates that there is no difference in pH between the samples and the buffer, thus the samples have pH 7,4. The lack of chemical shift change also indicates that no considerable degradation of the sample has occurred. The storing conditions, the use of argon gas during sample preparation and the low experimental temperature did not change the pH. However, **table 4.1** reveals differences in the chemical shift of water between samples, as much as up to 0,09 ppm. The experiments were performed on the samples in numerical order, and there is no trend in the chemical shifts change. It is assumed that the differences are not due to changes in the temperature because the instrumental temperature control is optimal. Presumably, the differences are not due to degradation since the buffer and samples´ chemical shifts match within each experiment, and the buffer is assumed to be stable. It is therefore assumed that the differences are not due to changes in the pH. However, the differences could be due to naturally occurring drift of the magnetic field. The field was calibrated in advance of every set of experiments, and the chemical shift reference was adjusted with one decimal. The lack of a more precise chemical shift reference can explain the differences in the chemical shifts.

5.1.2 Temperature

According to **equation 3.1** and the pH, the water signal at 298 and 277 K should appear at 4,71 and 4,93 ppm respectively. The change in the chemical shift between the two temperatures should be 0,22 ppm. The ^{1}H NMR spectra in **figure 4.2** show the water signal in a pituitary sample (sample 12) at different temperatures. The chemical shifts are at 4,61 and 4,75 ppm, at 298 and 277 K respectively. The change in the chemical shift is 0,14 ppm between the temperatures. The chemical shifts of water is 0,1 and 0,18 ppm off the theoretical values at 298 and 277 K respectively. The difference between the theoretical and experimental chemical shift values can be due to small magnetic interactions that differ in the samples. The magnetic field is calibrated in advance of every set of experiment, therefore it is assumed that the chemical shifts in the samples are accurate. However, the magnetic field was not adjusted during the 24 hours one experiment set requires, since it is assumed that the field drift is neglible during the experimental time. **Figure 4.3** reveals that it is only the chemical shift of water that changes with temperature, leaving all other signals unchanged. The resonances in the spectra can be processed without a chemical shift adjustment.

5.2 T_2 filter

Figure 4.4 and **4.5** depicts spectra with and without applied T_2 filter. The intensity of the signals are noticeably reduced in the filtered experiment, and some signals disappear. The reduction of the broad signals in the spectra confirms that the applied T_2 filter was effective. The resolution was improved with the applied filter, but there was no new signals revealed in the areas with initially broad signals, after applied T_2 filter. Nonetheless, the experiment resulted in signals appearing from intramolecular mobile molecules like the amino acid side groups.

5.3 Quantification of the water signal

The spectra show water resonances with undesirable shapes (**figure 4.6**), which indicate that the samples are contaminated, and can not be used for quantification. However, the volume percentage of water in each sample can be found within a spectra. By integrating the water peak of the spectrum with no presaturation, and integrating over all the peaks in the spectrum the proton fraction is shown. **Table 4.2** shows the integrated fraction of the water in each sample. All the samples have more than 90% water, leaving less than 10% of other proton containing molecules in the samples. The similarity indicates that the samples are all from identical tissue. The samples in this study have low proton content (**table 4.2**), and with only 10 % of the protons are from hormones this yields low concentrations of the samples. This is not preferable for a method where the signal intensity is relative to the sample content. However, if the spectra only contain signals from water and hormones it is possible to analyse it using presaturation of water.

5.4 Signal interpretation

Sample 1 is not taken into account in the analysis because it has been differently treated. However, it has been used for optimizing the method. The result of sample 9 is not used in the analysis as the 1D spectrum yielded broad and improper results.

Since the pituitary extraction from the fish was performed in a period with no dominating hormone activity it is assumed that the concentration of hormones are similar (according to information given by Geir-Lasse Taranger at HI). However, the distribution of amino acids in the different hormones differ, and there are higher concentrations of some amino acids (**appendix 2**). Assuming that the hormone distribution is similar, it is expected to be highest concentrations of the amino acids Leucine (Leu) and Serine (Ser).

To interpret the spectra, the chemical shifts of the 20 common amino acids that are present in the hormones need to be assigned. Experimental proton NMR spectra of the different amino acids are collected from two different databases: The Human Metabolome Database (HMDB) and The Biological Magnetic Resonance Data Bank (BMRB), where the obtained spectra are acquired at 298 K with pH 7,4. An example of the expected signals in both 1D

and 2D ^{1}H NMR spectra are shown for the amino acid Isoleucine (Ile). **Figure 5.1** depicts the chemical structure of Ile and the chemical shifts of the different proton environments in the side chain of the molecule (in ppm). The expected 1D ^{1}H NMR spectrum of Ile is presented in **figure 5.2**, and the H,H-COSY spectrum in **figure 5.3**.

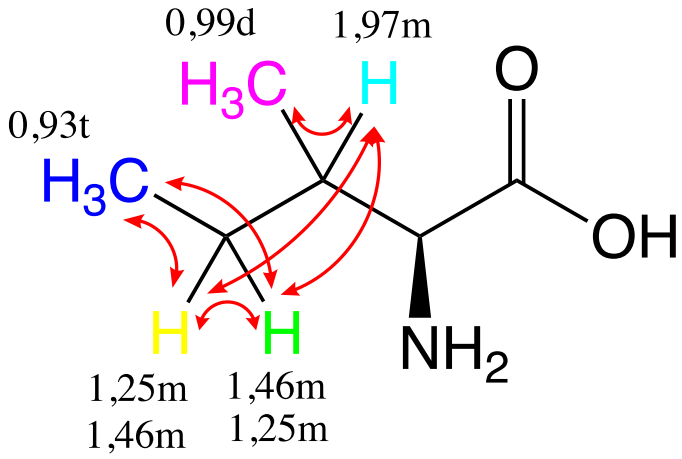

Figure 5.1: The molecular structure of the amino acid Isoleucine (Ile). The letters assigned to the chemical shift values describe the shape of the signal; singlet (s), doublet (d), quartet (q) or multiplet (m). The red arrows in the figure shows which protons that are J-coupled. The figure is drawn with adjustments from figure at Wikipedia.org 12.03.2019.

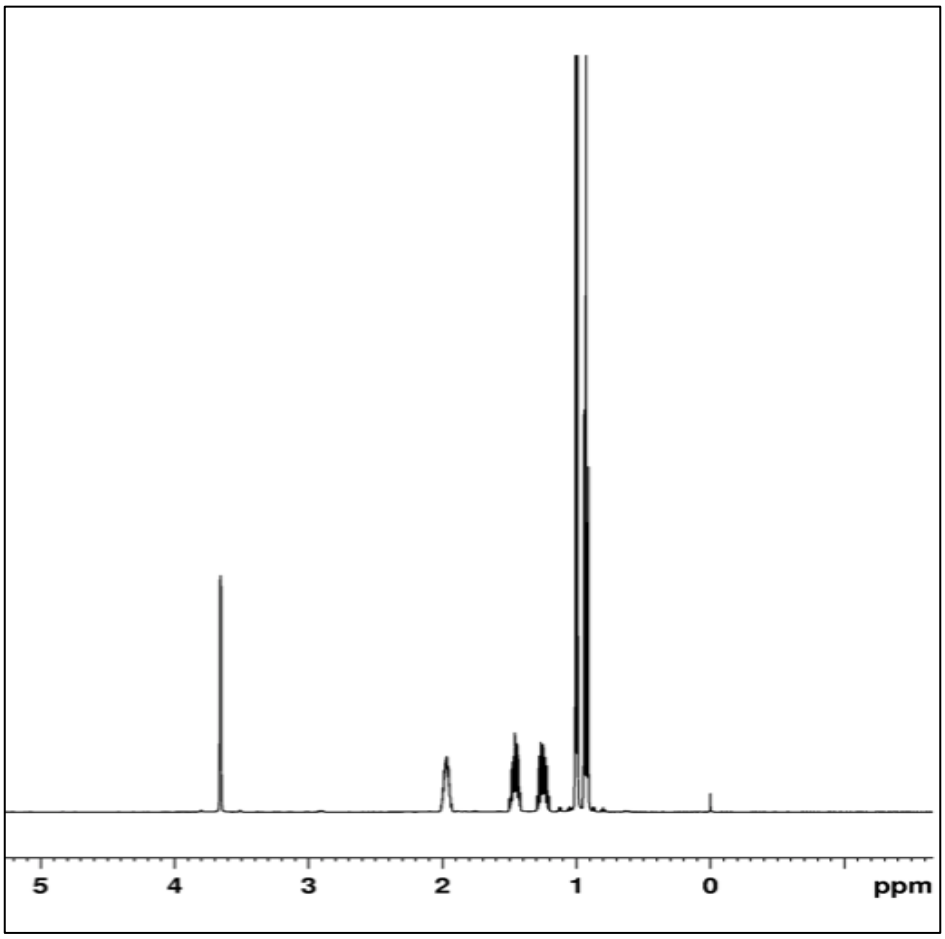

Figure 5.2: The experimental 1D ^{1}H NMR spectrum of the amino acid Isoleucine (Ile) referenced to 4,4-dimethyl-4-silapentane-1-sulfonic acid (DSS) collected from BMRB.

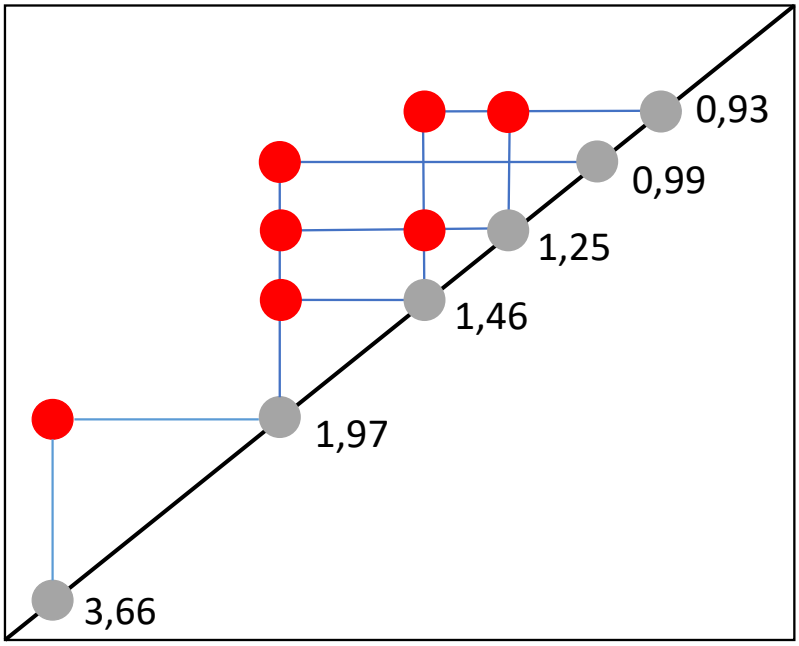

Figure 5.3: The H,H-COSY spectrum of Isoleucine (Ile) showing which protons are J-coupled in the side chain of the molecule.

The spectra of all the samples show similar features with the exception of the observation of a singlet at 2,0 ppm or a triplet at 0,9 ppm. The two signals do not occur simultaneously, but all the samples contain one of the two signals, except sample 8. The samples are taken from mature fish. Further, length, weight, sex of the fish and all other information concerning the fish were provided from The Institute of Marine Research at Matre. There is no trend that separates the signals dependent on the sex or size of the fish. Thus, it is impossible to know why these two signals appear only in some of the spectra. With more detailed background information about the fish, it would be possible to get a better analysis.

5.4.1 The Methyl signal at 0,9 ppm

The samples 1, 2, 7 and 10 show the presence of a triplet at 0,9 ppm in the 1D NMR spectra (**figure 4.7)**. The signal has a chemical shift value characteristic for a methyl signal. Alanine (Ala), Isoleucine (Ile), Leucine (Leu), Valine (Val), Threonine (Thr) and Methionine (Met) are all amino acids with a methyl group on their side chain. However, only Ile, Leu and Val yield methyl signal in the same chemical shift area as the observed triplet (**Figure 5.2 and**

5.4), and the signal can appear from these amino acids. The methyl signal from the amino acid Leu is a triplet, Val yields a doublet and Ile yields both a doublet an a triplet in the same chemical shift area. The observed triplet does not state that there is only Ile or Leu present, the resonances from the doublets might overlap in the triplet signal.

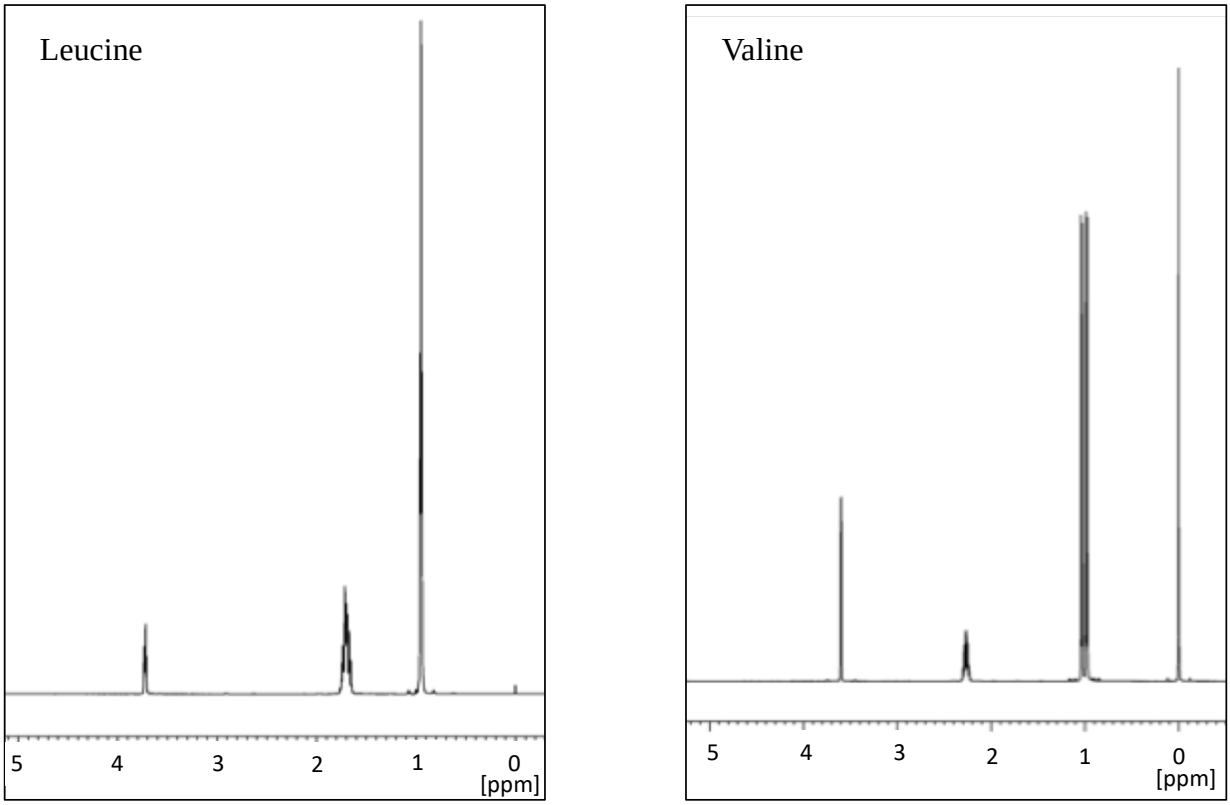

Figure 5.4: The ^{1}H NMR spectra of Leucine (Leu) (left) and Valine (Val) (right) referenced to DSS taken from the Biological Metabolite Resonance bank (BMRB).

To accompany the 1D NMR spectra, a 2D COSY spectrum of every sample was aquired. The triplet shows four cross peaks in the COSY spectrum (**figure 4.8)**. However, it is important to remember that the COSY spectra were not acquired with T_2 filter. The coupling to the signal at 2.15 ppm indicates that the amino acid Val is present in the sample. If the signal at 2.15 ppm originates from Val it is supposed to be coupled further with the signal at 3,5 and 1,03 ppm. From **figure 4.10** it is shown that the signal at 2,15 ppm is coupled to a resonance at 3,38 ppm. The coupling pattern partly supports the presence of Val. The expected couplings to the triplet of Ile and Leu are not observed in the COSY NMR spectra.

These couplings can still be present, but due to short relaxation times the couplings can be broad and concealed by noise, and therefore not visible.

The signal at 3,38 ppm is the broadest and most intense cross peak to the triplet. There are probably several couplings present here, but it is hard to define the different signals because of overlapping resonances. A signal around 3,5 ppm is typically observed in all spectra of the three amino acids: Leu, Ile and Val. However, this signal will not make a cross peak with the methyl signal. The methyl and alpha protons in the three amino acids are separated with more than 3 bond lengths. All of the 20 common amino acids have signals in this area.

The two cross peaks with chemical shift at 5,84 and 7,11 ppm are not typical for any of the three amino acids, nor other common amino acids. The signals around 5,84 ppm are often from carbon-carbon double bonds, and the signals around 7,11 ppm are aromatic, and the appearance of these signals are not unambiguous. The signals only appear under the diagonal and are not observed above. It is likely that these signals in fact are noise.

The signal at 0,9 ppm is characteristic for a methyl-group in the three amino acids as mentioned above, and there might be a sufficient quantity of them in the samples of the pituitary. If the signal originates from these amino acids they are expected to be visible in all spectra. Especially based on the amount of these amino acids that are present in the pituitaries. However, there are also glycoproteins present in the samples. These molecules are rigid and signals from glycoproteins are not expected to appear in the spectra when T_2 filter is applied. However, small chains in glycoproteins might be more mobile and cause signals in the spectra. Signals from sugars and molecules that are mobile might be visible in the COSY spectra since the T_2 filter is not applied in the COSY experiment. In addition, the triplet has the chemical shift as the end-methyl groups in fatty acids [24]. This can also be visible in the COSY spectra with no applied T_2 filter.

It is assumed that the triplet signal can originate from the amino acids as all the samples are expected to contain Ile, Val and Leu, however, the resonance can also originate from sugars or fat.

5.4.2 The singlet at 2,0 ppm

The samples 3, 4, 5, 6, 11 and 12 have a distinct singlet signal with high intensity at 2,0 ppm as shown in the 1D NMR spectrum (**figure 4.12)**. None of the common 20 amino acids yield a singlet at this chemical shift. There are amino acids that give signals at this chemical shift, but these are doublets and multiplets. The position and intensity of the signal is characteristic for the brain metabolite N-acetyl aspartate (NAA) [71] (**figure 5.5**). This is the metabolite of highest concentration present in the brain, but is not supposed to occur in healthy pituitaries. However, the pituitary gland is directly connected to the brain, and it is possible that some brain tissue has polluted the pituitary sample. The samples have been extracted from the fish mechanically and might contain impurities. Not all the samples yield spectra with the intense signal described, and there are no observed trends in the spectra about the appearance of the singlet. The distribution of the signal indicates that its appearance is random, and this might support that the sample is contaminated with brain tissue, and if so, the characteristic singlet at 2,0 ppm occurs from NAA.

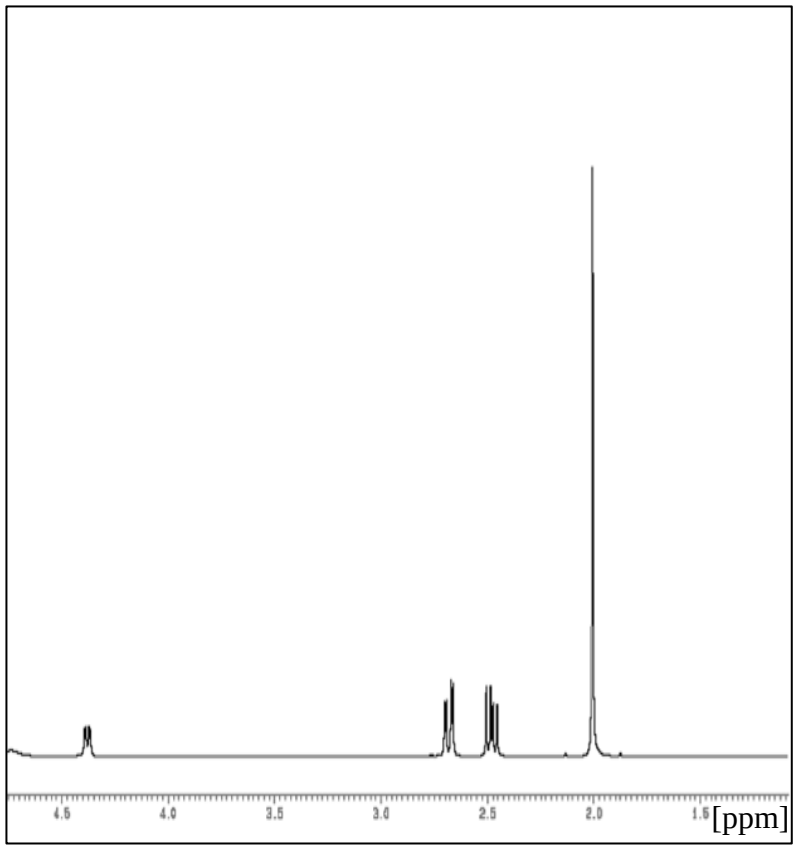

Figure 5.5: The [1]H NMR spectrum of N-acetyl aspartate (NAA) taken from the Biological Metabolite Resonance bank (BMRB).

5.4.3 The doublets at 1.13 and 1,27 ppm

All the samples in this study yield spectra with two distinct doublets. The two doublets have chemical shifts at 1,13 and 1,27 ppm as shown in **figure 4.14**. The doublet at 1,13 ppm can originate from a methyl group. This can support the presence of Valine with methyl signals at both 0,99 and 1,03 ppm (BMRB) **figure 5.4**. However, the couplings between the resonances at 1,13 and 2,26 does not appear in the COSY spectra. The expected couplings of Val is illustrated in **figure 5.6**. There could be Val present in the samples if the coupling is broad and concealed by noise.

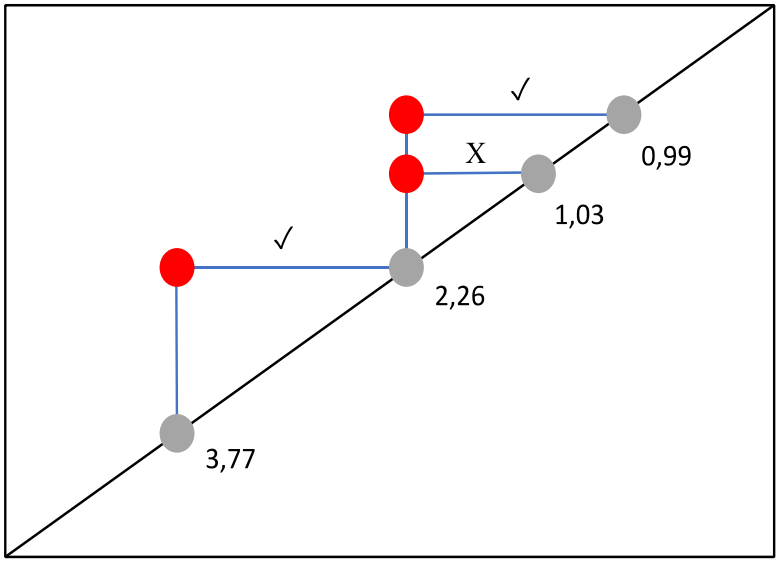

Figure 5.6: An illustration of how the H,H-COSY spectrum of Valine (Val) is with chemical shifts in ppm. The couplings found in the samples is marked with a check sign, and the missing coupling is marked with an X.

The methyl group in Threonine (Thr) contributes to a doublet at 1,31 ppm (BMRB) **figure 5.7.** If small changes in the chemical shift is considered, the doublet at 1,27 ppm can originate from Thr. The amino acid also yields signals at 3,58 and 4,24 ppm. The experimental spectra have signals around 3,58 and at 4,14 ppm. Regarding the 1D spectra, it can be assumed that Thr is present in the samples. **Figure 4.15** illustrates how the doublet´s resonances are coupled. The doublet at 1,27 ppm is coupled to a signal at 1,74

ppm and another signal at 3,64 ppm. The two signals at 1,74 and 3,64 ppm are also coupled. None of the detected couplings match the expected couplings for Thr.

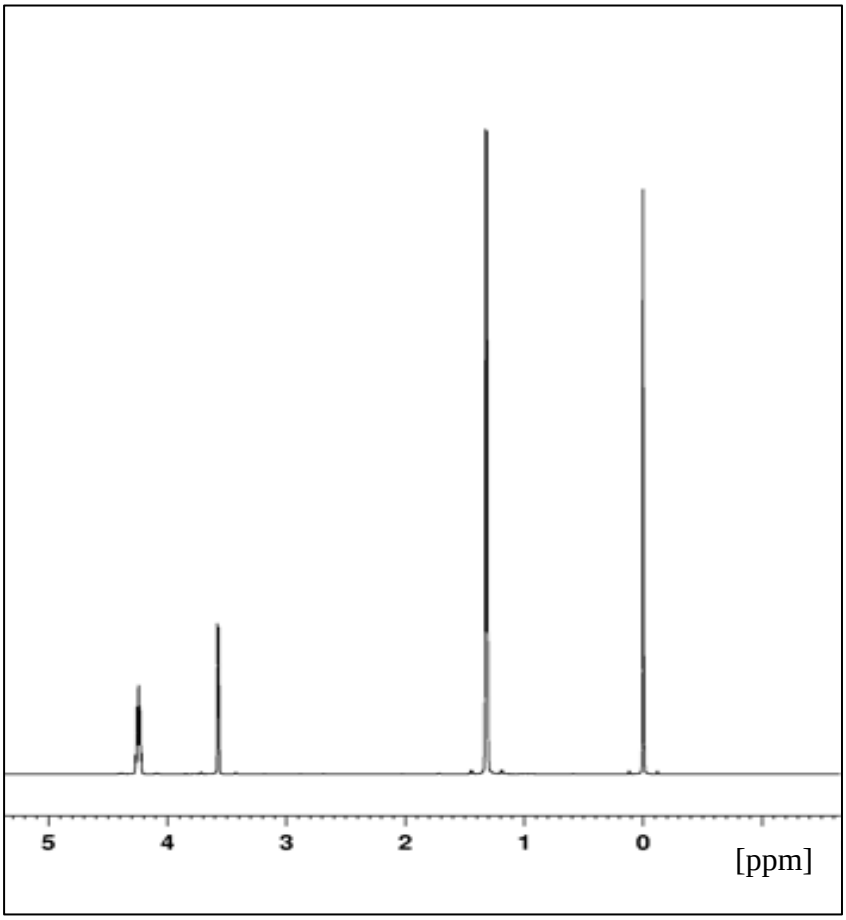

Figure 5.7: The ^{1}H NMR spectrum of Threonine (Thr) referenced to DSS taken from the Biological Metabolite Resonance bank (BMRB).

However, the cross peak between 1,27 and 3,58 ppm can appear from the amino acid Alanine (Ala)(**figure 5.8**). The resonances of Ala at the same experimental conditions are 1,47 and 3.77 ppm (BMRB) and the signals are J-coupled. **Figure 4.15** shows how the signals are coupled to an additional signal at 1,70 ppm that do not correspond to the presence of Ala. The coupling from a corresponding proton might cause overlapping, or the signals do not originate from Ala.

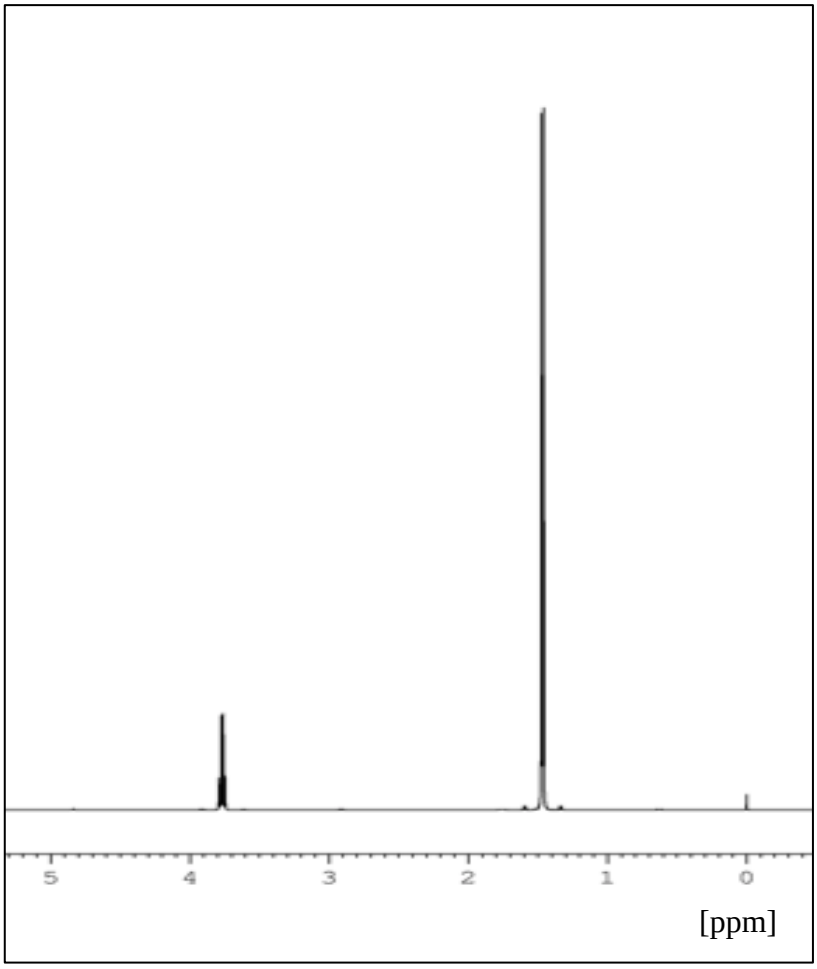

Figure 5.8: The ^{1}H NMR spectrum of Alanine (Ala) referenced to DSS taken from the Biological Metabolite Resonance bank (BMRB).

Figure 4.15 also depicts how the doublet at 1,13 ppm is coupled to two other signals at 3,93 and 4,10 ppm. None of the common 20 amino acids contributes to these signals or couplings and their appearance are not conclusive.

The doublet at 1,27 ppm can be recognizable as lactate, this molecule yields a doublet at 1,32 and a quartet at 4,10 ppm (BMRB) (**figure 5.9**). Lactate is a brain metabolite that

stimulates the pituitary and is produced at the connection between the brain and the pituitary gland. The metabolite is not supposed to be found in healthy pituitaries, but it is not unlikely that some brain tissue is present in the pituitary sample. However, the couplings that are observed in **figure 4.15** do not support that Lactate is present in the samples.

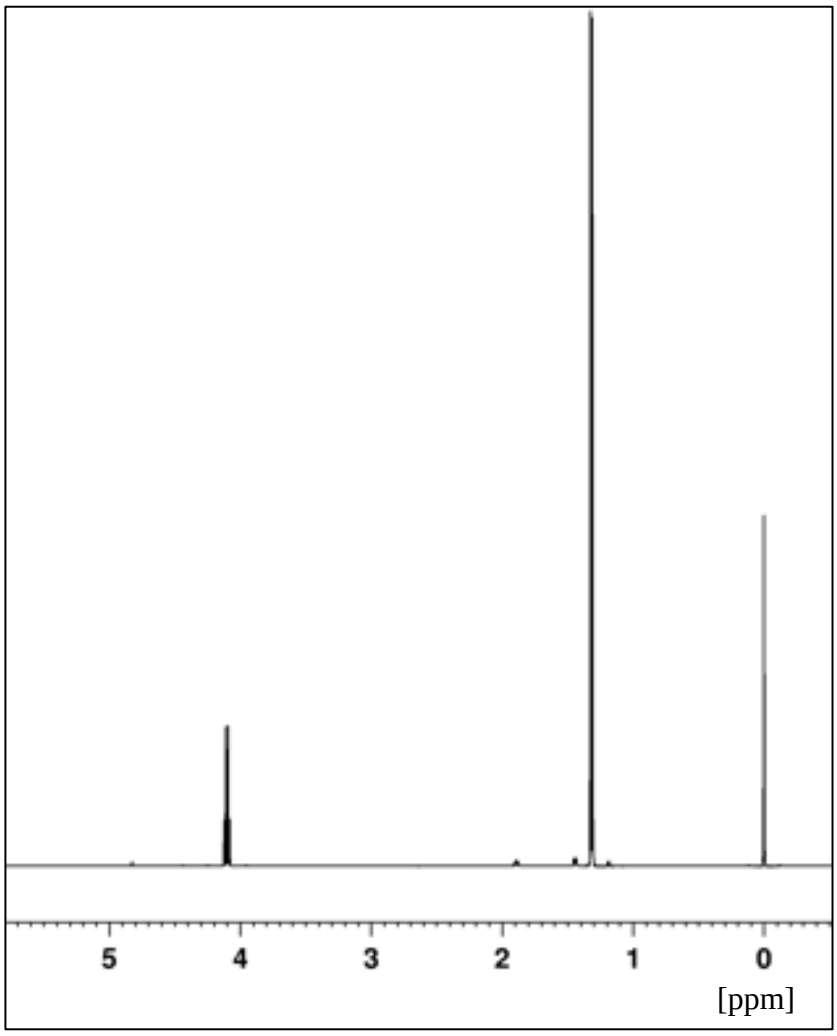

Figure 5.9: The ^{1}H NMR spectrum of Lactate referenced to DSS taken from the Biological Metabolite Resonance bank (BMRB).

5.4.4 Additional Resonances

Figure 4.17 depicts the signals with chemical shifts lower than 3,0 ppm which shows similar features for all the samples. **Figure 4.18** depicts the H,H-COSY spectrum of chemical shifts between 0 and 4,2 ppm (sample 7). The three signals at 0,79, 1,52 and 2,82 ppm correlate in the COSY spectra, and the signal at 1,52 ppm is also coupled to a resonance at 3,54 ppm (**figure 4.18**). The signal at 0,79 ppm is broad and none of the common 20 amino acids yield signal in this area: its origination is unknown. However, there are amino acids with signals around 1,52 and 2,82 ppm.

The amino acid Alanine (Ala) yields only two signals in proton NMR; at 1,47 and 3,77 ppm (BMRB). The possibility that the resonance at 1,27 ppm is the methyl doublet from Ala is mentioned earlier, further the resonance at 1,52 ppm might also correspond to the presence of Ala. In addition, the signals at 1,52 and 3,54 ppm are coupled as expected for Ala. However, the shape of the signal at 1,52 ppm does not correspond to the expected doublet of the methyl group. The two signals correlates with two additional resonances in the COSY spectrum at 0,79 and 2,82 ppm. This observation do not correspond to the presence of Ala, although these correlations could appear from other molecules with similar chemical shifts.

Lysine (Lys) yields signals at 1,47, 1,72, 1,89, 3,0 and 3,75 ppm (BMRB) (**figure 5.10**). In the 1D NMR spectrum of healthy fish pituitary, signals are observed around 1,52, 1,71, 1,88, 3,0 and, 3,74 ppm. However, the COSY spectrum only shows one out of four expected cross peaks that indicate the presence of Lys, which is between the resonances at 1,88 and 3,55 ppm.

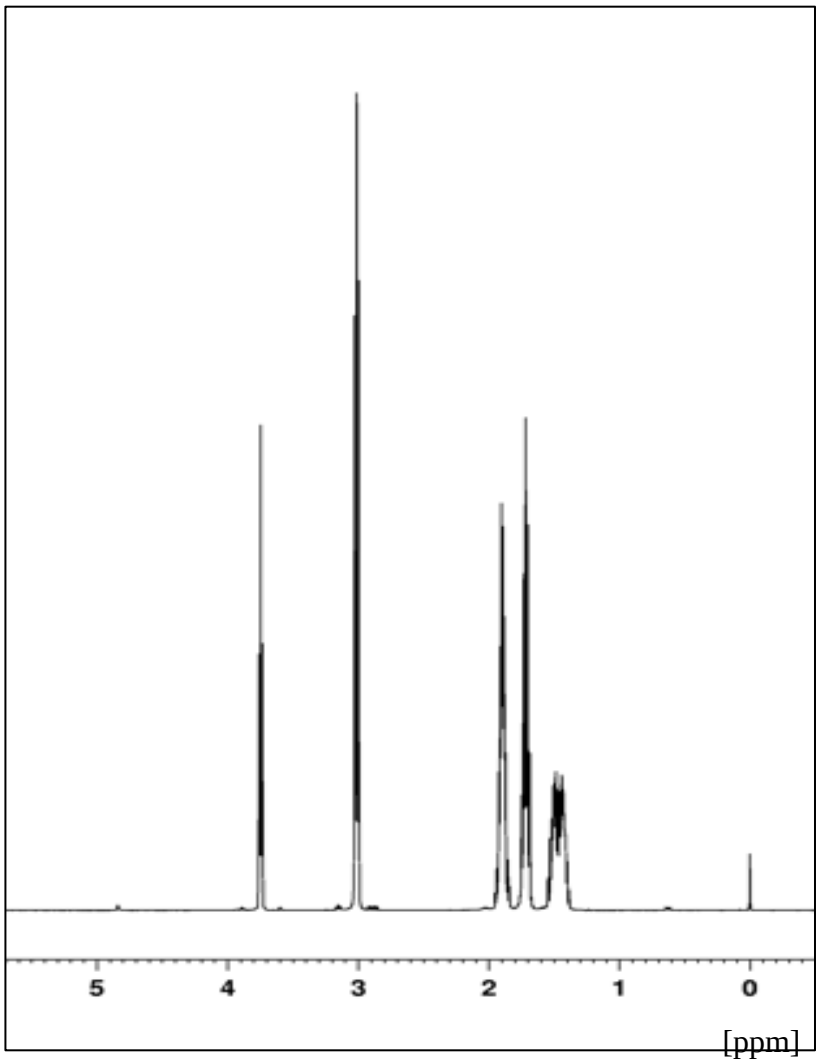

Figure 5.10: The ^{1}H NMR spectrum of Lysine (Lys) referenced to DSS taken from the Biological Metabolite Resonance bank (BMRB).

Aspartic Acid (Asp) yields signal at 2,66, 2,80 and 3,88 ppm (BMRB) (**figure 5.11**). There are signals at 2,82 and 3,71 ppm which are coupled in the 1D spectra of the pituitary samples. A resonance at 2,61 ppm is visible in the COSY spectrum (**figure 4.18**). However, the rest of the expected couplings of Asp are not observed in the COSY spectra, furthermore, the shapes of the signals are not at all corresponding to the expected spectrum of Asp.

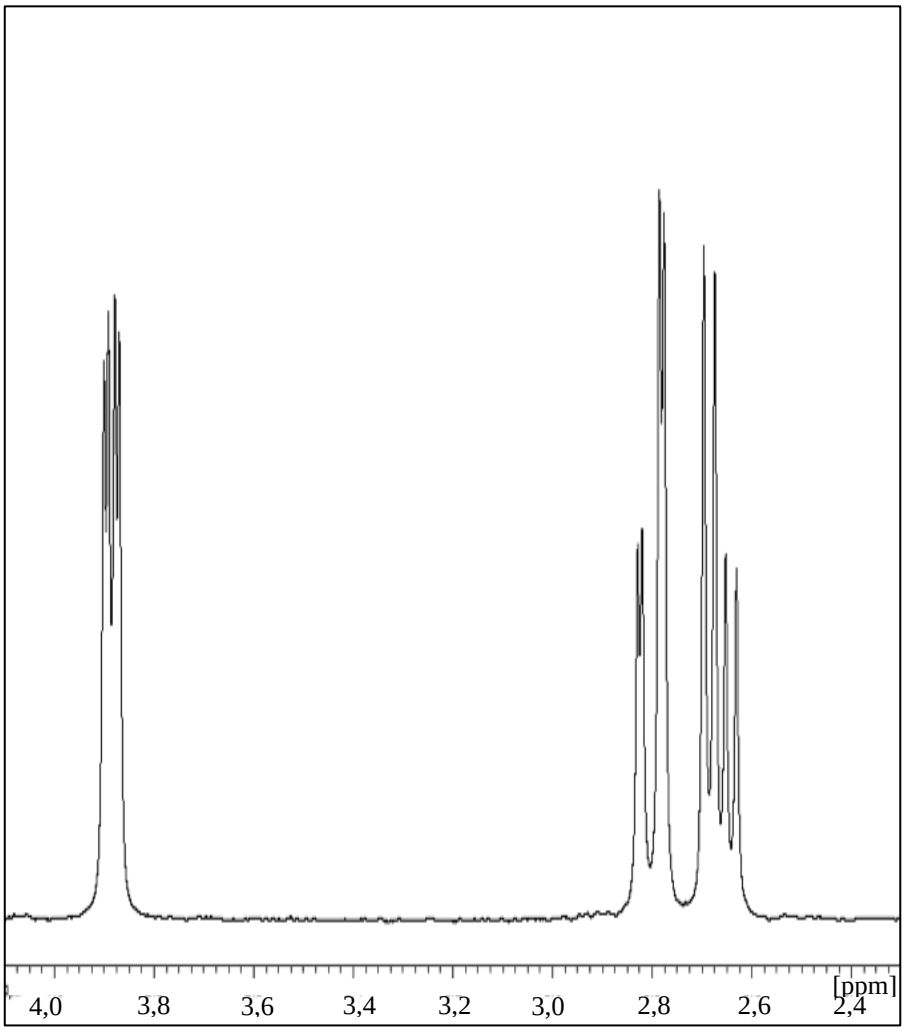

Figure 5.11: The ^{1}H NMR spectrum of Aspartic Acid (Asp) referenced to DSS taken from the Biological Metabolite Resonance bank (BMRB).

Asparagine (Asn) is the last amino acid with signals resembling the observed signals in the spectrum below 3,0 ppm. The amino acid have signals at 2,84, 2,94 and 4,0 ppm (BMRB) (**figure 5.12**). In the 1D spectra signals at 2,8 and 4,0 ppm are observed, but these are not correlated in the COSY spectrum, and indicates that Asn is not present in the sample. In addition, the shapes of the signals are different from the expected spectra of Asn.

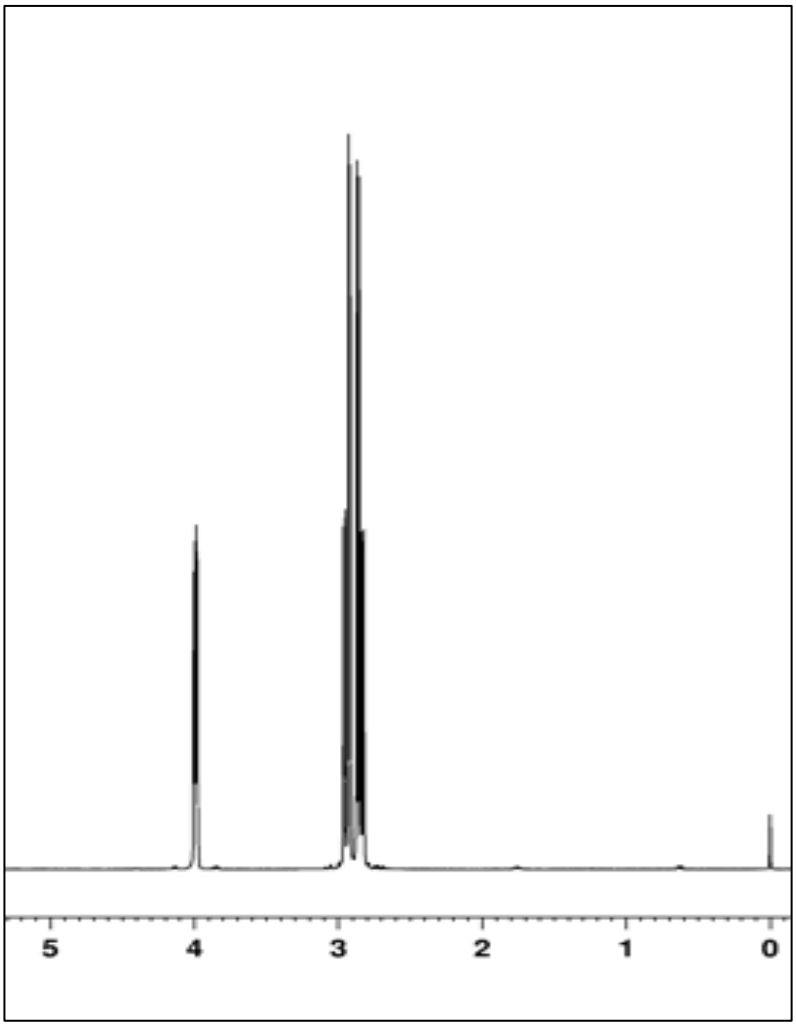

Figure 5.12: The ^{1}H NMR spectrum of Asparagine (Asn) referenced to DSS taken from the Biological Metabolite Resonance bank (BMRB).

Figure 4.20 depicts all the signals with chemical shifts between 3,0 and 8,0 ppm. There are many overlapping signals between 3,0 and 4,0 ppm making the interpretation of the

spectrum difficult. The cross peaks between signals from this area are shown in the COSY spectrum (**figure 4.21)**.

The amino acid Cysteine (Cys) yields only two signals which are correlated, the resonances are at 3,04 and 3,95 ppm (BMRB) (**figure 5.13**). The pituitary spectra yield signals at 3,08 and 3,91 ppm, but it is difficult to see if they are correlated in the COSY spectra due to overlapping signals. The signals might originate from Cys.

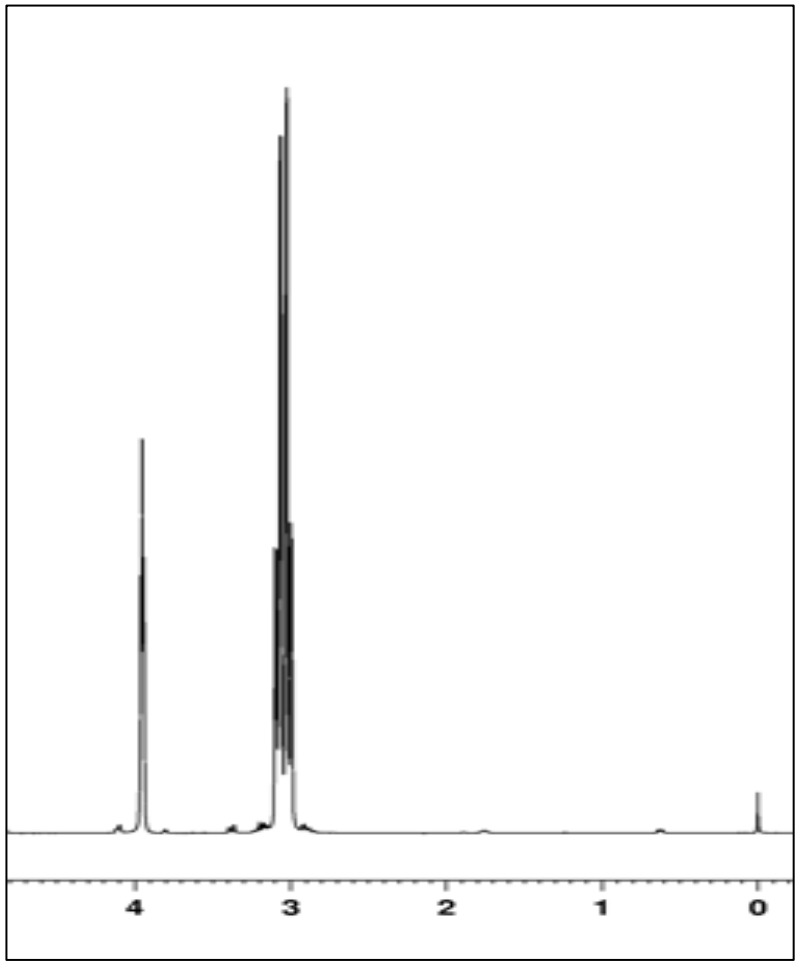

Figure 5.13: The ^{1}H NMR spectrum of Cysteine (Cys) referenced to DSS taken from the Biological Metabolite Resonance bank (BMRB).

There are three signals with resonances between 6,0 and 8,0 ppm observed in the COSY spectra, and two of them are correlated as seen in **figure 4.21**. The signals in the pituitary samples are at 6,73, 7,02 and 7,15 ppm. Tyrosine (Tyr) is an aromatic amino acid with

resonances at 3,06, 3,20, 3,94, 6,89 and 7,19 (BMRB) (**figure 5.14**). The two signals at 6,73 and 7,02 ppm are correlated which might correspond to Tyr, but the signals are also coupled to resonances at 3,27 ppm. In addition, the signal at 3,08 ppm are coupled with the signal at 3,91 which matches the coupling pattern of Tyr. The expected couplings of Tyr is illustrated in **figure 5.15**. Even though some signals are missing, the observed signals might originate due to the presence of Tyr.

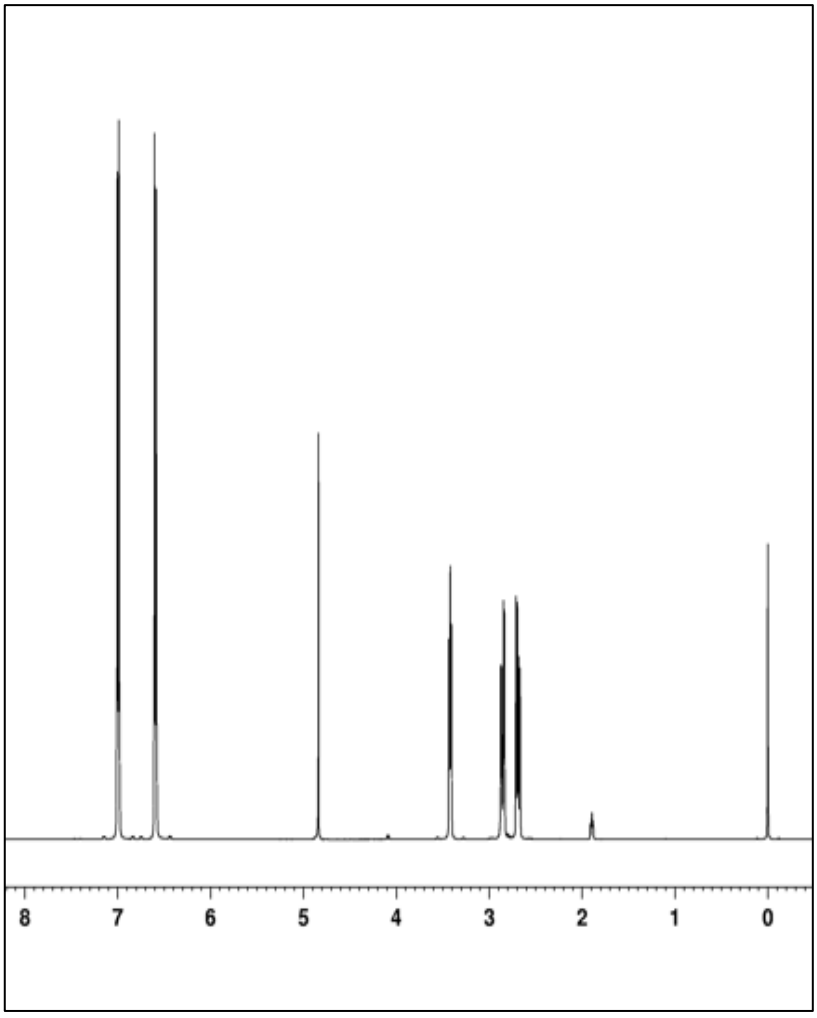

Figure 5.14: The ^{1}H NMR spectrum of Tyrosine (Tyr) referenced to DSS taken from the Biological Metabolite Resonance bank (BMRB).

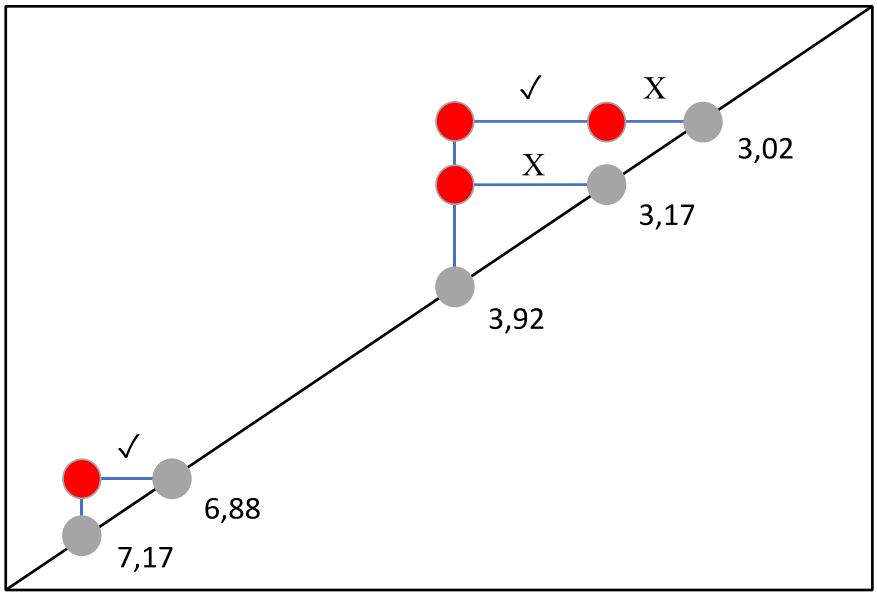

Figure 5.15: The H,H-COSY spectrum of Tyrosine (Tyr) showing which proton environments are J-coupled in the side chain of the molecule.

6. Conclusion

The signals in the spectra of healthy salmon pituitaries in this study are assumed to originate from amino acids. The study lead to three main findings.

The triplet at 0,9 ppm is assumed to originate from a methyl group. All the hormones in the pituitary gland contain several methyl groups at the chemical shift of the observed triplet, presumably from the amino acids Ile, Leu and Val. Val is the amino acid which is proven to be present, however the methyl signal is only present in the spectra of some samples. The lack of the methyl signal in these spectra could be due to low concentrations of the hormones making it difficult to detect. The doublets at 1,13 and 1,27 ppm are also considered due to the presence of methyl groups. Val might be present, confirmed by the presence of a doublet at 1,13 ppm. The amino acid Ala can also be considered proven by specific coupling in the 2D COSY spectra. The methyl signal in Ala is assumed to be overlapping with methyl signals from other amino acids. In addition, the 1D NMR spectra show the methyl and other signals specific for the amino acid Thr.

Further, several other signals in the 1D and 2D NMR spectra were attempted to be assigned, and the amino acids Lys and Cys are also assumed present in the samples.

Another finding is a high intensity singlet at 2,0 ppm appearing in six of the spectra. This signal is characteristic for the brain metabolite NAA, and is assumed present in the samples as a contamination. The contamination appears due to the mechanical extraction of the pituitary from the fish.

The attempt to distinguish hormones from each other in healthy salmon pituitaries using HR-MAS NMR was challenging. However, the results from this pilot can be used to design a study where all the salmons are comparable considering maturity, breeding conditions and genetic background. In addition, the samples should be collected from the fish at another time in their life cycle with higher hormone activity.

7. References

1. FaO, F. a. A. O. o. t. U. N., The State of World Fisheries and Aquaculture. *The State of the World* **2018**, 210.
2. Gjedrem, T., Improving Farmed Fish Quality by Selective Breeding. In *Improving Farmed Fish Quality and Safety*, Lie, Ø., Ed. Woodhead: 2008; pp 265-274.
3. Gjedrem, T.; Baranski, M., *Selective breeding in aquaculture : an introduction*. Springer: Dordrecht ; New York, 2009; p xiv, 221 p.
4. McClure, C. A.; Hammell, K. L.; Moore, M.; Dohoo, I. R.; Burnley, H. J. A., Risk factors for early sexual maturation in Atlantic salmon in seawater farms in New Brunswick and Nova Scotia, Canada. **2007,** *272* (1-4), 370-379.
5. Taranger, G. L.; Carrillo, M.; Schulz, R. W.; Fontaine, P.; Zanuy, S.; Felip, A.; Weltzien, F. A.; Dufour, S.; Karlsen, O.; Norberg, B.; Andersson, E.; Hansen, T., Control of puberty in farmed fish. *Gen Comp Endocrinol* **2010,** *165* (3), 483-515.
6. Weltzien, F.-A.; Andersson, E.; Andersen, Ø.; Shalchian-Tabrizi, K.; Norberg, B., The brain–pituitary–gonad axis in male teleosts, with special emphasis on flatfish (Pleuronectiformes). *Comparative Biochemistry and Physiology Part A: Molecular & Integrative Physiology* **2004,** *137* (3), 447-477.
7. Pickford, G. E.; Atz, J. W., Physiology of the pituitary gland of fishes. *Physiology of the pituitary gland of fishes* **1957**.
8. Matty, A.; Matty, J., A histochemical investigation of the pituitary glands of some teleost fish. *J Cell Sci* **1959,** *3* (50), 257-267.
9. Peute, J.; de Bruyn, M. G. A.; Seldenrijk, R.; van Oordt, P. G. W. J., Cytophysiology and innervation of gonadotropic cells in the pituitary of the Black Molly (Poecilia latipinna). *Cell Tissue Res* **1976,** *174* (1), 35-54.
10. Weltzien, F.-A.; Norberg, B.; Helvik, J. V.; Andersen, Ø.; Swanson, P.; Andersson, E., Identification and localization of eight distinct hormone-producing cell types in the pituitary of male Atlantic halibut (Hippoglossus hippoglossus L.). *Comparative Biochemistry and Physiology Part A: Molecular & Integrative Physiology* **2003,** *134* (2), 315-327.
11. Kaneko, T.; Kakizawa, S.; Yada, T.; Hirano, T., Gene expression and intracellular localization of somatolactin in the pituitary of rainbow trout. *Cell Tissue Res* **1993,** *272* (1), 11-16.
12. Levavi-Sivan, B.; Bloch, C. L.; Gutnick, M. J.; Fleidervish, I. A., Electrotonic coupling in the anterior pituitary of a teleost fish. *Endocrinology* **2005,** *146* (3), 1048-1052.
13. Oka, Y., Electrophysiological characteristics of gonadotrophin-releasing hormone 1–3 neurones: insights from a study of fish brains. *Journal of neuroendocrinology* **2010,** *22* (7), 659-663.
14. Au - Fontaine, R.; Au - Hodne, K.; Au - Weltzien, F.-A., Healthy Brain-pituitary Slices for Electrophysiological Investigations of Pituitary Cells in Teleost Fish. *JoVE* **2018,** (138), e57790.
15. Benjamin, M., A morphometric study of the pituitary cell types in the freshwater stickleback, Gasterosteus aculeatus, form leiurus. *Cell Tissue Res* **1974,** *152* (1), 69-92.
16. Ruijter, J., Development and aging of the teleost pituitary: qualitative and quantitative observations in the annual cyprinodont Cynolebias whitei. *Anatomy and embryology* **1987,** *175* (3), 379-386.
17. Takeda, M.; Jardetzky, O., Proton magnetic resonance of simple amino acids and dipeptides in aqueous solution. *The Journal of Chemical Physics* **1957,** *26* (5), 1346-1347.

18. Opella, S. J.; Lu, P., *NMR and Biochemistry: A Symposium Honoring Mildred Cohn [Philadelphia, June 22-23, 1978]*. Dekker: 1979.
19. Shulman, R. G.; Brown, T.; Ugurbil, K.; Ogawa, S.; Cohen, S.; Den Hollander, J., Cellular applications of 31P and 13C nuclear magnetic resonance. *Science* **1979,** *205* (4402), 160-166.
20. Cheng, L. L.; Lean, C. L.; Bogdanova, A.; Wright Jr, S. C.; Ackerman, J. L.; Brady, T. J.; Garrido, L., Enhanced resolution of proton NMR spectra of malignant lymph nodes using magic-angle spinning. *Magnet Reson Med* **1996,** *36* (5), 653-658.
21. Aursand, M.; Gribbestad, I.; Martinez, I., Omega-3 fatty add content of intact muscle of farmed Atlantic salmon (Salmo salar) examined by 1 H MAS NMR spectroscopy. In *Modern magnetic resonance*, Springer: 2008; pp 941-945.
22. Roy, U.; Conklin, L.; Schiller, J.; Matysik, J.; Berry, J. P.; Alia, A., Metabolic profiling of zebrafish (Danio rerio) embryos by NMR spectroscopy reveals multifaceted toxicity of β-methylamino-L-alanine (BMAA). *Sci Rep-Uk* **2017,** *7* (1), 17305.
23. Howell, N.; Shavila, Y.; Grootveld, M.; Williams, S., High-resolution NMR and magnetic resonance imaging (MRI) studies on fresh and frozen cod (Gadus morhua) and haddock (Melanogrammus aeglefinus). *Journal of the Science of Food and Agriculture* **1996,** *72* (1), 49-56.
24. Nestor, G.; Bankefors, J.; Schlechtriem, C.; Brännäs, E.; Pickova, J.; Sandström, C., High-resolution 1H magic angle spinning NMR spectroscopy of intact Arctic char (Salvelinus alpinus) muscle. Quantitative analysis of n− 3 fatty acids, EPA and DHA. *Journal of agricultural and food chemistry* **2010,** *58* (20), 10799-10803.
25. Totland, C.; Seland, J. G.; Steinkopf, S.; Nerdal, W., Analysis of wild and farmed salmon using C-13 solidstate NMR and MRI directly on fillet tissue. *Anal Methods-Uk* **2017,** *9* (8), 1290-1296.
26. Martinez, I.; Bathen, T.; Standal, I. B.; Halvorsen, J.; Aursand, M.; Gribbestad, I. S.; Axelson, D. E., Bioactive compounds in cod (Gadus morhua) products and suitability of 1H NMR metabolite profiling for classification of the products using multivariate data analyses. *Journal of agricultural and food chemistry* **2005,** *53* (17), 6889-6895.
27. Castejón, D.; Villa, P.; Calvo, M. M.; Santa-María, G.; Herraiz, M.; Herrera, A., 1H-HRMAS NMR study of smoked Atlantic salmon (Salmo salar). *Magn Reson Chem* **2010,** *48* (9), 693-703.
28. Alam, T. M.; Jenkins, J. E., HR-MAS NMR spectroscopy in material science. In *Advanced aspects of spectroscopy*, IntechOpen: 2012.
29. Hawkes, R.; Holland, G.; Moore, W.; Corston, R.; Kean, D.; Worthington, B., The application of NMR imaging to the evaluation of pituitary and juxtasellar tumors. *American Journal of Neuroradiology* **1983,** *4* (3), 221-222.
30. Maxwell, R. J.; Prysor-Jones, R. A.; Jenkens, J. S.; Griffiths, J. R., Vasoactive intestinal peptide stimulates glycolysis in pituitary tumours; 1H-NMR detection of lactate in vivo. *Biochimica et Biophysica Acta (BBA)-Molecular Cell Research* **1988,** *968* (1), 86-90.
31. Prysor-Jones, R.; Silverlight, J.; Jenkins, J.; Stevens, A.; Rodrigues, J.; Griffiths, J., VIP enhances TRH-stimulated prolactin secretion of pituitary tumours: Studies with 31P NMR. *Febs Lett* **1984,** *177* (1), 71-75.
32. Usenius, J.-P.; Kauppinen, R. A.; Vainio, P. A.; Hernesniemi, J. A.; Vapalahti, M. P.; Paljärvi, L. A.; Soimakallio, S., Quantitative metabolite patterns of human brain tumors: detection by 1H NMR spectroscopy in vivo and in vitro. *Journal of computer assisted tomography* **1994,** *18* (5), 705-713.
33. Ijare, O. B.; Baskin, D. S.; Pichumani, K., Ex Vivo 1 H NMR study of pituitary adenomas to differentiate various immunohistochemical subtypes. *Sci Rep-Uk* **2019,** *9* (1), 3007.

34. Bloch, F.; Hansen, W. W.; Packard, M., Nuclear Induction. *Phys Rev* **1946,** *69* (3-4), 127-127.
35. Purcell, E. M.; Torrey, H. C.; Pound, R. V., Resonance Absorption by Nuclear Magnetic Moments in a Solid. *Phys Rev* **1946,** *69* (1-2), 37-38.
36. Friebolin, H., *Basic one- and two-dimensional NMR spectroscopy*. 2nd enl. ed.; VCH Verlagsgesellschaft ;
VCH Publishers: Weinheim, Germany
New York, NY, USA, 1993; p xxi, 368 p.
37. Hore, P. J., *Nuclear Magnetic Resonance*. Oxford Science Publications: USA, 1995; p 90.
38. Fyfe, C. A., Solid State NMR for Chemists. *C.F.C. Press* **1983**, 1-150.
39. Penzel, S.; Smith, A. A.; Ernst, M.; Meier, B. H., Setting the magic angle for fast magic-angle spinning probes. *J Magn Reson* **2018,** *293*, 115-122.
40. Bone, Q.; Moore, R. H., Biology of fishes. *Taylor & Francis group* **2008,** *3rd*, 437-458.
41. Stien, L. H.; Bracke, M. B. M.; Folkedal, O.; Nilsson, J.; Oppedal, F.; Torgersen, T.; Kittilsen, S.; Midtlyng, P. J.; Vindas, M. A.; Øverli, Ø.; Kristiansen, T. S., Salmon Welfare Index Model (swim 1.0): a semantic model for overall welfare assessment of caged Atlantic salmon: review of the selected welfare indicators and model presentation. *Reviews in Aquaculture* **2012**, 33-57.
42. Schreibman, M. P.; Leatherland, J. F.; McKEOWN, B. A., Functional morphology of the teleost pituitary gland. *Am Zool* **1973,** *13* (3), 719-742.
43. Ando, H.; Urano, A., Molecular regulation of gonadotropin secretion by gonadotropin-releasing hormone in salmonid fishes. *Zoolog Sci* **2005,** *22* (4), 379-89.
44. Schwyzer, R., ACTH: a short introductory review. *Annals of the New York Academy of Sciences* **1977,** *297* (1), 3-26.
45. Martin, S. A. M.; Wallner, W.; Youngson, A.; Smith, T., Differential expression of Atlantic salmon thyrotropin β subunit mRNA and its cDNA sequence. *J Fish Biol* **1999,** *54* (4), 757-766.
46. Male, R.; Nerland, A. H. H.; Lorens, J. B. B.; Lossius, I.; Telle, W.; Totland, G., The complete nucleotide sequence of Atlantic Salmon growth hormone I gene. *Nucleic Acids Res* **1991**, The National Center for Biotechnolofy Information(NCBI).
47. Andersen, O.; Skibeli, V.; Gautvik, K. M., Purification and characterization of Atlantic salmon prolactin. *Gen. Comp. Endocronol.* **1989**, 354-360.
48. Chong, K. L.; Wang, S.; Melamed, P., Isolation and characterization of the follicle-stimulating hormone β subunit gene and 5'flanking region of the Chinook salmon. *Neuroendocrinology* **2004,** *80* (3), 158-170.
49. Kato, Y.; Gen, K.; Maruyama, O.; Tomizawa, K.; Kato, T., Molecular cloning of cDNAs encoding two gonadotropin beta subunits (GTH-I beta and -II beta) from the masu salmon. *J. Mol. Endocrinol.* **1994,** *11*, 275-282.
50. Kithara, N.; Nishizawa, T.; Gatanaga, T.; Okazaki, H.; Andoh, T.; Soma, G.-I., Primary structure of two mRNAs encoding putative salmon alpha-subunits of pituitary glycoprotein hormone. *Comp. Biochem. Physiol.* **1993,** *91*, 551-556.
51. Lin, X.-W.; Peter, R. E., Expression of salmon gonadotropin-releasing hormone (GnRH) and chicken GnRH-II precursor messenger ribonucleic acids in the brain and ovary of goldfish. *Gen Comp Endocr* **1996,** *101* (3), 282-296.
52. Kawauchi, H.; Adachi, Y.; Tsubokawa, M., Occurrence of a new melanocyte stimulating hormone in the salmon pituitary gland. *Biochem Bioph Res Co* **1980,** *96* (4), 1508-1517.

53. Britannica, T. E. o. E., Perch. January 03, 2016 ed.; Encyclopædia Britannica, inc.: https://www.britannica.com/animal/perch, 2016.
54. Quentin, B.; Moore, R. H., *Biology of Fishes*. 3rd ed.; Taylor & Francis Group: 2008; p 478.
55. Morcombe, C. R.; Zilm, K. W., Chemical shift referencing in MAS solid state NMR. *J Magn Reson* **2003,** *162* (2), 479-86.
56. Reich, H. J. C-13 Chemical Shifts.
57. Wishart, D. S.; Bigam, C. G.; Yao, J.; Abildgaard, F.; Dyson, H. J.; Oldfield, E.; Markley, J. L.; Sykes, B. D., 1 H, 13 C and 15 N chemical shift referencing in biomolecular NMR. *Journal of biomolecular NMR* **1995,** *6* (2), 135-140.
58. Aursand, M.; Jorgensen, L.; Grasdalen, H., Quantitative High-Resolution C-13 Nuclear-Magnetic-Resonance of Anserine and Lactate in White Muscle of Atlantic Salmon (Salmo-Salar). *Comp Biochem Phys B* **1995,** *112* (2), 315-321.
59. Risa, O.; Melo, T. M.; Sonnewald, U., Quantification of amounts and C-13 content of metabolites in brain tissue using high-resolution magic angle spinning C-13 NMR spectroscopy. *Nmr Biomed* **2009,** *22* (3), 266-271.
60. Stephan Grzesiek, A. B., The Importance og Not Saturating H20 in Protein NMR. Application to Sensitivity Enhancement and NOE Measurements. *Laboratory of Chemical Physics National Institute of Diabetes and Digestive and Kidney Diseases* **1993**.
61. Reeves, R. B., The interaction of body temperature and acid-base balance in ectothermic vertebrates. *Annu Rev Physiol* **1977,** *39*, 559-86.
62. HARTEL, A. J.; LANKHORST, P. P.; ALTONA, C., Thermodynamics of Stacking and of Self-Association of the Dinucleoside Monophosphate m62A-U from Proton NMR Chemical Shifts: Differential Concentration Temperature Profile Method. *Eur J Biochem* **1982,** *129* (2), 343-357.
63. Wind, R. A.; Hu, J. Z.; Rommereim, D. N., High-resolution (1)H NMR spectroscopy in organs and tissues using slow magic angle spinning. *Magn Reson Med* **2001,** *46* (2), 213-8.
64. Oliveira, A. L. d.; Martinelli, B. C. B.; Lião, L. M.; Pereira, F. C.; Silveira-Lacerda, E. P.; Alcantara, G. B., 1H HR-MAS NMR and S180 Cells: Metabolite Assignment and Evaluation of Pulse Sequence. *Journal of the Brazilian Chemical Society* **2014**.
65. Taylor, J. L.; Wu, C. L.; Cory, D.; Gonzalez, R. G.; Bielecki, A.; Cheng, L. L., High-resolution magic angle spinning proton NMR analysis of human prostate tissue with slow spinning rates. *Magnetic Resonance in Medicine: An Official Journal of the International Society for Magnetic Resonance in Medicine* **2003,** *50* (3), 627-632.
66. Bax, A., A Spatially Selective Composite 90-Degrees Radiofrequency Pulse. *Journal of Magnetic Resonance* **1985,** *65* (1), 142-145.
67. Hahn, E. L., Spin Echoes. *Phys Rev* **1950,** *80* (4), 580-594.
68. Carr, H. Y.; Purcell, E. M., Effects of Diffusion on Free Precession in Nuclear Magnetic Resonance Experiments. *Phys Rev* **1954,** *94* (3), 630-638.
69. Hore, P.; Jones, J.; Wimperis, S., *NMR: The toolkit: How pulse sequences work*. Oxford University Press, USA: 2015.
70. Levitt, M. H., *Spin dynamics: basics of nuclear magnetic resonance*. John Wiley & Sons: 2001.
71. Govindaraju, V.; Young, K.; Maudsley, A. A., Proton NMR chemical shifts and coupling constants for brain metabolites. *NMR in Biomedicine: An International Journal Devoted to the Development and Application of Magnetic Resonance In Vivo* **2000,** *13* (3), 129-153.

8. Appendix

8.1 Appendix 1

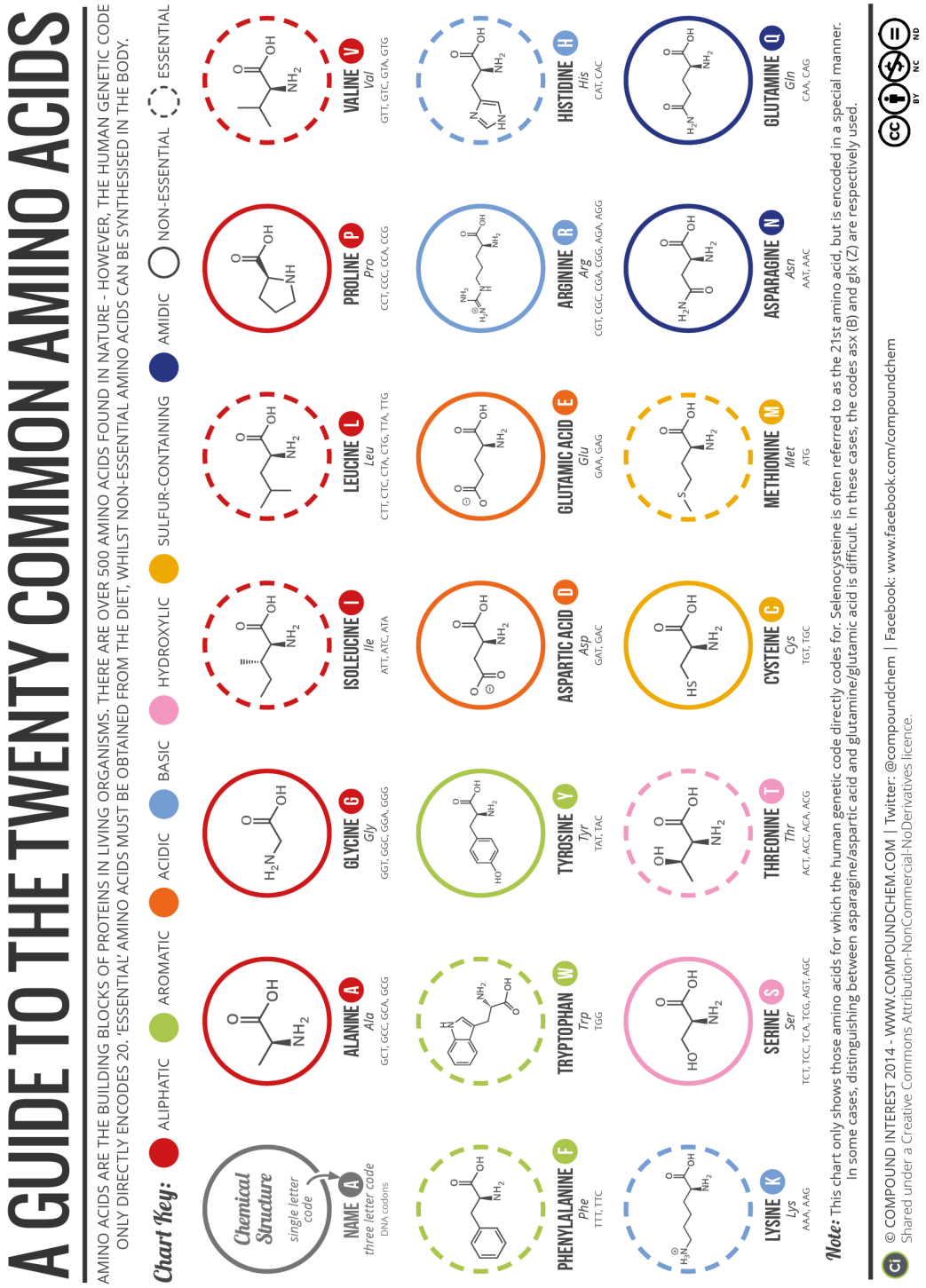

Figure A.1: An overview of the 20 common amino acids. The figure is taken from compoundchem.com 29.04.2019.

8.2 Appendix 2

Table A.1: The different pituitary hormones consist of a number of amino acids, which are presented in this table.[44-52]

ACTH	GH	PRL	FSH β	LH β	TSH β	FSH/LH/TSH α	sGnRH	MSH α	MSH β
S	M	M	M	M	M	S	M	G	D
Y	G	A	Y	L	E	L	E	Y	G
S	Q	R	C	G	L	I	G	S	S
M	V	R	T	L	S	L	K	M	Y
E	F	S	H	H	V	S	G	E	R
H	L	Q	L	N	A	I	R	H	M
F	L	G	K	G	M	L	V	F	G
R	M	T	T	T	C	L	L	R	H
W	P	K	L	L	G	Y	V	W	F
G	V	L	Q	I	L	M	Q	G	R
K	L	H	L	S	L	A	L	K	W
P	L	L	V	L	C	D	L	P	G
M	V	A	V	S	L	S	M	V	S
G	S	V	M	L	L	Y	L		P
R	C	C	A	C	F	Q	A		T
K	F	L	T	I	S	N	C		A
R	L	V	L	L	Q	S	V		I
R	S	V	W	L	A	D	L		
P	Q	S	V	E	V	M	E		
I	G	C	T	P	P	T	V		
K	A	H	P	V	M	N	S		
V	A	A	V	E	C	V	L		
Y	M	I	R	G	V	G	C		
P	E	G	A	S	P	C	Q		
N	N	L	G	L	T	E	H		
S	Q	S	T	M	D	E	W		
F	R	D	D	Q	Y	C	S		
E	L	L	C	P	T	K	Y		
D	F	M	R	C	L	L	G		
E	N	E	Y	Q	Y	K	W		
S	I	R	G	P	E	E	L		
V	A	A	C	I	E	N	P		
E	V	S	R	N	R	K	G		
N	N	Q	L	Q	R	V	G		
M	R	R	N	T	E	F	K		
G	V	S	N	V	C	S	R		
P	Q	D	M	S	D	N	S		
E	H	K	T	L	F	P	V		
L	L	L	I	E	C	G	G		

H	H	T	K	V	A	E
L	S	V	E	A	P	V
M	L	E	G	I	V	E
A	S	R	C	N	Y	A
Q	T	E	P	T	Q	T
K	L	D	T	T	C	F
M	S	C	C	I	T	R
F	T	H	L	C	G	M
N	K	G	V	M	C	M
D	D	S	I	G	C	D
F	L	I	Q	F	F	S
E	D	T	T	C	S	G
G	S	I	P	Y	R	D
T	H	T	I	S	A	A
L	F	T	C	R	Y	V
L	P	C	S	D	P	L
P	P	A	G	S	T	S
D	M	G	H	N	P	I
E	G	L	C	M	L	P
R	R	C	I	K	Q	M
R	V	E	T	E	S	D
Q	M	T	K	L	K	S
L	M	T	E	A	K	P
N	P	D	P	G	A	M
K	R	L	V	P	M	E
I	P	N	F	R	L	R
F	S	Y	R	F	V	L
L	M	Q	S	L	P	S
L	C	S	P	I	K	P
D	H	T	F	Q	N	I
F	T	W	T	R	I	H
C	S	L	V	G	T	I
N	S	P	Y	C	S	V
S	L	R	Q	T	E	S
D	Q	S	H	Y	A	E
S	T	Q	V	D	T	V
I	P	G	C	Q	C	D
V	K	V	T	V	C	A
S	D	C	Y	E	V	E
P	K	N	R	Y	A	G
I	E	F	D	R	K	L
D	Q	K	V	T	E	P
K	A	E	R	V	G	L
L	L	W	Y	I	E	K
E	K	S	E	L	R	E
T	V	Y	M	P	V	Q

Q	S	E	I	G	V	R
K	E	K	R	C	D	F
S	N	V	L	P	N	P
S	E	Y	P	L	I	N
V	L	L	D	H	K	R
L	I	E	C	A	L	R
K	S	G	P	N	T	G
L	L	C	P	P	N	R
L	A	P	W	L	H	D
H	R	S	V	F	T	
I	S	G	D	T	E	
S	L	V	P	Y	C	
F	L	D	H	P	W	
R	L	P	V	V	C	
L	A	F	T	A	N	
I	W	F	Y	L	T	
E	N	I	P	S	C	
S	D	P	V	C	Y	
W	P	V	A	H	H	
E	L	A	L	C	H	
Y	L	K	S	G	K	
P	L	S	C	T	S	
S	L	C	D	C		
Q	S	D	C	N		
T	S	C	S	T		
L	E	I	L	D		
T	A	K	C	S		
I	P	C	N	D		
S	T	K	M	E		
N	L	T	D	C		
S	P	D	T	A		
L	H	N	S	H		
M	P	T	D	K		
V	S	D	T	A		
R	N	C	I	S		
N	G	D	E	S		
S	D	R	I	G		
N	I	I	L	D		
Q	S	S	S	G		
I	S	M	P	A		
S	K	A	D	R		
E	I	C	F	C		
K	R	P	C	S		
L	E	S	I	K		
S	L	C	T	P		
D	Q	I	Q	L		

L	D	V	R	R
K	Y	N	V	H
V	S	P	L	I
G	K	L	T	Y
I	S	E	D	H
N	L	M	G	T
L	G		D	L
L	D		M	A
I	G		W	
K	L			
G	D			
S	I			
Q	M			
D	V			
G	N			
V	K			
L	M			
S	G			
L	P			
D	S			
D	S			
N	Q			
D	Y			
S	I			
Q	S			
Q	S			
L	I			
P	P			
P	F			
Y	K			
G	G			
N	G			
Y	D			
Y	L			
Q	G			
N	N			
L	D			
G	K			
G	T			
D	S			
G	R			
N	L			
V	I			
R	N			
R	F			
N	H			

Y	F
E	L
L	M
L	S
A	C
C	F
F	R
K	R
K	D
D	S
M	H
H	K
K	I
V	D
E	S
T	F
Y	L
L	K
T	V
V	L
A	R
K	C
C	R
R	A
K	T
S	M
L	R
E	P
A	E
N	T
C	C
T	
L	

Table A.2: The amino acids in codes and letters

Code	Letter	Code	Letter	Code	Letter
Ala	A	Asp	D	Asn	N
Gly	G	Glu	E	Gln	Q
Ile	I	Arg	R		
Leu	L	His	H		
Pro	P	Lys	K		
Val	V	Ser	S		
Phe	F	Thr	T		
Trp	W	Cys	C		
Tyr	Y	Met	M		

8.3 Appendix 3

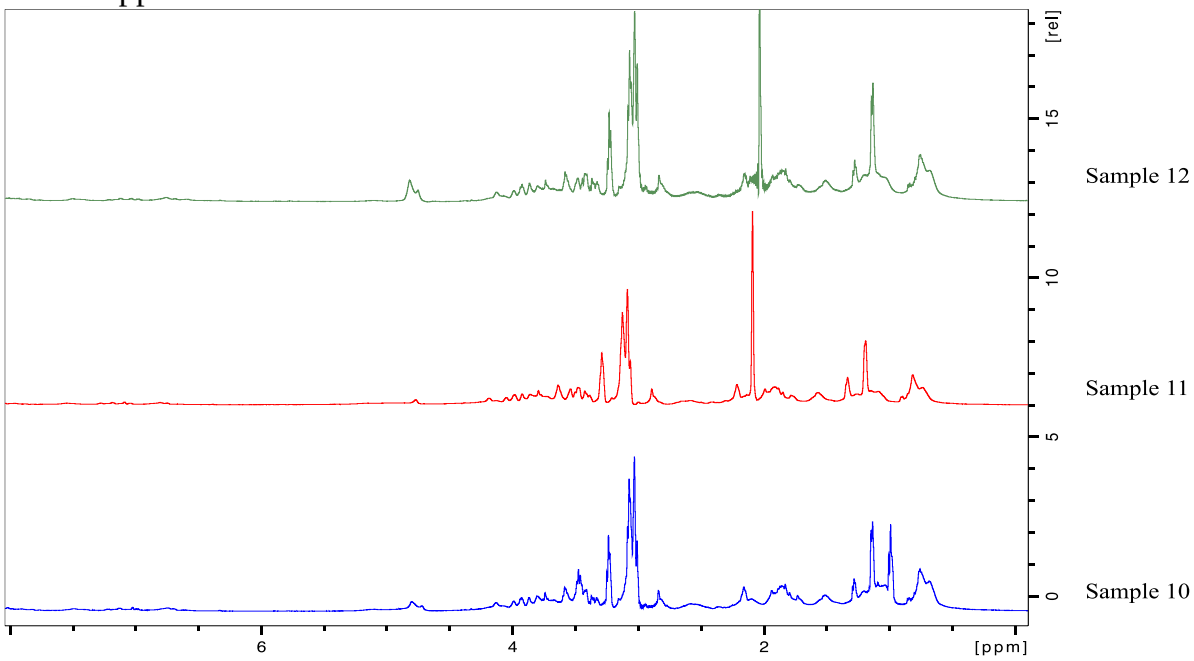

Figure A.2: The 1D proton spectra of healthy salmon pituitaries. Samples 10, 11 and 12 are presented.

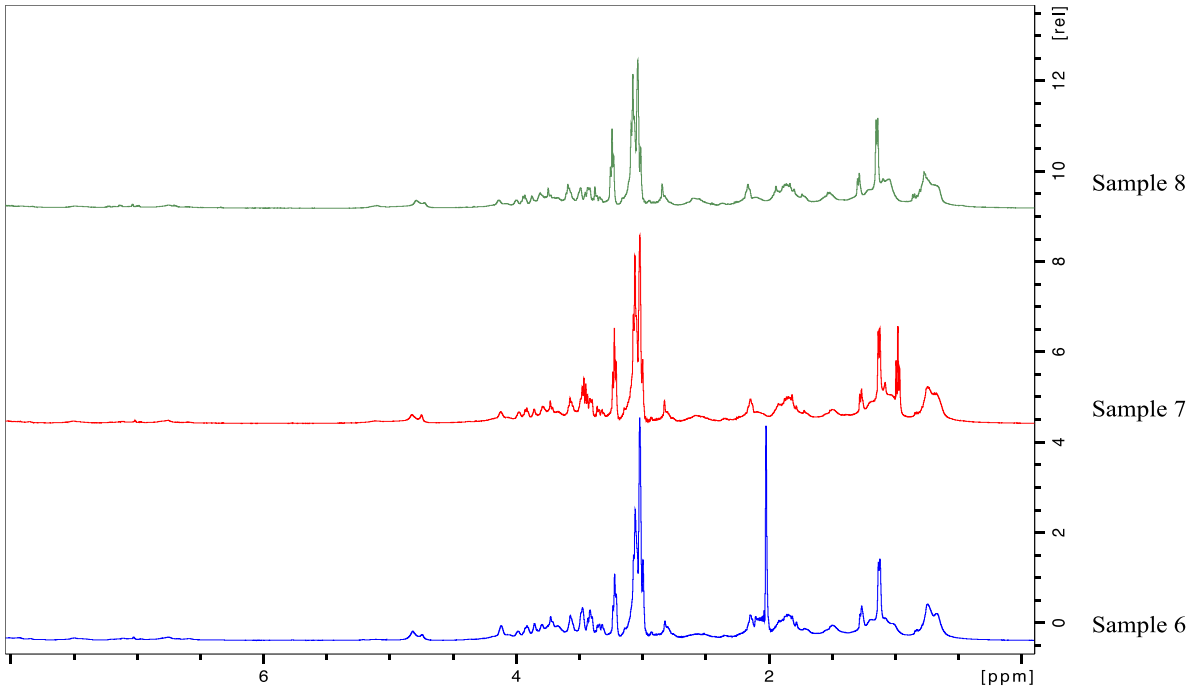

Figure A.3: The 1D proton spectra of healthy salmon pituitaries. Samples 6, 7 and 8 are presented.

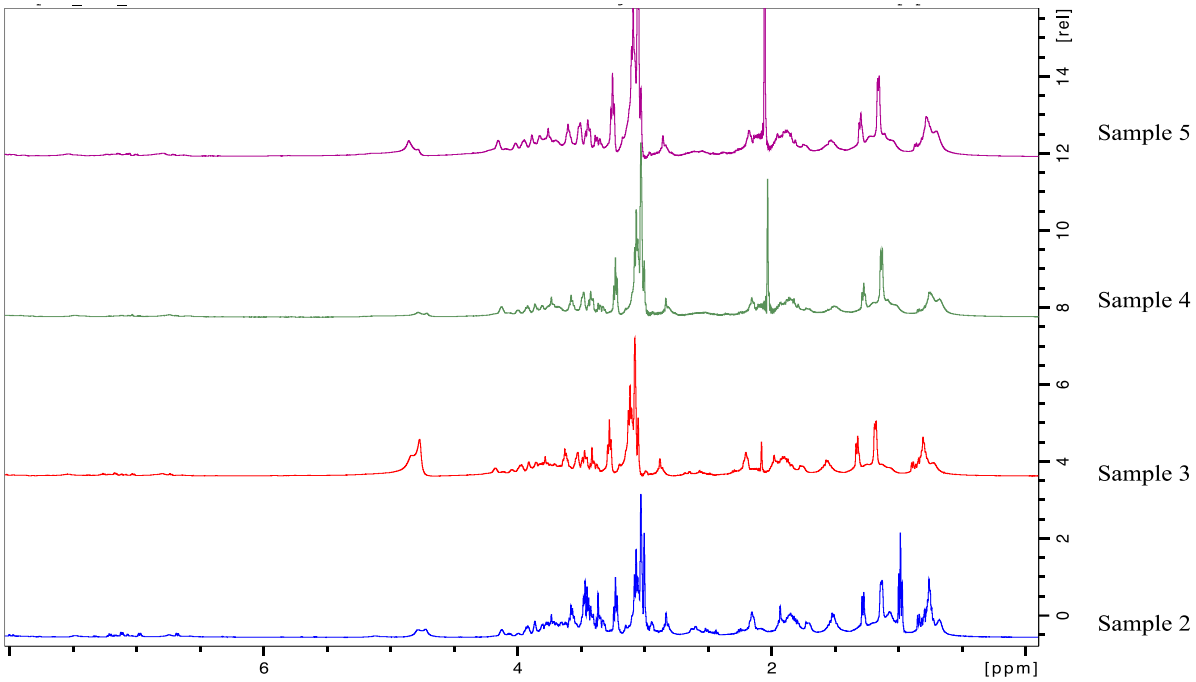

Figure A.4: The 1D proton spectra of healthy salmon pituitaries. Samples 2, 3, 4 and 5 are presented.

8.4 Appendix 4

Table A.3: An overview of the parameters used in the ^{13}C experiment of a pituitary on a 500MHz magnet. d1 is measured in seconds, the pulse width p1 is measured in micro seconds and the experimental time is measured in hours.

Pulse prog.	Temp. [K]	d1 [s]	p1 [μs]	ns	Spin [Hz]	Exp.time [h]
hpdec	277	5	3,9	44000	2500	62,37

Table A.4: An overview of the parameters used in the ^{1}H "onepulse" experiments to detect water signal in the pituitaries. The temperature is measured in kelvin, d1 is measured in seconds and the pulse width p1 is measured in micro seconds

Pulse prog.	Temp. [K]	d1 [s]	p1 [μs]	ns	Spin [Hz]
onepulse	277	5	2,5	8	4000

Table A.5: An overview of the parameters used for all the experiments of water. The temperature is measured in kelvin, d1 is measured in seconds and the pulse width p1 is measured in micro seconds.

Sample	Puls.prog.	Temp. [K]	d1[s]	p1 [μs]	Spin [Hz]	Rg
Distilled water	onepulse	277	5	2,5	0	8
Pituitary	onepulse	277	5	2,5	4000	8

Table A.6: *An overview of the parameters used in the ^{1}H 1D "zgcppr" experiment performed on the pituitaries with a 500MHz magnet. The temperature is measured in kelvin, d1 is measured in seconds, the pulse width p1 is measured in micro seconds and the p19 is measured in decibel.*

Puls.prog.	Temp. [K]	d1 [s]	p1[μs]	p19 [dB]	Spin [Hz]	ns	Time [h]
zgcppr	277	10	2,5	30	4000	512	1,5

Table A.7: An overview of the parameters used to adjust the echo value in the "cmpgpr1d" pulse sequence. The temperature is measured in kelvin, d1 is measured in seconds, the pulse width p1 is measured in micro seconds and the p19 is measured in decibel.

Puls.prog.	**Temp. [K]**	**d1 [s]**	**p1 [μs]**	**p2 [μs]**	**d20 [ms]**	**L4**	**Spin [Hz]**	**ns**	**Echo time [ms]**
cpmgpr1d	277	10	2,5	5	2	20	4000	261	88

Table A.8: An overview of the parameters used to adjust the echo value in the "cosydfphpr" pulse sequence. The temperature is measured in kelvin, d1 is measured in seconds, the pulse width p1 is measured in micro seconds and the p19 is measured in decibel.

Puls.prog.	**Temp. [K]**	**d1 [s]**	**p1 [μs]**	**d0 [μs]**	**Spin [Hz]**	**ns**
cpmgpr1d	277	2	3,5	95,5	4000	128